Evaluation of Gait and Muscle Function with Ankle Foot Orthoses

Hwan Choi

A dissertation

submitted in partial fulfillment of the

requirements for the degree of

Doctor of Philosophy

University of Washington

2016

Reading Committee:

Katherine M. Steele, Chair

Mark A. Ganter

Kristie F. Bjornson

Program Authorized to Offer Degree:

Mechanical Engineering

University of Washington

Abstract

Evaluation of Gait and Muscle Function with Ankle Foot Orthoses

Hwan Choi

Chair of the Supervisory Committee:
Assistant Professor Katherine M. Steele
Mechanical Engineering

Many individuals with cerebral palsy (CP) and stroke are prescribed ankle foot orthoses (AFOs) for use during daily life. AFOs have been shown to improve pathologic gait and walking speed in CP and stroke by providing support and alignment. There are many different types of AFOs available such as posterior leaf spring AFOs, rigid AFOs, and articulated AFOs. Further, there are many parameters that can be customized or tuned for each type of AFO, such as stiffness, heel height, shank to vertical angle, and foot plate length. However, how different types of AFOs and the customization of specific parameters impact muscle function remains unclear.

The goals of this dissertation were to evaluate how different types of AFOs and different tuning parameters impact gait kinematics and muscle function. Of particular interest is the gastrocnemius, a key muscle that crosses the knee and ankle joints and is commonly tight among individuals with CP or stroke. Gastrocnemius operating length, defined as the total muscle and tendon length during a functional activity, influences ankle and knee kinematics during gait.

Therefore, understanding and potentially controlling gastrocnemius operating length may help to properly select and optimize the design of AFOs to improve gait. To understand the impact of AFOs on gastrocnemius function, this dissertation includes four primary aims.

The first aim was to evaluate how current methods for tuning, or adjusting patient-specific properties of AFOs, impact gastrocnemius operating length and gait kinematics using musculoskeletal modeling. We performed a case study of an adult stroke survivor who received three AFOs that were tuned by a trained orthotist. The orthotist observed the individual's shank to vertical angle (SVA, the angle of the tibia with respect to vertical, which is commonly assessed by orthotists during gait analysis) and adjusted the AFO's fixed plantarflexion angle and heel height to make the SVA more similar to unimpaired individuals. For this case study, we found that tuning the AFOs based on SVA resulted in a decrease in gastrocnemius operating length and increased knee flexion angle during swing. These results demonstrated how musculoskeletal modeling can be used to evaluate muscle function during walking and the impacts of adjusting SVA for stroke survivors.

The second aim was to evaluate how different types of AFOs, representing the current standard of care, alter gastrocnemius operating length and gait kinematics in children with CP. We evaluated gastrocnemius operating length for eleven children with CP who each received two types of AFOs. Since individuals wear AFOs all day, we sought to evaluate if the gastrocnemius operated in a stretched or shortened position. For individuals with CP with more mild involvement, we found both types of AFOs stretched the gastrocnemius during walking for the majority of individuals. However, for individuals with CP and more severe involvement, we found only the more solid, Cascade AFOs stretched the gastrocnemius in some individuals. This

study suggested AFOs can potentially be a rehabilitation modality by providing dynamic stretching exercise for a short and tight gastrocnemius during gait.

The third aim was to create a flexible platform for fabricating AFOs with 3D printing and scanning technology, which could support research on how AFO stiffness impacts joint and musculotendon function. The current standard AFO designs are not only cost and time ineffective, but also provide limited control of AFO stiffness. This study demonstrated a novel method for fabricating a variable stiffness AFO using a 3D scanner and printer. To adjust the stiffness, elastic polymer bands were fabricated with varying stiffness. The 3D printed AFO is cost and labor effective compared to current AFO fabrication methods. 3D printed AFOs can also can provide adjustable AFO stiffness, as well as versatility to combine with various measurement tools such as ultrasound and electromyography.

The forth aim was to evaluate how AFO stiffness and walking speed impact joint kinematics, gastrocnemius muscle length, and Achilles tendon (AT) length in unimpaired individuals. In this study we used the 3D printed AFO created in Aim 3. We found that as AFO stiffness increased, peak AT length, peak gastrocnemius activation level, and peak ankle dorsiflexion angle significantly decreased. However, peak gastrocnemius muscle length and peak AFO dorsiflexion moment increased with increasing AFO stiffness. Gastrocnemius muscle length and lengthening velocity significantly decreased with slower walking speeds. This study illustrated how human musculoskeletal system interplays with different stiffness AFOs. Building on these methods, future research can inform AFO prescription for individuals with neurologic injuries to maximize stretching or other rehabilitation or performance goals during walking.

This dissertation provides important evidence for how humans adapt to various AFO properties and suggests important implications for the design and prescription of AFOs. This work provides a quantitative evaluation of how AFOs impact musculotendon dynamics among individuals with stroke (Aim 1) and cerebral palsy (Aim 2). The fabrication methods in Aim 3 creates a powerful and flexible research platform for evaluating AFO design, which may be extended to fabrication of AFOs for daily use with further improvements in additive manufacturing materials and methods. The final study (Aim 4), provides the first experimental evidence combining ultrasound and musculoskeletal modeling to understand how muscle and tendon length are impacted by AFO design. These evaluations provide guidance for future AFO design and prescription that can not only augment human mobility for unimpaired individuals, but also provide improve metrics for improving function and guiding rehabilitation for individuals with neurologic impairments.

ACKNOWLEDGEMENTS

I am so excited to have finally taken a small step towards my life-time mission to be “the salt and light” for the humankind by contributing to research aimed at improving the dynamic motion of individuals with neurologic impairments. This accomplishment is not just a reflection of my ability but the unlimited support from my father, Dayeon Choi, and mother, Taere Jeong. In addition to providing me an education, and teaching me persistence, I appreciate my parents and life-time mentors for their support, encouraging words, and prayers.

To my eternal friend and the light of my life, Song Hyeon Lee, you are the key me finishing my doctoral degree. Every time I felt exhausted and frustrated, you have encouraged me to keep pursuing my research. Celebrating every milestone has been so much sweeter with you at my side. .As a spouse and a mother of two children, Emmelyn Choi and Adelle Choi, your dedication not only allowed me keep pursuing my doctoral program but has also nurtured a wonderful family. Without your dedication, I would not have been to start my life-time mission. I would like to thank my daughters, Emmelyn Choi and Adelle for giving me all the joys and responsibilities of being a father and putting up with me studying during weekends when I should be playing with them.

I would like to thank my advisor, Katherine Steele. She has provided a great opportunities to do biomechanics research and supported me through my doctoral program. I learned a lot from you beyond research. There are so many lessons I have learned from my adviser but the most valuable lessons are communication skill with one’s adviser and other lab members, mentorship skill, actively participating in meetings by throwing ideas even it is non-sense without judgment and connecting with the other researchers outside campus. I especially

enjoyed discussing research ideas during our meetings. The meetings motivated and spurred me to take steps forward towards reaching my goals. I really appreciate your patience and dedication, which led me to a successful doctoral program. I also thank my first year adviser Michael Hahn and Kristie Bjornson who supported me during my first year PhD and gave me an opportunity to make a solid corner stone of my doctoral program.

To the members of Steele Lab, it has been my pleasure to see develop into successful researchers. Thank you my urban dictionary, Benjamin Shuman, lab manager, Keshia Peters, network bank, Gaurav Mukherjee, and quasi-professional cyclist, Michael Rosenberg for your collaborations, advice, proofreading, and all the conversations which broaden my perspective. To my trusty mentees Michael MacConnell, Katie Ly, Matthew Yang, and Eric Eckert: I really appreciate all of your contributions processing huge amount of data and enabling me to finish my research. I really enjoyed instructing and learning from you.

It has been blessing to have developed friendships at the University of Washington. I thank to my sous-chef Stefan Bjornson who had kept the office with me late in the night. David Schipf and Michael Au-yeung thank you for keep praying for me. I also thank to my “sun-bae” (Mentors) Jae Hyeuk Suk, Se-yeun Lee, Sangyun Han, Heesuk Kim, and Jong Yoon for giving me advice how to manage the PhD program as a Korean. I also thank my fellow church members Young Kim, Jinhong Kim for blessing my family and my studies.

Lastly, finishing my doctoral program is just beginning of my research journey and I appreciate all of many people who have helped me begin this adventure. I believe the God will help me to finish my journey and serve people with the knowledge I have learned.

TABLE OF CONTENTS

LIST OF FIGURES

LIST OF TABLES

AIMS OVERVIEW

AIM 1: Evaluate the Effect of Ankle Foot Orthoses Tuning on Musculotendon Dynamics during Gait after Stroke

The efficacy of AFO-footwear combination (AFO-FC) is thought to be related to gastrocnemius function; however, the impacts of tuning an AFO-FC on gastrocnemius were unclear. We analyzed the impact of tuning an AFO-FC in a case study of an individual with left hemiplegia following stroke who had gastrocnemius contracture and a stiff-knee gait. Tuning an AFO-FC altered gastrocnemius operating length, ankle internal plantarflexor moment, and knee kinematics.

AIM 2: Quantify Changes in Gastrocnemius Operating Length with Different Types of Ankle Foot Orthoses in Children with Cerebral Palsy

Many types of AFOs are available, but impacts on gastrocnemius operating length and kinematics with different types of AFOs have not been previously evaluated. We analyzed the effects of two different types of AFOs on medial gastrocnemius operating length. Medial gastrocnemius operating length during gait was compared to the passive threshold of the gastrocnemius, defined as the length of gastrocnemius at maximum ankle dorsiflexion with the knee fully extended measured in physical exam. This comparison was used to evaluate whether the medial gastrocnemius was stretched beyond the passive threshold during gait. The results suggested that AFOs can stretch the gastrocnemius during gait for some individuals and AFOs have potential for rehabilitation to stretch the gastrocnemius during walking in daily life.

AIM 3: Fabricate Customized 3D Printed Variable Stiffness Ankle Foot Orthoses to Evaluate Muscle Function

To evaluate how varying AFO stiffness impacts musculotendon operating length, an AFO with interchangeable elastic polymer bands was fabricated that can be used as a research platform for evaluating muscle function with AFOs. The AFO fabrication process uses an affordable 3D portable scanner and computer aid design tools to customize the fit of the AFO to an individual's leg. A fuse deposition modeling 3D printer with polylactic acid filament was used to fabricate the AFOs and negative molds of elastic polymer bands. Varying the stiffness of the elastic polymer bands, attached posteriorly parallel to the Achilles tendon, can be used to adjust sagittal plane stiffness of the AFOs. The 3D printed variable stiffness AFOs are compatible with other measurement tools such as ultrasonography and electromyography (EMG) by the virtue of flexible AFO design.

AIM 4: Evaluate Changes in Kinematics and Gastrocnemius Function during Gait with Different Stiffness Ankle Foot Orthoses in Unimpaired Individuals

We evaluated impacts of AFO stiffness on medial gastrocnemius length, Achilles tendon (AT) length, and joint kinematics during gait of unimpaired adults using 3D printed variable stiffness AFOs, ultrasonography, and electromyography (EMG). Analyzing the interplay between different stiffness AFOs and AT and muscle length can provide insight into how our body adapts to different AFOs. The results demonstrate that as AFO stiffness increased, peak AT length, peak gastrocnemius activation level, and peak gastrocnemius eccentric velocity decreased. Slower

walking speed reduced peak gastrocnemius eccentric velocity, suggesting the muscle may produce less force due to muscle's force-velocity properties. The results demonstrate the complex musculotendon dynamics with varying AFO properties and provide methods that can be extended to inform the design and prescription of AFOs for individuals with neurologic injuries.

INTRODUCTION

Cerebral Palsy

Cerebral Palsy (CP) is a neurological disorder that stems from a non-progressive brain lesion or malformation of the immature brain, which causes heterogeneous impairments in movement, sensory abilities, and language. CP negatively affects mobility and can create long-term financial burdens. For example, in the United States, the prevalence of CP is 3.3 per 1000 children [1]. Among children with CP, 58.2% of children can walk independently but their gait pattern deviates from unimpaired individuals, 11.3% rely on hand-held assistive devices to walk, and 30.6% have a limited ability to walk independently [2]. The medical costs for children with CP is a crucial social issue. Among children who enrolled in Medicaid in 2005, medical expenditures for children with CP without co-occurring intellectual disability (ID) were $15,047 higher per child per year than typically developing children, and CP with co-occurring ID were $41,664 higher [3]. Although caused by an injury to the brain, secondary musculoskeletal impairments commonly develop among individuals with CP. Muscle contracture is common in individuals with CP and may lead to bone deformities [4]. Muscle contracture can also impair movement and cause hip dislocation and degenerative arthritis and joint pain if left untreated [5].

There are several common factors which can increase the risk of CP. Inadequate level of oxygen in the blood due to altered heart rate, respiratory distress or a collapsed lung can cause intrapartum asphyxia and damage areas of the brain that are crucial to development and motor function [6]. Intracranial hemorrhage, which is a pathological accumulation of blood within the brain, is one of most common causes of CP [7]. Intracranial hemorrhage can be related to blood coagulation in the placenta from pathologies such as placenta abruption and placenta previa, in

which the placenta partially or entirely covers the cervix [8]. Brain damage from bacterial infection is another risk factor of CP. The brain can be broadly classified into white matter and grey matter. Grey matter consists of dendrites, axon terminals of neurons, cell bodies of neurons, synapses, and capillaries [9]. Grey matter plays a role in muscle control, sensory perception and self-control [10]. White matter is composed of long-range myelinated axons and it responsible for the signal transmission of nerve impulses that control motor function [11].

When the white matter and grey matter are damaged near the time of birth, CP can result. Periventricular leukomalacia (PVL) is a type of brain damage of periventricular white matter and it results in necrosis of affected cells and generates an empty area in the brain [12]. It is believed that intrauterine infections may be an underlying contributing cause of these injuries, where abnormal bacteria can infect the amniotic fluid [13]. PVL also can be caused by intraventricular hemorrhage [14]. Traumatic brain damage can also lead to CP when children are exposed to abuse, motor vehicle accident, or infected by meningitis which causes inflammation of brain and spinal cord membranes. Since every brain lesion is unique, every individuals with CP has different pathologic gait patterns, thus orthoses and other assistive devices need to be customized to each individual.

Pathologic Gait Patterns and Muscle Characteristics

Because there are many types of brain injuries that can cause CP, there are also many different gait patterns among individuals with CP. The most common pathologic gait patterns include stiff knee in swing, equinus, intoeing, increased hip flexion, and crouch gait [15]. Among the common pathologic gait patterns, equinus and crouch gait are thought to be related to gastrocnemius contracture and spasticity. Since AFOs directly influence the gastrocnemius and the soleus by

controlling ankle joint movements during gait, evaluating AFO's impact on muscle function is crucial to better understand these pathologic gait patterns. Equinus gait is caused by excessive activation of the triceps surae and/or inadequate tibialis anterior muscle contractile force [16]. Equinus can be classified into true equinus and apparent equinus. True equinus is characterized by a large plantarflexion ankle angle with a fully extended knee or mild recurvatum, fully extended hip, and neutral to anteriorly tilted pelvis. Jump gait is a combination of true equinus with contracture and spasticity of biarticular muscles which cross the knee, such as the rectus femoris, gastrocnemii, and hamstrings. Thus, jump gait is characterized by normal ankle angle range with excessive knee joint flexion, excessive hip joint flexion, and normal or anteriorly tilted pelvis angle during stance. Apparent equinus has similar characteristics with jump gait except that the ankle is not plantarflexed but exhibits a neutral angle when in anatomic position. When the ankle angle is dorsiflexed from jump gait it classified as crouch gait (Fig. 1) [17].

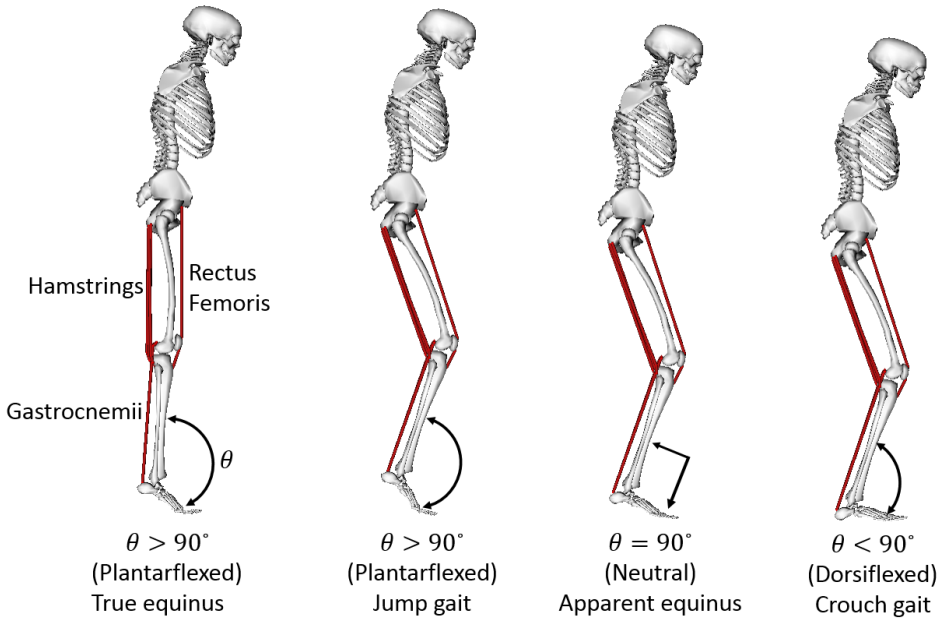

Figure 1. Common pathologic gait patterns of individuals with cerebral palsy.
Red lines depicts biarticular muscles which cross the knee joint including the hamstrings, gastrocnemii, and rectus femoris.

Equinus gait patterns also have different joint kinetics during gait compared to unimpaired individuals. For example, continuous ankle plantarflexor contraction during stance phase results in an inadequate ankle plantarflexion moment during terminal stance. The ankle plantarflexors also have two phases of activation during stance, which results in double bump ankle moment pattern during equinus gait, demonstrating a rapid change in plantarflexor moment. Extensor knee moments of individuals with CP are often larger compared to unimpaired individuals to prevent collapse with excess knee flexion [18]. The quadriceps muscles, which are knee extensors, continuously maintain contraction during pathologic gait patterns such as crouch gait. In some cases, activation of knee flexors present different moment patterns. The knee flexor activation patterns can also contribute to different knee moments during gait.

Altered muscle characteristics are one contributor to pathologic gait patterns. Individuals with CP have muscle characteristics that are different than those of unimpaired individuals [20]. Common symptoms of CP include muscle spasticity and contracture. Spasticity is characterized by an abnormal velocity-dependent resistance to stretch. Muscles with spasticity have larger intrinsic and reflex stiffness than unimpaired muscles where muscle resistance increases as muscle stretching velocity increases [21]. Muscle contracture may result from protracted spasticity and these muscles have a permanent reduction in muscle operating length, which can limit joint range of motion [22,23]. Operating length is defined as the length of the musculotendon unit from origin to insertion during movement. Muscles with spasticity and contracture have different muscle morphologies and structures compared to unimpaired muscle. For example, among individuals with CP muscles have been shown to have reduced fascicle length, physiological cross-sectional area, pennation angle, and muscle volume [24]. The muscle fiber is also stiffer compared to typically developing individuals [25]. Thus, spasticity and contracture hinder muscles from

achieving an effective length for generating force and executing daily activities. Muscles of individuals with CP also have altered activation patterns during gait compared to unimpaired individuals [26]. They cannot voluntarily fully activate their muscles and have excess co-activation [27,28]. These altered muscle characteristics and activations impair movement.

There are many possible treatments for children with CP to correct pathologic muscle functions and gait patterns. In general, pharmaceutical treatment such as benzodiazepines [29], baclofen [30], and botullinum toxin [31] in addition to multi-level orthopedic surgeries [32-34] have been suggested as possible treatments. However, pharmaceutical treatments and surgical treatments not only often have side effects [35], but outcomes are also inconsistent and often unsatisfactory [36,37]. Physical therapy such as stretching [38], strengthening [39], ambulation training [40] and functional activity training [41] may offer alternative treatments to reduce muscle tone. For example physical therapy techniques are associated with improvements in gait [42]. Although physical therapy is non-invasive compared to surgical and pharmaceutical treatments, the beneficial effects of therapy often cease once therapy is discontinued [43] and therapy can be time and resource intensive [3]. Therefore, it is both desirable and important to have repeatable and sustainable rehabilitation exercise strategies that can be integrated with daily life. Ankle foot orthoses (AFOs) are an assistive device to improve mobility in individuals with CP by providing support and alignment during gait. Moreover, AFOs also could be an alternative treatment to extend therapy into daily life. Compared to surgical and pharmaceutical treatment, AFOs cost less, avoid perilous aspects of operations, and can be discontinued if unsuccessful. In order to maximize benefits of AFOs, understanding the underlying mechanisms by which AFOs impact pathologic muscle and gait are required.

Ankle Foot Orthoses

AFOs are commonly prescribed for individuals with CP. Different types of AFOs are commonly prescribed depending on an individual's gait pattern and musculoskeletal deformities. Broadly, AFOs can be classified into articulated AFOs, posterior leaf spring (PLS) AFOs, and rigid AFOs (Fig. 2). Articulated AFOs use hinges to permit unrestricted ankle motion over a range that can be adjusted with a plantarflexion or dorsiflexion stop, as necessary. The articulated AFO gives flexibility to transition between common motions (*e.g.,* walking, sit to stand, and stair climb). However, prior research has suggested articulated AFOs should be cautiously prescribed to individuals with tight gastrocnemii or crouch gait. Increasing the muscle length at the ankle (with a plantarflexion stop) may result in a compensatory increases in knee flexion angle (developing or exacerbating crouch gait), preventing changes in gastrocnemius muscle length [44].

Figure 2. Three typical type of AFOs. Rigid AFO (left), posterior leaf spring AFO (middle), and hinged AFO (right).

Rigid AFOs consist of a single rigid piece of material. A rigid AFO locks ankle motion during gait. The primary goal of rigid AFOs are to provide stability and are commonly used for individuals with equinus deformity [45]. If rigid AFOs are used for a long time, they may cause atrophy of ankle plantarflexors and dorsiflexors since they restrict ankle motion [46]. PLS AFOs are similar to rigid AFOs being of a single continuous piece of plastic, or calf cuff, behind the ankle, but are designed to be non-rigid. PLS AFO stiffness is determined by changing the thickness and width of the calf cuff [47-49] or by choosing different materials [50]. Advantages of PLS AFOs are that they can 1) prevent foot drop in swing and support alignment of the foot promoting appropriate heel contact, 2) store energy during stance and (3) help during push-off to move the body forward by releasing stored energy [51]. The flexibility to design different stiffness is one strength of PLS AFOs, but once the fabrication of a PLS AFO is completed with a specific stiffness it cannot be changed. Determining the optimal stiffness for each individual is challenging because gait patterns are unique among different individuals and individual responses to a given AFO are difficult to predict [52].

Many studies have shown AFOs can alter gait kinematics and kinetics. For example, AFOs can improve temporal-spatial gait characteristics by increasing stride length, step length, and gait velocity [53-55]. Other studies have reported that AFOs do not improve or can even aggravate pathologic gait patterns. For instance, one study reported decreased gait velocity with articulated AFOs and rigid AFOs compared to barefoot walking [56], while another study reported that rigid AFOs increased double limb support time [57]. Rigid AFOs, articulated AFOs, and PLS AFOs have been shown to reduce cadence compared to walking without AFOs for some individuals [58]. PLS AFOs mechanically contribute to improved gait patterns by

creating additional plantarflexion moment during terminal stance [59,60]. AFOs can also reduce the tibialis anterior activation [61,62] and metabolic cost [63,64].

Along with selecting a specific type of AFO, there are some parameters that can be tuned such as adjusting shank-to-vertical angle (SVA, figure 4) and stiffness in the sagittal plane. These parameters affect not only gait kinematics and kinetics but can also influence muscle function. To adjust SVA, wedges of different heights are attached on the bottom of the AFOs to make the shank slightly inclined to the ground, which can enable more normal gait kinematics by adjusting the heel contact at gait initiation (Fig. 3). Adjusting SVA has the potential to effectively correct and accommodate tight or contracted gastrocnemius [65,66] and help prevent knee recurvatum [67]. On the other hand, AFOs with wedges do not contribute to increasing the stride length or the moments at the knee and ankle [68].

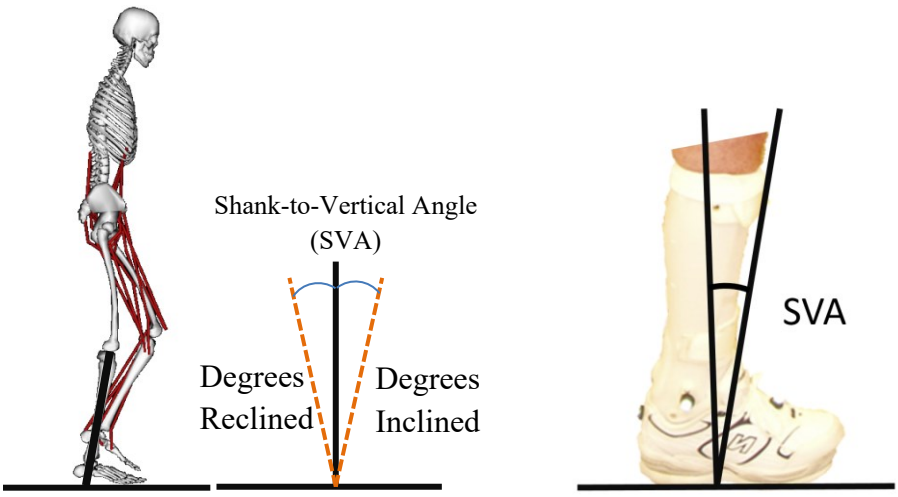

Figure 3. Shank-to-vertical angle (SVA). SVA is defined as being either reclined or inclined during standing. SVA can be adjusted using a wedge on the bottom of the shoe (right).

Gait kinematics and kinetics can change in response to AFO stiffness. Gök et al. suggested that stiffer AFOs which were made of metal, contributed to better walking speed, step

length, ankle dorsiflexion moments and reduced knee flexion moment compared to less stiff AFOs made of plastic [69]. Stiffness level alters the AFO's contribution to the total plantarflexion moment during terminal stance; however, the level of contribution is not proportional to stiffness level [52]. There is evidence that neuromuscular control of ankle plantarflexors and dorsiflexors change in response to AFO stiffness, specifically the excitation level of the soleus has been shown to not be proportional to stiffness level [70]. While ambulation energy cost could potentially be minimized with an optimal AFO stiffness, prior research has suggested that this stiffness is not concurrent with the stiffness level that maximizes energy storage [71].

AFOs are clearly beneficial to individuals with neuromuscular injuries, but a greater understanding of the underlying mechanisms by which AFOs contribute to improved gait and impact pathologic muscle function is required to determine the optimal AFO prescription for each individual. Considering that even children with Gross Motor Function Classification System (GMFCS) Level III still take over one thousand steps per day [72], quantifying muscle function and impact of AFOs on daily life is crucial. For example, if AFOs can stretch affected muscles during ambulation for individuals with neurological disorders, these AFOs can be utilized as a rehabilitation tool for repetitive stretching that may increase gastrocnemius fascicle length and reduce passive force for individuals with CP [73]. Therefore, optimally tuned AFOs may improve gait patterns and enable AFOs to be used as a supplement to traditional stretching and physical therapy.

Musculoskeletal Modeling

Understanding and quantifying muscle function with AFOs not only allows us to better understand mechanisms that may contribute to pathologic gait, but also provide crucial insight into how to optimally prescribe customized AFOs, pharmaceutical prescriptions, and surgical treatments. The human musculoskeletal system is extremely complex, which makes determining the effects of treatments such as AFOs on muscle function and pathologic motion challenging. For example, biarticular muscles cross two joints and have multiple attachment points on each bone segment thus, evaluating these biarticular muscle is particularly difficult. Musculoskeletal modeling and simulation has recently provided new tools to quantify how muscles contribute to pathologic motion. OpenSim, an open-source 3D musculoskeletal modeling and simulation software, lets users analyze the dynamics of human movement [74,75].

Musculoskeletal modeling has been used to evaluate pathologic gait patterns [76]. For example, prior research has examined how different muscles contribute to accelerating the body during crouch gait [77,78] and stiff-knee gait compared to unimpaired individuals [79,80]. Simulation can also be used to evaluate the impact of different factors like muscle strength. A prior musculoskeletal simulation study demonstrated that crouch gait reduces the capacity of many lower-extremity muscles to extend the hip and knee [81].

Musculoskeletal modelling has also been used to calculate musculotendon lengths for individuals with CP. Limited musculotendon operating lengths and muscle moment arms due to bone deformities (altered bone geometry) in individuals with CP can be key factors contributing to pathologic gait patterns. For example, tight hamstrings due to spasticity and contracture were thought to cause crouch gait, and crouch gait was often treated with hamstring lengthening

surgery. Arnold et al. showed individuals with CP and crouch gait had shorter semitendinosus and psoas operating lengths compared to unimpaired gait, potentially contributing to crouch gait [82]. She also demonstrated that key muscles such as the hamstrings, adductor brevis, adductor longus and gracilis had an external rotation moment arm or very small internal rotation moment arms during pathologic gait [83]. However, even though hamstring lengthening surgery often improved excessive knee flexion during gait, it also could lead to decreased knee flexion during swing, increased hip flexion during stance, or increased anterior pelvic tilt [84-86]. The majority of individuals with CP and crouch gait did not have short hamstrings operating length, but rather had normal or longer hamstrings length compared to unimpaired individuals [87]. Arnold et al further used a musculoskeletal model to combine hamstring lengths and lengthening velocities with gait kinematics for individuals with CP who have crouch gait. Her results suggested that individuals with CP who walked with short hamstring lengths or slow lengthening velocity preoperatively, and individuals whose hamstrings had short operating lengths with normal musculotendon length or faster lengthening velocity postoperatively, were both unlikely to improve knee extension from hamstring surgery [88]. Similar methods have also been used to evaluate the impact of AFOs during gait. Thompson et al utilized musculoskeletal modeling and demonstrated that rigid AFOs increased peak hamstring operating length in with children with CP [89].

Musculoskeletal modeling has limitations. In particular, these methods often use muscle properties obtained from unimpaired individuals, which may be very different from those of individuals with CP. Further, while modeling can be used to quantify the overall musculotendon operating length, it is challenging to quantify the relative changes in length of the muscle and tendon, independently. To achieve better simulation outcomes, pathologic muscle structure such

as fascicle length, pennation angle, muscle length, and tendon length should be quantified and integrated with experimental techniques like ultrasonography to better understand muscle function.

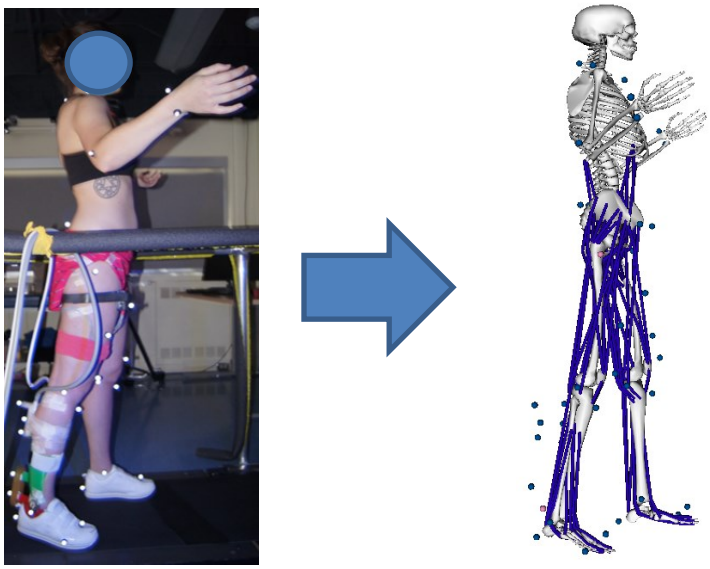

Figure 4. Musculoskeletal model.
Based on experimental marker position on the participant, a musculoskeletal model can be scaled and used to perform inverse kinematics which calculates joint angles. The musculoskeletal model used in Aim 4 of this research consists of 37 degrees of freedom and 92 muscle actuators, including the lower extremities [74] and upper extremities [75]. The degrees of freedom in the model included a ball-and-socket joint at each shoulder, a hinge joint at each elbow, a combination of saddle joint and condyloid joint at each wrist, three translations and three rotations of the pelvis, a ball and socket joint between the pelvis and the torso located at the third lumbar vertebrae, a ball-and-socket joint at each hip, a combination joint of translations and rotations at each knee, and a revolute joint at each ankle.

Ultrasonography

Ultrasound is defined as a high-frequency sound wave that humans cannot hear; the range of frequencies humans hear is 20 to 20,000 Hz with ultrasound frequency above 20,000 Hz. Ultrasonography is a diagnostic imaging technique which utilizes ultrasound ranging between 1 MHz and 30 MHz. Ultrasound waves are produced by a piezoelectric transducer which converts electric current into mechanical sound waves. The transducer should have an identical acoustic impedance to that of the human body, high permittivity, wide dynamic range and frequency response for pulse operation, high efficiency as a transmitter, and a high sensitivity receiver. The lead zirconate titanate (PZT) transducer satisfies these characteristics and has been widely used for clinical purposes [90]. Ultrasonography operates in the following way: First, activating a transducer transmit pulser, $P(t)$, in order to transform electric signals into ultrasound waves and then transmitting the ultrasound wave signals into the human body. Second, detecting reflected ultrasound wave signals with the transducer. Next, the transducer transforms the ultrasound wave signal into electric signals. Finally, the transformed electric signals is processed with the signal processor to display on a monitor [91] (Fig. 5).

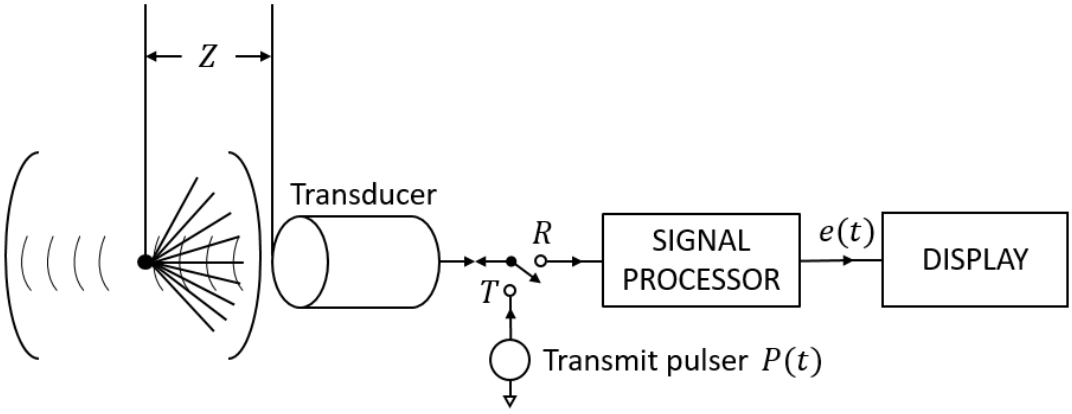

Figure 5. Block diagram of ultrasonography

Medical imaging such as X-ray, computed tomography (CT), magnetic resonance imaging (MRI), and ultrasonography are non-invasive which is beneficial to examine human internal structures, such as muscle. Each method has pros and cons for examining different structures in the human body. For example, individuals are exposed to radiation when subjected to X-ray and computed tomography. MRI supports high resolution images, but it has limitations to acquire real-time images and is very expensive compared to the other imaging methods. Ultrasonography is not only one of the least expensive imaging modalities but also the only method which can currently be used while a person is walking. Ultrasonography supports real-time measurement, but the images have a low resolution relative to CT and MRI. Image processing techniques and hardware developments make ultrasonography reliable and has, thus, contributed to many studies on changes in pathologic muscle morphologies. For example, changes in muscle architecture and contractile performance have been studied with ultrasonography for older adults who have sarcopenia [92]. Ultrasonography has also been utilized to study differences in muscle morphologies. For example, quadriceps femoris and longissimus muscle thickness is significantly different according to Gross Motor Functional Classification System Level [93] for children with CP. Prior research with ultrasonography has also demonstrated that gastrocnemius fascicle length, muscle thickness, muscle length, and muscle volume in the paretic limb are reduced compared to the non-paretic limb in individuals with hemiplegic CP [94,95].

This dissertation evaluates how tuning AFO parameters impacts gastrocnemius function and gait kinematics. The first aim evaluated how tuning the SVA influence gastrocnemius operating length and gait kinematics of an individual with stroke. The second aim evaluates how different types of AFOs alter gastrocnemius operating length and gait kinematics in children with

CP, including five children with mild involvement and six children with more severe involvement. In order to evaluate muscle function and gait kinematics with respect to different AFO properties, the third aim introduces a flexible research platform which can incorporate sensors, such as ultrasound, into AFOs with variable stiffness fabricating using 3D printing and scanning technology. The fourth aim demonstrates how different AFO stiffness impacts gait kinematics and gastrocnemius function with the variable stiffness AFOs during unimpaired gait.

AIM 1: USING MUSCULOSKELETAL MODELING TO EVALUATE THE EFFECT OF ANKLE FOOT ORTHOSIS TUNING ON MUSCULOTENDON DYNAMICS: A CASE STUDY

Published in: Hwan Choi, Kristie Bjornson, Stefania Fatone, Katherine M. Steele. Disability and Rehabilitation: Assistive Technology, 2015, **11**(7) pp. 613-8. DOI: 10.3109/17483107.2015.1005030

1.1 Abstract

This case study examines the influence of an Ankle Foot Orthosis Footwear Combination (AFO-FC) on musculotendon lengths and gait kinematics and kinetics after right thrombotic stroke resulting in left hemiplegia. Gait analysis was performed over three visits where the participant walked with an AFO-FC with two shank-to-vertical angle (SVA) alignments, a posterior leaf spring AFO (PLS AFO), and shoes alone. Biomechanical and musculoskeletal modeling was used to evaluate musculotendon lengths, kinematics, and kinetics for each condition. The AFO-FC improved walking speed and non-paretic kinematics compared to the PLS AFO and shoes alone. The operating length of the paretic gastrocnemius decreased with the AFO-FC improving knee kinematics in swing, but not stance. As the SVA of the AFO-FC was reduced from 15˚ to 12˚, internal ankle plantarflexor moment increased. Musculoskeletal modeling demonstrated that the AFO-FC altered gastrocnemius operating length during post-stroke hemiplegic gait. Using these tools to evaluate muscle operating lengths can provide insight into underlying mechanisms that may improve gait and guide future AFO-FC design.

This study was published in Disabil and Rehabil: Assist Technol 2015. ***11****(7): pp.613-8.*

1.2 Background

Stroke negatively affects mobility with 50% of stroke survivors achieving only a limited level of functional ambulation [96]. To achieve better outcomes we need an improved understanding of the mechanisms that hinder mobility and better methods for prescribing and optimizing function of assistive devices. Ankle Foot Orthoses (AFOs) are an assistive device commonly used to improve gait after stroke, with many designs available to provide support and alignment, compensate for muscle weakness, and help prevent secondary musculoskeletal deformities. Recently, Ankle Foot Orthosis Footwear Combinations (AFO-FCs) have been suggested to improve gait for individuals with neuromuscular problems [97–101]. AFO-FCs comprise a rigid, non-articulated AFO set at an ankle angle (AA) predicated on muscle length [102], a shank-to-vertical angle (SVA) modified by intrinsic or extrinsic heel wedges to center the knee over the middle of the foot during mid-stance [103], and footwear modified to allow stance phase roll-over given restriction of ankle and possibly metatarsophalangeal joint motion [104]. By dynamically adjusting the SVA and rocker profile of the footwear, orthotists can "tune" the sagittal plane orientation of the vertical ground reaction force vector with respect to the knee and hip during terminal stance and pre-swing [67,97]. Tuning an AFO-FC was previously shown to improve walking speed, knee kinematics, and knee pain in an individual after stroke [105] and walking speed, step length and cadence in eight individuals after stroke [98].

The efficacy of AFO-FCs is thought to be related to musculotendon dynamics during gait [67]; however, the impact of AFO-FCs on muscle function during gait remains unclear. Contracture, spasticity, and increased muscle tone are common after stroke and can contribute to pathologic gait patterns [106]. For example, contracture or spasticity of the gastrocnemius, which crosses both the knee and ankle, may contribute to reduced push-off in terminal stance, excessive

knee flexion in stance, and inadequate knee flexion in swing [77,107]. If the gastrocnemius is too tight to achieve full knee extension and the 10-20 degrees of ankle dorsiflexion required during terminal stance, compensations such as increasing ankle plantar flexion or knee flexion must occur. Tuning an AFO-FC to reduce the operating length of the gastrocnemius during gait may help to reduce the effect of contracture and spasticity on these abnormal kinematics, but the impact of AFO-FCs on musculotendon operating lengths has not been previously investigated.

A muscle's operating length is defined as the length of the muscle-tendon unit from origin to insertion during movement. Estimating a muscle's operating length requires knowledge of not only joint angles, but also musculoskeletal geometry such as segment length, muscle moment arms, and musculotendon paths. Thus, estimating a muscle's operating length during movements such as walking is challenging, especially for bi-articular muscles like the gastrocnemius. Recent advances in musculoskeletal modeling and simulation have created detailed models of the musculoskeletal system that can be used to estimate muscle operating lengths [74]. For example, musculoskeletal modeling has been used to evaluate the length of the hamstrings during crouch gait, a common gait pathology among children with cerebral palsy, and has been used to predict surgical outcomes after hamstring lengthening [88,108]. It is thought that orthotists can adjust AFOs to alter the operating length of the gastrocnemius and other muscles during gait [109], so understanding how musculotendon operating lengths change with AFO-FCs may improve orthotic prescription, design, and tuning.

This case study evaluated whether tuning an AFO-FC altered musculotendon operating lengths and contributed to improved kinematics during gait. We evaluated a participant with left hemiplegia post-stroke who presented with gastrocnemius contracture and a stiff-knee gait. Evaluations were conducted over three visits while walking with shoes alone, a posterior leaf

spring AFO (PLS AFO), and an AFO-FC with two shank-to-vertical angles. We hypothesized that the AFO-FC would decrease gastrocnemius operating length and improve knee kinematics during gait.

1.3 Methods

Participant

A 56 year old male (height = 190 cm, weight = 88.5 kg) who sustained a right middle cerebral artery injury with subsequent left hemiplegia was first evaluated using instrumented gait analysis eleven months post-stroke. Clinical exam indicated that the participant had restricted passive ankle range of motion on the left due to gastrocnemius shortening: 10˚ dorsiflexion (knee at 90˚ flexion) and 5˚ plantarflexion (knee at 0˚). The left knee also had 5˚ hyperextension. The university's Institutional Review Board approved this study and written informed consent was obtained from the participant prior to participation.

Orthotic Conditions

The participant visited the motion analysis laboratory on three occasions. As part of his preceding clinical care the participant had been provided an off-the-shelf polypropylene PLS AFO. At the first visit (11 months post-stroke), his gait was assessed with the PLS AFO. The participant was also fitted with a custom polypropylene AFO-FC with an ankle angle of 8˚ plantarflexion (based on passive ankle range of motion with the knee extended) and an SVA of 15˚ after tuning (Fig. 6). The AFO-FC was tuned by a certified orthotist with over 20 years of experience in the orthotic management of individuals post-stroke. The participant wore this AFO-FC full-time for 5 months

between the first and second visit. At the second visit (16 months post-stroke), the participant's gait was evaluated with the same AFO-FC.

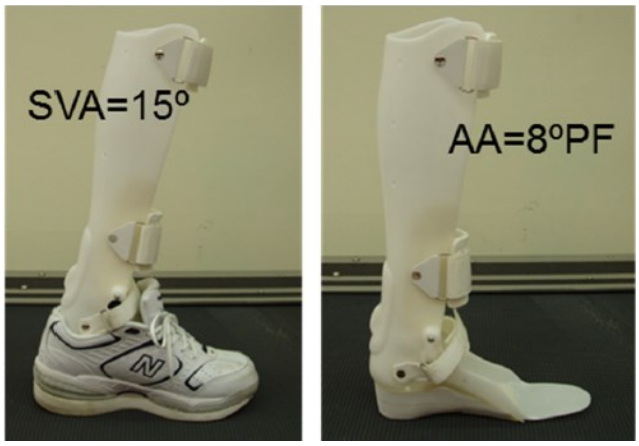

Figure 6. Alignment of the AFO-FC. Ankle Angle (AA) set at 8° plantarflexion and SVA of 15° inclination when the orthosis is placed inside a modified shoe.

Based upon this analysis, the AFO-FC was adjusted (*i.e.,* re-tuned) by the same orthotist, reducing the SVA from 15˚ to 12˚ by removing material from beneath the heel of the shoe. This was done to improve the sagittal plane orientation of the vertical ground reaction force vector with respect to the knee joint such that greater knee extension might be achieved in terminal stance. The participant returned 1 month later (17 months post-stroke) to evaluate the re-tuned AFO-FC, which was worn full-time during the intervening month. During this final visit, the participant's gait was also evaluated with shoes alone to determine if gait had changed due to recovery compared to the initial visit. The participant walked with a quad cane when using the PLS AFO and shoes alone but ambulated without an assistive device when the AFO-FC was worn. At the first visit, the participant refused to walk with shoes alone, which is why the PLS AFO was used as the comparison condition. At the final visit, the participant agreed to walk with shoes alone, suggesting some level of recovery and improvement in comfort and confidence in walking without AFOs. Unfortunately, the PLS AFO was no longer available for testing at the final visit.

Gait Analysis

An eight-camera real-time motion capture system (Motion Analysis Corporation, Santa Rosa, CA) was used to acquire three-dimensional marker data at 120 Hz. Markers were placed on the participant by the same investigator for all analyses based on a modified Helen-Hayes marker set [110]. Ground reaction forces were acquired at 960 Hz using six force plates (Advanced Mechanical Technology Inc., Watertown, MA).

Musculoskeletal Modeling

OpenSim, an open-source musculoskeletal modeling and simulation software platform [74], was used to calculate gait kinematics and estimate musculotendon lengths. A generic musculoskeletal model with 19 degrees of freedom and 92 muscles [74] was scaled to the participant based upon anatomical landmarks. For each trial, inverse kinematics was used to calculate joint angles, minimizing the distance between the three-dimensional marker trajectories from gait analysis and virtual markers placed on the model.

Musculotendon operating lengths of major lower-limb muscles were calculated from the distance of each muscle's path from origin to insertion during the gait cycle. Muscle paths are based upon cadaveric and imaging data and have previously been used to evaluate muscle lengths and velocities in unimpaired individuals and individuals with neurologic disorders [88]. To facilitate comparison with unimpaired individuals, musculotendon lengths were normalized by the length of each muscle with the hip, knee, and ankle joints in anatomic position. The maximum operating length of the gastrocnemius was also estimated by calculating the length of the gastrocnemius with the knee in full extension and the ankle dorsiflexed to the maximum angle measured during the clinical exam. Joint kinetics were calculated using inverse dynamics. Joint

kinematics, kinetics, and musculotendon operating lengths were normalized to 101 points for each gait cycle and averaged over a minimum of 9 gait cycles for each condition.

Musculotendon operating lengths have previously been shown to be dependent on walking speed [112]. Hence, results were compared to previously collected kinematics and musculotendon lengths of a group of unimpaired participants walking at very slow speeds (N=8, data available at: https://simtk.org/home/mspeedwalksims) [113].

1.4 Results

Compared to unimpaired individuals, the participant walked with inadequate hip extension, excessive stance phase knee flexion, reduced stance phase ankle dorsiflexion, and reduced swing phase knee flexion on the paretic side when wearing shoes alone or the PLS AFO (Figs. 7 A, B, C). On the non-paretic side, hip, knee, and ankle kinematics were also abnormal with shoes alone and PLS AFO, with a prolonged support time (Figs. 7 D, E, F). For the same conditions (shoes alone and PLS AFO), the paretic side hamstrings operated at near normal maximum length at initial contact (Fig. 8 A, solid and dotted gray lines) while paretic side gastrocnemius length (Fig. 8 B, solid and dotted gray lines) was reduced during stance compared to unimpaired gait. Maximum paretic side gastrocnemius length in terminal stance was similar to the maximum length measured during passive ankle dorsiflexion in the clinical exam (Fig. 8 B, red horizontal line).

Paretic limb kinematics at the hip, knee and ankle improved with the AFO-FC at the second and third visits (Figs. 7 A, B, C). The AFO-FC reduced support time and improved joint motion on the non-paretic side compared to gait with shoes alone and the PLS AFO. At the second visit, the AFO-FC with SVA of 15˚ reduced toe-off time from 88% to 76% of the gait cycle on the non-

paretic side and 77% to 61% of the gait cycle on the paretic side. Knee range of motion remained less than unimpaired gait, but improved from 19.3 ˚ and 13.4 ˚ with shoes alone and the PLS AFO, respectively, to 26.1˚ in the AFO-FC with SVA of 12˚ at the final visit.

Musculotendon operating lengths and joint moments on the paretic side were altered with the AFO-FCs (Figs. 8 A, B, C). In contrast to the shoes alone and PLS AFO conditions, the medial gastrocnemius did not exceed the maximum passive gastrocnemius length with the AFO-FCs because of the fixed plantarflexion angle. Although gastrocnemius operating length was reduced, paretic side knee extension during stance did not improve with the AFO-FCs (Fig. 7 B, solid and dotted black lines). However, changing the AFO-FC's SVA from 15 ˚ to 12 ˚ improved knee flexion during swing. Knee flexion during swing increased from 30.4˚ to 36.5˚ after re-tuning the AFO-FC. Hip flexion at heel contact improved from 14.1˚ to 18.8˚ with the retuned AFO-FC, but overall range of motion decreased. Reducing the AFO-FC's SVA from 15 ˚ to 12 ˚ also increased the internal ankle plantarflexor moment and decreased the internal knee extensor moment during terminal stance, helping to decrease the stiff-knee gait pattern.

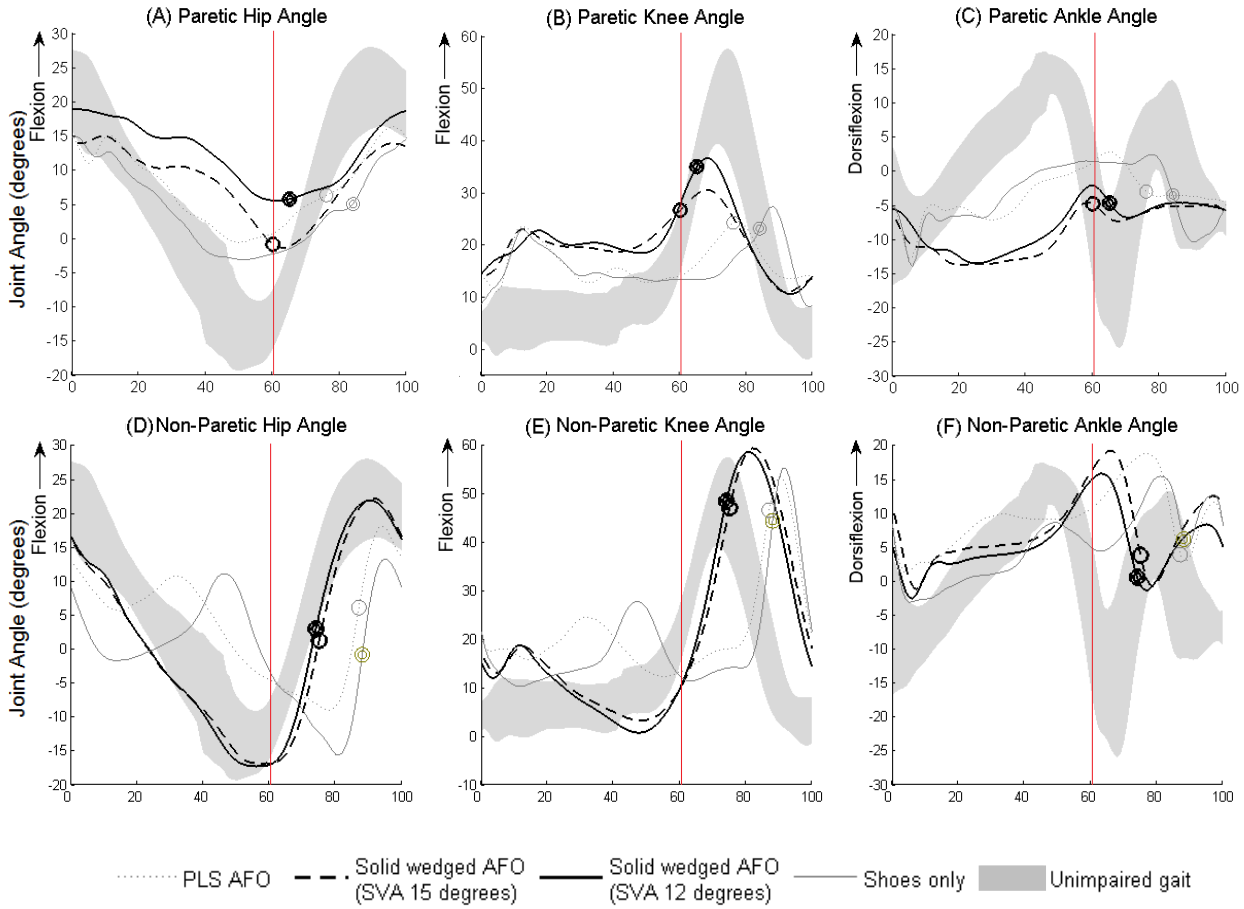

Figure 7. Sagittal plane gait kinematics with two different type AFO-FC, PLS AFO, and barefoot walking.

Average sagittal plane kinematics at the hip, knee, and ankle of the non-paretic and paretic sides with shoes alone (solid gray lines), PLS AFO (dotted gray lines), AFO-FC with 15˚ SVA (dotted black line) and AFO-FC with 12˚ SVA (solid black lines) normalized to one gait cycle. The gray shaded band depicts the average ± one standard deviation of unimpaired gait at very slow speeds. Circles and vertical lines indicate toe-off for each condition for the participant with stroke and unimpaired individuals, respectively. Positive values of hip and knee angles are flexion and positive values of ankle angle are dorsiflexion.

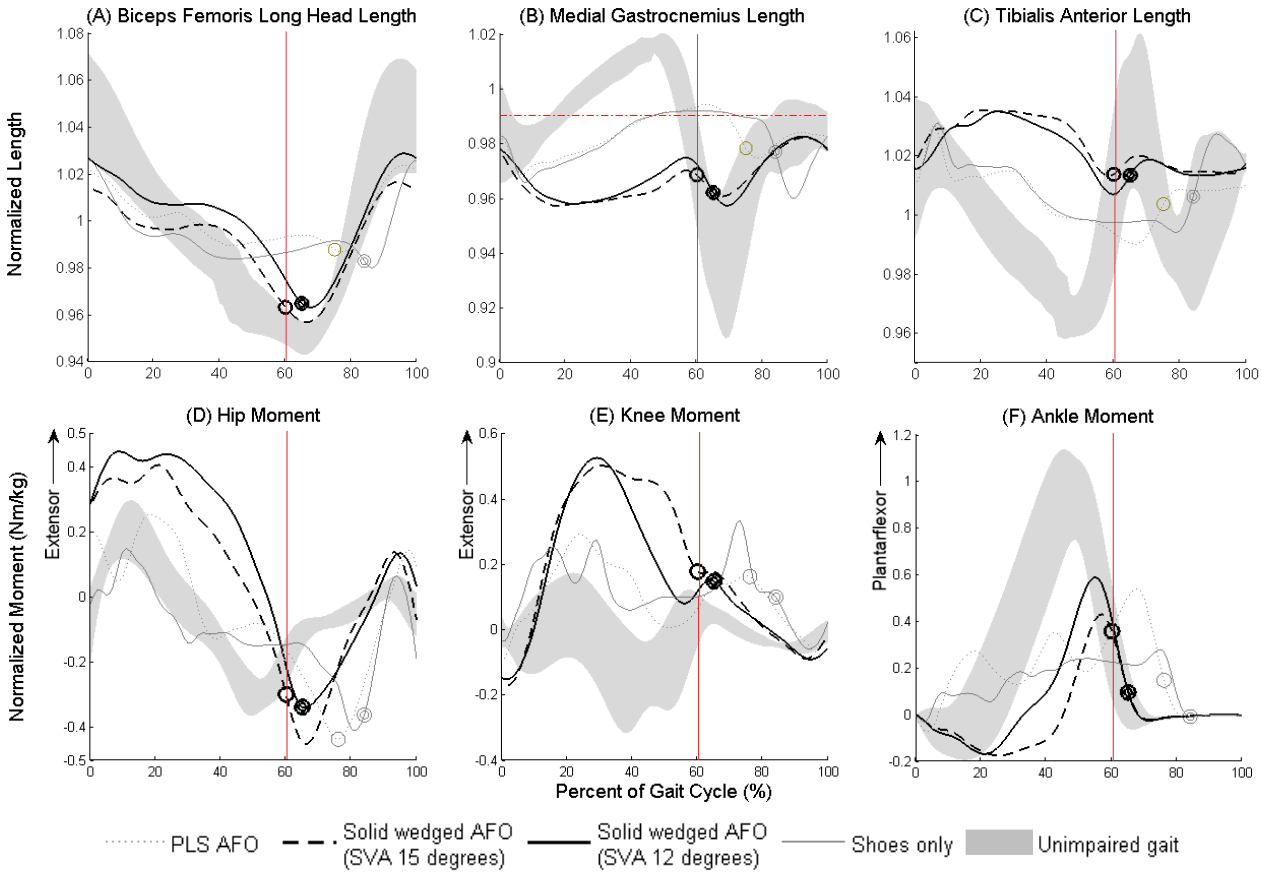

Figure 8. Musculotendon operating length with two different type AFO-FC, PLS AFO, and barefoot walking.

Average musculotendon operating length on the paretic side for the biceps femoris long head (A), medial gastrocnemius (B), and tibialis anterior (C) during trials with shoes alone (solid gray line), PLS AFO (dotted gray line), AFO-FC with SVA of 15˚ (dotted black line), and AFO-FC with SVA of 12˚ (solid black line) normalized to one gait cycle. The gray shaded band depicts the average ± one standard deviation of musculotendon operating lengths during very slow unimpaired gait. Circles and vertical lines indicate toe-off for each condition for the participant with stroke and unimpaired individuals, respectively. The horizontal red dotted line in (B) depicts gastrocnemius length at maximum ankle dorsiflexion with the knee extended from the clinical exam. Musculotendon lengths were normalized by the length of each muscle in the anatomic position. Also shown are average sagittal plane internal joint moments at the hip (D), knee (E), and ankle (F) of the paretic side with shoes alone (solid gray lines), PLS AFO (dotted gray lines), AFO-FC with 15˚ SVA (dotted black line) and AFO-FC with 12˚ SVA (solid black lines) normalized to one gait cycle.

Walking speed was also significantly improved with the AFO-FC. The participant's speed was 0.20 and 0.26 m/s (0.07 and 0.09 nondimensional velocity) with the shoes alone and PLS AFO, respectively. With the initial AFO-FC, the speed was 0.59 m/s (0.21 nondimensional

velocity) and improved to 0.66 m/s (0.24 nondimensional velocity) when the AFO-FC was re-tuned to an SVA of 12˚. However, these speeds are still substantially less than the unimpaired participants' very slow speed, which had an average nondimensionalized velocity of 0.54 ± 0.04 (Table 1).

Table 1. Temporal-spatial and kinematic changes in gait with each condition.
*The nondimensional velocity normalizes walking velocity by $\sqrt{\boldsymbol{g} * \boldsymbol{L_{leg}}}$. Where $\boldsymbol{g}$ is gravity and $\boldsymbol{L_{leg}}$ is participant leg length. PLS AFO=posterior leaf spring ankle foot orthosis; AFO-FC= ankle foot orthosis-footwear combination; SVA=shank-to-vertical angle.

	First visit (11 months post-stroke)	Second visit (16 months post-stroke)	Third visit (17 months post-stroke)	
	PLS AFO	AFO-FC (SVA 15˚)	AFO-FC (SVA 12˚)	Shoe only
Stride Length (cm)	45.5	72.8	76.0	47.3
Nondimensional Velocity*	0.09	0.21	0.24	0.07
Walking Speed (meters/sec)	0.26	0.59	0.66	0.20
Cadence (steps/min)	68.8	98.0	104.2	50.1
Step Width (cm)	27.7	23.7	23.7	32.8
Paretic Toe Off Time (%)	77	61	66	85
Paretic Hip Range of Motion (˚)	17	16.4	13.4	18.1
Paretic Knee Range of Motion (˚)	13.4	19.7	26.1	19.3
Paretic Ankle Range of Motion (˚)	15.7	9.2	11.4	16.4

1.5 Discussion

In this case study, we used musculoskeletal modeling to evaluate the influence of AFO-FCs on musculotendon lengths and gait kinematics and kinetics. Our results indicate that the AFO-FC reduced gastrocnemius operating length during gait and improved walking speed, stiff-knee gait, and non-paretic limb kinematics compared to both shoes alone and a PLS AFO. Since the PLS

AFO was not retested on the participant at the end of the study, we cannot rule out the possibility that some of the improvement seen in the AFO-FC conditions were the result of motor recovery over time and that further improvements in gait with the PLS AFO may have also been achieved at the final visit. However, stance phase kinematics were highly similar between walking with shoes alone and PLS AFO, suggesting that the PLS AFO had minimal effects on gait kinematics and the participant used a similar gait pattern without AFO-FCs at the initial visit (11 months after stroke) and final visit (17 months after stroke). Given that PLS AFOs are designed primarily to assist swing phase ankle alignment, this similarity was unsurprising.

We had hypothesized that a shortened gastrocnemius was contributing to impaired knee motion and that reducing gastrocnemius operating length during gait with an AFO-FC would improve knee kinematics. Our hypothesis was partially supported by our results: we demonstrated that the gastrocnemius was operating at its maximum length during gait with the PLS AFO and shoes alone; while the AFO-FC reduced gastrocnemius operating length and knee kinematics improved in swing, but not stance.

Sagittal plane joint moments provide insight into the mechanisms underlying changes in knee kinematics. First, since gastrocnemius operating length was reduced throughout the gait cycle to below the participant's maximum length based on clinical exam, a shortened gastrocnemius no longer contributed to inadequate dorsiflexion or excessive knee flexion in stance. However, reducing the effect of a stiff/shortened gastrocnemius does not directly translate to improved knee kinematics. In swing, maximum knee flexion is largely dependent upon ankle and knee moments in terminal stance. With the AFO-FCs, the participant had greater internal ankle plantarflexor and knee extensor moments in terminal stance than with shoes alone (Figs. 9 E and F), which helped improve knee flexion in swing. With the initial AFO-FC (SVA of 15˚), the internal ankle

plantarflexor moment increased in terminal stance, but there was also an excessive internal knee extensor moment. Reducing the SVA from 15˚ to 12˚ shifted the orientation of the ground reaction force such that the internal ankle plantar flexor moment increased and the internal knee extensor moment decreased, improving knee flexion in swing [114]. This demonstrates the importance of tuning the SVA of AFO-FCs and that even a small change in SVA can have a dramatic effect on knee kinetics.

In stance, knee extension did not improve with the AFO-FCs, even though the gastrocnemius operating length was reduced. With shoes and the PLS AFO, the gastrocnemius was operating at its maximum length and likely contributed to inadequate ankle dorsiflexion and knee extension. While, the AFO-FC dramatically changed the dynamics of the ankle joint, a reduced gastrocnemius operating length did not translate to improved ankle and knee kinematics in stance. In unimpaired gait, the ankle plantarflexors play an important role in helping to extend the knee through dynamic coupling: the ankle plantarflexion-knee extension couple [114, 115]. In an AFO-FC the ankle is held rigid and the ankle plantarflexor muscles can no longer contribute to knee extension acceleration. Furthermore, as SVA increases, the forward tilt of the shank causes greater knee flexion and increases the internal knee extensor moment required to maintain a stable posture. Additionally, increasing SVA shortens the foot lever, similar to high heels, creating a smaller effective moment arm about the ankle [116]. These changes highlight the complex, interacting factors that must be considered when tuning orthoses.

This case study illustrates how musculoskeletal modeling can be used to evaluate the role of individual muscles during walking, informing orthotic design to improve gait. We quantified changes in musculotendon lengths, kinematics, and kinetics when wearing an AFO-FC. The AFO-FC reduced gastrocnemius length but did not improve knee extension in stance compared to shoes

alone and the PLS AFO. However, overall gait improved with the AFO-FC, including faster walking speed and reduced stiff-knee gait. Further studies are needed to determine if changes in gastrocnemius operating length and effects on joint moments during gait are consistent across multiple participant s and evaluate differences between orthotic designs. We believe that finding the balance between optimizing musculotendon operating lengths and lower extremity joint moments can help improve orthotic designs.

AIM 2: GASTROCNEMIUS OPERATING LENGTH WITH ANKLE FOOT ORTHOSES IN CEREBRAL PALSY

Published in: Hwan Choi, Tishya A.L. Wren, and Katherine M. Steele. Prosthetics and Orthotics International, 2016. DOI: 10.3109/17483107.2015.1005030

2.1 Abstract

Many individuals with cerebral palsy wear ankle foot orthoses during daily life. Orthoses influence joint motion, but how they impact muscle remains unclear. In particular, the gastrocnemius is commonly stiff in cerebral palsy. Understanding whether orthoses stretch or shorten this muscle during daily life may inform orthosis design and rehabilitation. This study investigated the impact of different ankle foot orthoses (AFOs) on gastrocnemius operating length during walking in children with cerebral palsy. We performed gait analyses for eleven children with cerebral palsy. Each child was fit with two types of orthoses: a dynamic ankle foot orthosis (Cascade DAFOs) and an adjustable dynamic response ankle foot orthosis (Ultraflex AFOs). Musculoskeletal modeling was used to quantify gastrocnemius musculotendon operating length and velocity with each orthosis. Walking with AFOs could stretch the gastrocnemius more than barefoot walking for some individuals; however, there was significant variability between participants and orthoses. At least one type of orthosis stretched the gastrocnemius during walking for 4/6 and 3/5 of the Gross Motor Functional Classification System (GMFCS) Levels I and III participants, respectively. AFOs also reduced peak gastrocnemius lengthening velocity compared to barefoot walking for some participants, with greater reductions among the GMFCS Level III participants. Changes in gastrocnemius operating length and lengthening velocity were related to changes in ankle and knee kinematics during gait. AFOs impact gastrocnemius operating length during walking and, with proper design, may assist with stretching tight muscles in daily life. Determining whether ankle

foot orthoses dynamic stretching tight muscles can inform future orthotic design and potentially provide a platform for integrating therapy into daily life. However, stretching tight muscles must be balanced with other goals of orthoses such as improving gait and preventing bone deformities.

This study was published in Prosthet and Orthot Int. 2016

2.1 Background

Ankle foot orthoses (AFOs) are commonly used to improve ambulation for individuals with cerebral palsy (CP). Many types of AFOs are available and are prescribed for different gait patterns and musculoskeletal deformities. AFOs are designed to improve gait, reduce energy costs, prevent bone deformities, provide stability, and achieve other patient-specific goals [54-56,58,117-120]. The majority of these goals focus on improving function and prior research has indicated that, if properly prescribed, AFOs can improve gait and other activities of daily living [120]. Since AFOs are worn daily, this research also suggests that AFOs may provide a tool for extending therapy and rehabilitation into daily life.

CP is caused by a brain injury at or near the time of birth [121]; however, secondary musculoskeletal impairments, such as bone deformities, contracture, and weakness commonly develop [122]. AFOs have been designed to help prevent bone deformities [123], but their impact on muscle is not as well understood. In particular, the gastrocnemius is a complex multi-articular muscle, which is commonly impaired among individuals with CP and may be influenced by AFO prescriptions [124,125]. Stretching has commonly been prescribed for individuals with CP, and repetitive stretching has been shown to increase gastrocnemius fascicle length and reduce passive force [73]. Since muscles adapt to the stretched or shortened positions experienced during daily life, understanding how AFOs influence gastrocnemius length could be important for optimizing

AFOs. If an AFO can stretch the gastrocnemius with every step, AFOs may help prevent contracture and improve long-term muscle function. Conversely, if an AFO decreases the gastrocnemius operating length it may further exacerbate contracture.

Musculotendon operating length is defined as the length of the muscle-tendon unit from origin to insertion during movement. Prior studies have indicated that individuals with CP often have a shortened gastrocnemius operating length compared to unimpaired individuals, which can contribute to excessive ankle plantarflexion and knee flexion in stance [126,127]. Spasticity, defined as a velocity-dependent resistance to stretch [128], is also common in individuals with CP and can contribute to increased ankle plantarflexion during gait [130]. However, quantifying musculotendon operating length and velocity during movement can be challenging because it requires information about an individuals' joint kinematics, musculoskeletal geometry, moment arms, and muscle paths. Gait analysis and musculoskeletal modeling can be used to quantify these parameters and estimate musculotendon operating length and velocity [74]. For example, musculoskeletal modeling has been used to evaluate hamstring operating length and velocity during crouch gait of children and adolescents with CP. These studies have demonstrated that hamstring operating length and velocity are related to outcomes after surgery and can be used for treatment planning [88,108]. A prior study also evaluated the impact of AFOs on hamstring operating length and demonstrated increased operating lengths with rigid AFOs compared to barefoot walking [89]. In a case study of an adult stroke survivor, a rigid AFO was also shown to decrease the operating length of the gastrocnemius during gait compared to barefoot walking [125]. Musculoskeletal modeling has also shown that, in CP, gastrocnemius length and velocity differ in children with spasticity and are dependent on walking speed [131]. Evaluating the impact

of AFOs on musculotendon operating lengths and velocities may have important implications for rehabilitation and long-term use of AFOs.

The goal of this study was to evaluate how AFOs impact gastrocnemius musculotendon operating length and velocity during gait among children with CP. We evaluated gastrocnemius operating length and velocity for each individual with two different types of AFOs: Cascade Dynamic AFOs (DAFOs) and Ultraflex Adjustable Dynamic Response AFOs (ADR AFOs). We sought to determine if currently available AFOs and prescription procedures tend to stretch or shorten the gastrocnemius during gait compared to barefoot walking and whether responses are dependent upon impairment level or type of AFO.

2.2 Methods

This study reports a secondary analysis of data from a trial comparing two types of AFOs and barefoot walking in children with CP. Details and results of the main study appear in a previous publication [132]. The current study extends that work by examining the effects of different types of AFOs on medial gastrocnemius (MG) operating length and velocity.

Participant

Data were analyzed for eleven children with CP, including six individuals in Gross Motor Function Classification System (GMFCS) Level I (mean ± standard deviation, height: 120.6 ± 15.2 cm, mass: 23.9 ± 9.6 kg, age: 7.9 ± 2.4 years) and five individuals in GMFCS Level III (height: 116.1 ± 10.7 cm, 23.5 ± 5.7 kg, age: 7.4 ± 2.2 years). Three hemiplegic, five diplegic, and two quadriplegic participants were included in this study. All participants had crouch and/or equinus gait patterns, as evaluated by the physical therapists' visual observations [15]. Participants were

not excluded based upon prior surgical or pharmaceutical treatment (Table 2). Children's Hospital Los Angeles Institutional Review Board approval was obtained for this study and participants and their guardians gave written informed assent and consent.

Orthotic Conditions

Each participant was prescribed two different types of AFOs: DAFOs and Ultraflex ADR AFOs. Participants wore each AFO for four weeks and the order of AFOs was randomized for each participant. The AFO prescriptions were determined by manufacturer recommendations based on range of motion, muscle tone, and observational gait analysis (barefoot and wearing the participant's current AFOs) performed by a physical therapist. Fitting was performed by a certified pediatric orthotist.

Due to the heterogeneity in walking patterns among individuals with CP, the DAFOs and ADR AFOs prescribed varied between participants (Table 2). For example, DAFO 3.5 provides moderate dorsiflexion resistance and aggressive plantarflexion resistance. DAFO 2, DAFO 3 and DAFO Tami 2 provide free dorsiflexion motion and limited plantarflexion motion. DAFO Turbo provides aggressive plantarflexion resistivity and limited plantarflexion motion. The ADR AFO uses elastomers to provide resistance and store energy, including four adjustment channels: anterior and posterior elastomers to resist dorsiflexion/plantarflexion (0 – 27.1 Nm/0 – 40.7 Nm) and anterior and posterior stops to limit dorsiflexion/plantarflexion. Table 1 provides the order of AFO prescription, dorsiflexion/plantarflexion resistance, heel wedge height, and DAFO type for each participant. The goal of this research was to determine, given the current standards of prescription, whether these different AFOs tend to stretch or shorten the MG during gait in children with CP.

Gait Analysis Procedure

Each participant visited the gait analysis laboratory three times over a two-month period for initial testing and testing with the two types of AFOs. During the first visit, the participant's gait was assessed without AFOs, in the barefoot condition. The participants were randomly assigned one type of AFO. The participants wore the first AFO for four weeks and then returned for gait analysis. Each participant was then fit with the other type of AFO and returned four weeks later for gait analysis. The same shoes were worn with both AFOs (Apis Answer 2 Shoes, Apis Footwear Company, South El Monte, CA).

For gait analyses, an eight-camera infrared motion-capture system (Vicon Motion Systems Ltd., Oxford, UK) was used to acquire three-dimensional marker data at 120 Hz. Markers were placed on each participant based on a modified Helen-Hayes marker set [110]. At each visit, a minimum of ten gait cycles was collected. Each participant's kinematic data were averaged over all gait cycles to compare the different conditions.

Musculoskeletal Modeling

OpenSim, an open-source musculoskeletal modeling software [111], was used to calculate joint angles and estimate musculotendon operating length of the MG. A generic musculoskeletal model with 19 degrees of freedom (DOF) and 92 musculotendon actuators was scaled to each participant based upon anatomical landmarks [74]. Three rotational and translational DOF at the pelvis, a ball-and-socket joint between the pelvis and torso, ball-and-socket joints at each hip, and a single DOF at each knee and ankle. Inverse kinematics was used to calculate joint angles by minimizing the distance between experimental marker trajectories and virtual markers in OpenSim. The MG

operating lengths were calculated along the musculotendon path from origin to insertion in the musculoskeletal model during the gait cycle.

For each individual, we evaluated musculotendon operating length from the scaled model over a gait cycle. The MG's peak operating length during gait was compared to each individual's passive threshold, which was defined as the length of the MG at maximum ankle dorsiflexion with the knee fully extended from physical examination. To compare between participants, MG operating length and passive threshold were normalized to the length of the MG when the musculoskeletal model was positioned in anatomic position, similar to previous studies [88,133]. Musculotendon velocity was calculated by numerically differentiating the normalized MG length with respect to time.

Since joint and musculotendon kinematics depend on walking speed [133], each participant's walking speed was calculated from the horizontal position of the sacrum marker. The walking speed of the GMFCS Level I and III participants were most similar to the slow and very slow walking speeds, respectively, of a group of typically-developing children analyzed in a prior study (N=8, data available at: http://simtk.org/home/mspeedwalksims) [113] and the average kinematics and MG operating length and velocity for the slow and very slow speeds from these children were used for comparison. Figure 9 shows an example of the average MG operating length for one participant over a gait cycle with each of the tested conditions.

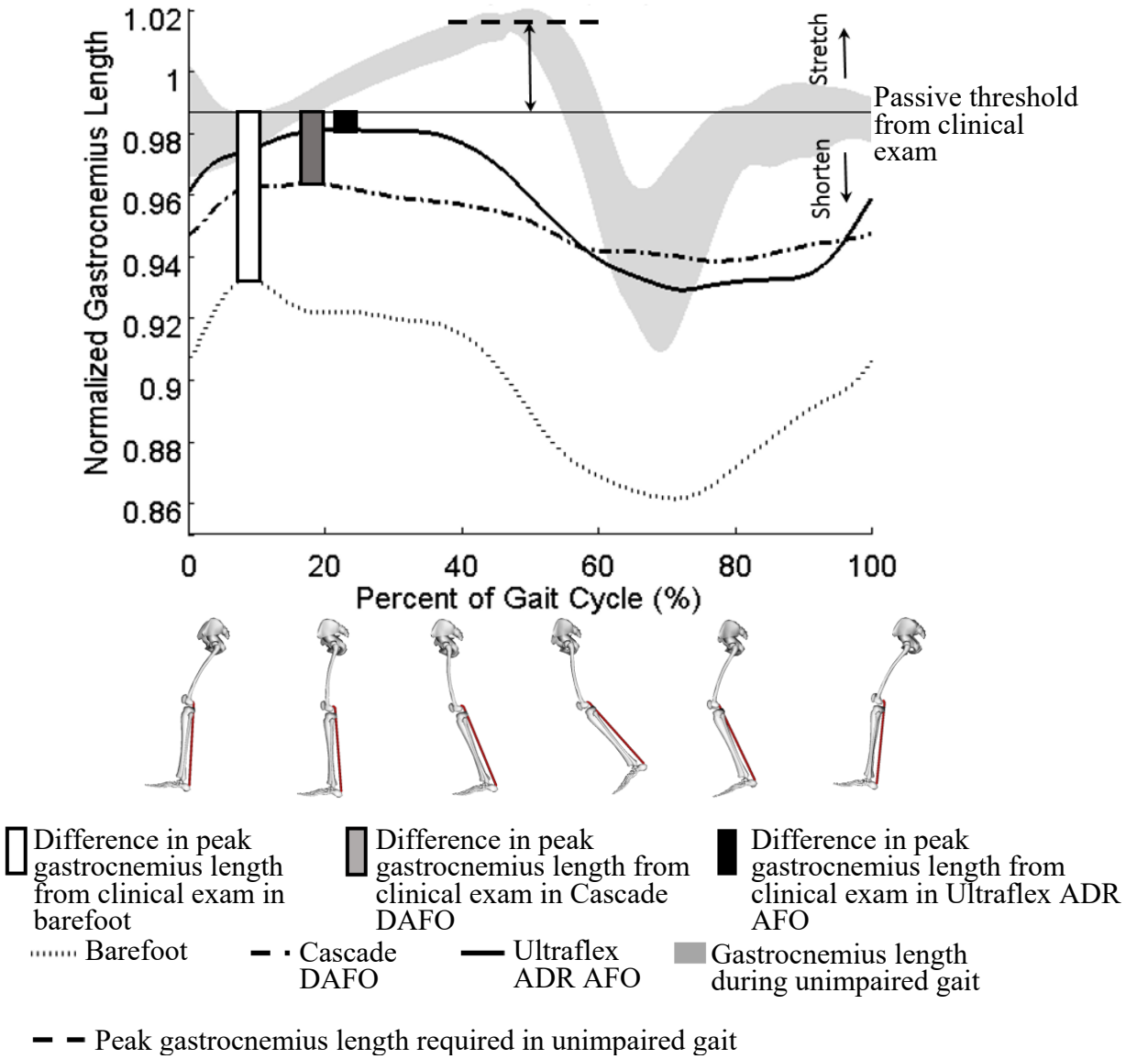

Figure 9. The average medial gastrocnemius operating length over a gait cycle across all conditions for one participant (P09, left limb). For each condition, the relative difference between peak gastrocnemius operating length and the passive threshold from physical exam was calculated (bars). The difference in the passive threshold and the peak gastrocnemius operating length required during unimpaired gait was also calculated (arrow). The gray shaded curve represents the average +/- one standard deviation in gastrocnemius operating length for unimpaired individuals walking in a very slow speed, similar to the speed of this participant. Thus, this participant's passive threshold was less than the peak length required during unimpaired gait. Further, when walking barefoot or with either AFO, this participant did not stretch the gastrocnemius beyond the passive threshold measured by the physical therapist during the physical exam.

Table 2. Participant information and prescribed AFOs.

*R=right; L=left; Bilat=bilateral; Post Tib=posterior tibialis; TAL=tendoachilles lengthening; Ant Tib=anterior tibialis; FRDO=femoral derotation osteotomy; TDRO=tibial derotation osteotomy; Ham=hamstrings; Gas=gastrocnemius

**UF Ultraflex ADR AFO; the number in parentheses after UF shows height of heel wedges in cm.

Participant	GMFCS Level	Diagnosis	Age	Height (cm)	Weight (kg)	Prior Treatments*	1st prescribed AFO**	2nd prescribed AFO**
1	I	Right Hemiplegia, Bilat Crouch	5.7	112.5	19.4		DAFO 3.5 DF: Resist PF: Resist	UF (0) DF: Resist PF: Resist
2		Spastic, Left Hemiplegia, Left Equinus	5.6	108.5	17.1	Serial casting	DAFO 3 DF: Free PF: Block	UF (0.75) DF: Resist PF: Resist
3		Right Hemiplegia, Bilat Crouch	8.3	114.5	16.8		DAFO 3.5 DF: Resist PF: Resist	UF (0.75) DF: Resist PF: Resist
4		Diplegia, Left Crouch	12.3	150.5	42.2	Multiple prior interventions including: Bilat TAL and Ham lengthening, R Post Tib lengthening, L Ant Tib and Post Tib transfers, Botox to Ham and Gas	UF (0.25) DF: Resist PF: Resist	DAFO Tami2 DF: Free PF: Block
5		Spastic, Right Hemiplegia, Bilat Crouch	7.6	118.2	22.6		UF (1) DF: Resist PF: Resist	DAFO 3.5 DF: Resist PF: Resist
6		Spastic, Diplegia, Bilat Equinus, Left Crouch	8.1	119.6	25.4		DAFO2 DF: Free PF: Block	UF (1.5 R, 0.75 L) DF: Resist PF: Resist
GMFCS Level I Average			7.9	120.6	23.9			
7	III	Diplegia, Right Crouch, Bilat Equinus, Bilat Crouch	10.0	128.9	29.8	Multiple prior interventions including: R FRDO, Bilat TDRO, Bilat hip adductor lengthening, Bilat Ham lengthening, 4 Times Botox to Ham and Gas with serial casting	DAFO 3.5 DF: Resist PF: Resist	UF (0.75) DF: Resist PF: Resist
8		Spastic, Quadriplegia, Bilat Equinus, Bilat Crouch	7.8	117.5	29.2		UF (0.5) DF: Resist PF: Resist	DAFO 3.5 DF: Resist PF: Resist
9		Spastic, Quadriplegia, Bilat Equinus, Bilat Crouch	8.7	122	21.6	Botox to Ham and Gas	DAFO 3 DF: Free PF: Block	UF (1.5) DF: Resist PF: Resist
10		Spastic, Diplegia, Bilat Equinus, Bilat Crouch	6.1	111	17.4	Botox to Ham and Gas	UF (1.5) DF: Resist PF: Resist	DAFO Tami2 DF: Free PF: Block
11		Spastic, Diplegia, Bilat Equinus, Bilat Crouch	4.4	101	19.5		UF (1.25) DF: Resist PF: Resist	DAFO Turbo DF: Block PF: Block
GMFCS Level III Average			7.4	116.1	23.5			

2.3 Results

Barefoot walking

We first evaluated if, during barefoot walking, the MG was stretched or shortened relative to the passive threshold measured from physical examination. For all but one participant (P04), the MG operated at a shorter length than the passive threshold during barefoot walking (Figs. 10A and 11A, white bars are less than 0). These results indicate that when walking barefoot, the MG was generally not stretched beyond the maximum length measured during passive stretching of the ankle by a therapist.

We next evaluated if each participant's passive threshold was sufficient to achieve normal walking kinematics (*i.e.*, the ankle dorsiflexion and knee extension required during unimpaired gait). The dotted lines in Figures 10A and 11A indicate the peak MG operating length required during unimpaired walking relative to each participant's passive threshold. The MG's passive threshold was less than the peak MG operating length required during unimpaired walking for all participants, except the left limb of P07 (Figs. 10A and 11A, dotted lines greater than 0). As a result, participants walked with either increased knee flexion (Figs. 10B and 11B) or decreased ankle dorsiflexion (Figs. 10C and 11C) in stance during barefoot walking compared to unimpaired gait. Both knee and ankle kinematics showed a linear relationship with the difference between the MG passive threshold and the MG length required for unimpaired gait (Fig. 12). This demonstrates that a short and stiff MG contributes to altered knee and ankle kinematics.

AFO: GMFCS Level I

The DAFOs increased peak MG operating length during gait compared to barefoot walking for 4/6 GMFCS Level I participants (Fig. 10 A, gray bars). For three of these participants (P04, P05, and P06) the MG was stretched beyond the passive threshold measured during physical exam due to increased knee extension or ankle dorsiflexion in stance (Fig. 10 B and 10 C, gray bars). There were variable changes in kinematics and MG operating length between the different types of DAFOs. Of the participants who had posterior leaf spring DAFOs that aggressively resisted plantarflexion and moderately resisted dorsiflexion (DAFO 3.5 – P01, P03, and P05), all had increased knee extension in stance (one into hyperextension). For the participants who had hinged or solid DAFOs that only blocked plantarflexion (DAFO 2, 3 or Tami2 – P02, P04, and P06), all had increased MG operating length compared to barefoot walking. This suggests that aggressively resisting plantarflexion with a DAFO may play a role in increasing MG operating length. The ADR AFO increased peak MG operating length during gait compared to barefoot walking for the same 4/6 GMFCS Level I participants. For three of these participants (P02, P05, and P06) the MG was stretched beyond the passive threshold (Fig. 10 A, black bars) due to increased knee extension and ankle dorsiflexion (Fig. 10 B and 10 C, black bars). However, two of the participants had knee hyperextension (P11 and P14) with the ADR AFO (Fig. 10 B, black bars). The other two participants (P01 and P03) had similar or slight decreases in MG operating length compared to barefoot walking. Peak MG velocity during gait for the GMFCS Level I participants was relatively similar to slow unimpaired gait (6.81x10-4 normalized length / second, Fig. 13 A dashed line) and was consistent across conditions. Only one participant (P05) had a large decrease in peak velocity with the DAFO and ADR AFO, while the other participants had similar or increased lengthening velocity with both types of AFOs.

These results with the DAFO and ADR AFO demonstrate that AFOs could stretch the MG length for some GMFCS Level I participants, although sometimes with undesirable changes in kinematics (*i.e.,* knee hyperextension). GMFCS Level I participants generally demonstrated similar changes in MG operating length and kinematics with the two different AFO prescriptions.

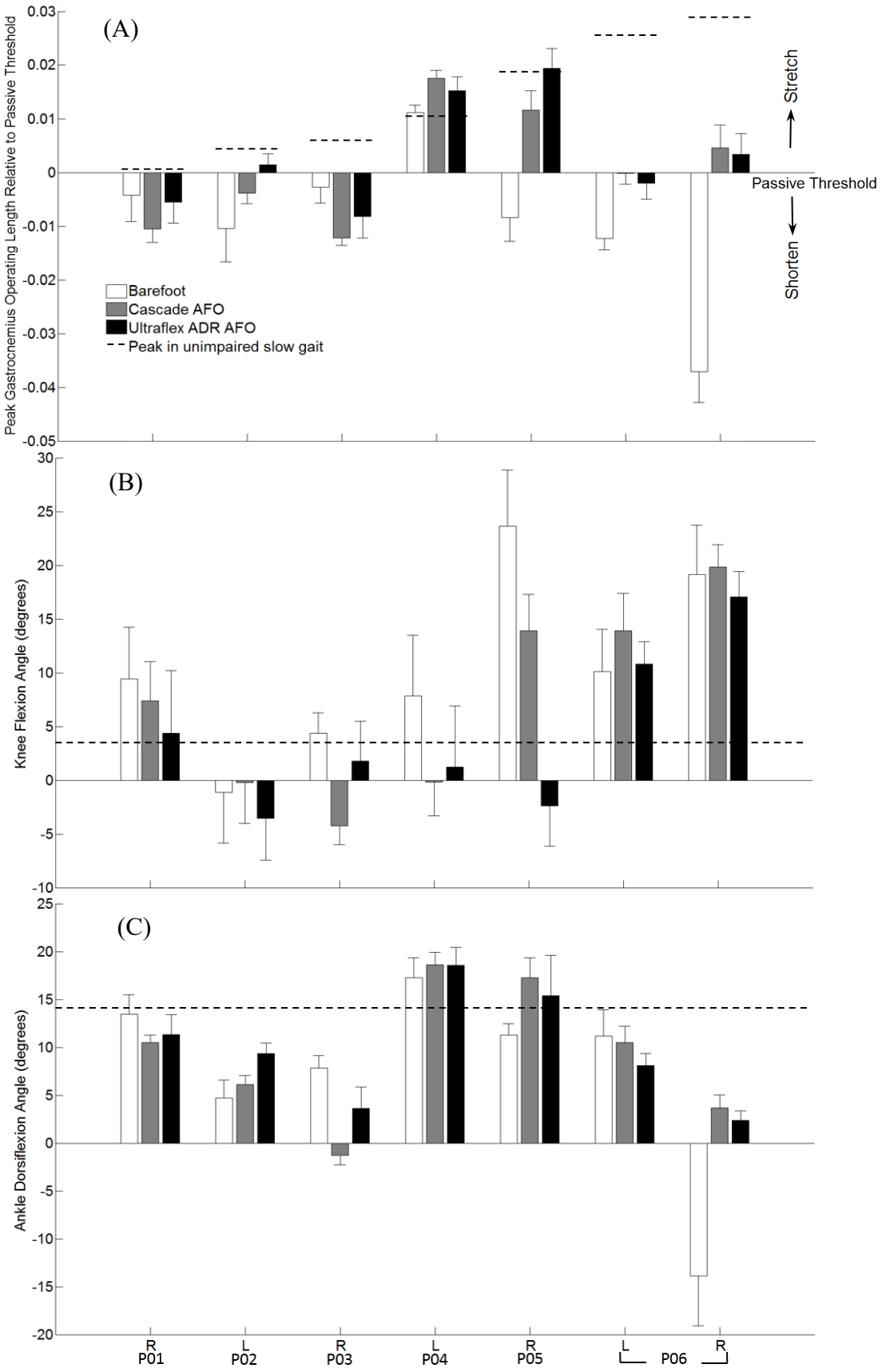
(A)
Peak Gastrocnemius Operating Length Relative to Passive Threshold
0.03
0.02
0.01
0
-0.01
-0.02
-0.03
-0.04
-0.05
Stretch
Passive Threshold
Shorten
Barefoot
Cascade AFO
Ultraflex ADR AFO
Peak in unimpaired slow gait
(B)
Knee Flexion Angle (degrees)
30
25
20
15
10
5
0
-5
-10
(C)
Ankle Dorsiflexion Angle (degrees)
25
20
15
10
5
0
-5
-10
-15
-20
R
P01
L
P02
R
P03
L
P04
R
P05
L
P06
R

Figure 10. GMFCS Level I Results: (A) Average normalized peak medial gastrocnemius operating length during gait compared to each individual's passive threshold from physical exam and sagittal plane kinematics at the knee (B) and ankle (C) at peak gastrocnemius operating length for all limbs that wore AFOs. Comparisons are shown during walking barefoot (white bars), with DAFOs (gray bars) and with ADR AFOs (black bars). Error bars describe one standard deviation across multiple gait cycles for each gait condition. Positive values of gastrocnemius length suggest stretching relative to the passive threshold and positive values of knee and ankle angles indicate flexion and dorsiflexion, respectively. Dashed lines depict the (A) peak operating length, (B) minimum knee flexion, and (C) maximum dorsiflexion during unimpaired gait at slow speeds. A dashed line in (A) greater than zero indicates that the participant's passive threshold measured from physical exam was lower than the operating length required during unimpaired gait.

AFO: GMFCS Level III

The DAFOs increased peak MG operating length during gait compared to barefoot walking for all GMFCS Level III participants (Fig. 11 A, gray bars), except P07 who already had a passive threshold similar to the peak length required during unimpaired gait. Changes in MG operating length with the DAFOs were primarily driven by increased knee extension or ankle dorsiflexion (Fig. 11 B and 11 C, gray bars). Unlike the GMFCS Level I participants, none of the GMFCS Level III participants had knee hyperextension with either AFO. Although MG operating length increased with the DAFOs, it only stretched the MG beyond the passive threshold for three of the participants (P08, P10, and P11). P11 had the greatest increase in MG operating length during gait with the DAFOs due to increases in both knee extension and ankle dorsiflexion. This participant had the most rigid DAFO, the Turbo, which likely contributed to the greater changes in kinematics and MG operating length.

The ADR AFOs increased peak MG operating length during gait compared to barefoot walking for 3/6 of the GMFCS Level III participants (Fig. 11, black bars). However, only one participant (P09) had a greater increase in MG operating length and improvements in knee extension and ankle dorsiflexion with the ADR AFO compared to the DAFO. With the ADR AFO, none of the participants had an MG operating length significantly greater than the passive threshold on both limbs, suggesting the MG was operating in a shortened state during gait with this AFO. Both DAFOs and ADR AFOs decreased peak MG lengthening velocity during gait compared to barefoot walking, except for P07 (Fig 13 B). MG lengthening velocity was generally greater with the ADR AFO compared to the DAFO, except for P07 and P11 right sides.

These results demonstrate that the MG length was generally short during gait relative to its passive threshold and MG lengthening velocity tended to decrease for GMFCS Level III participants with both types of AFOs.

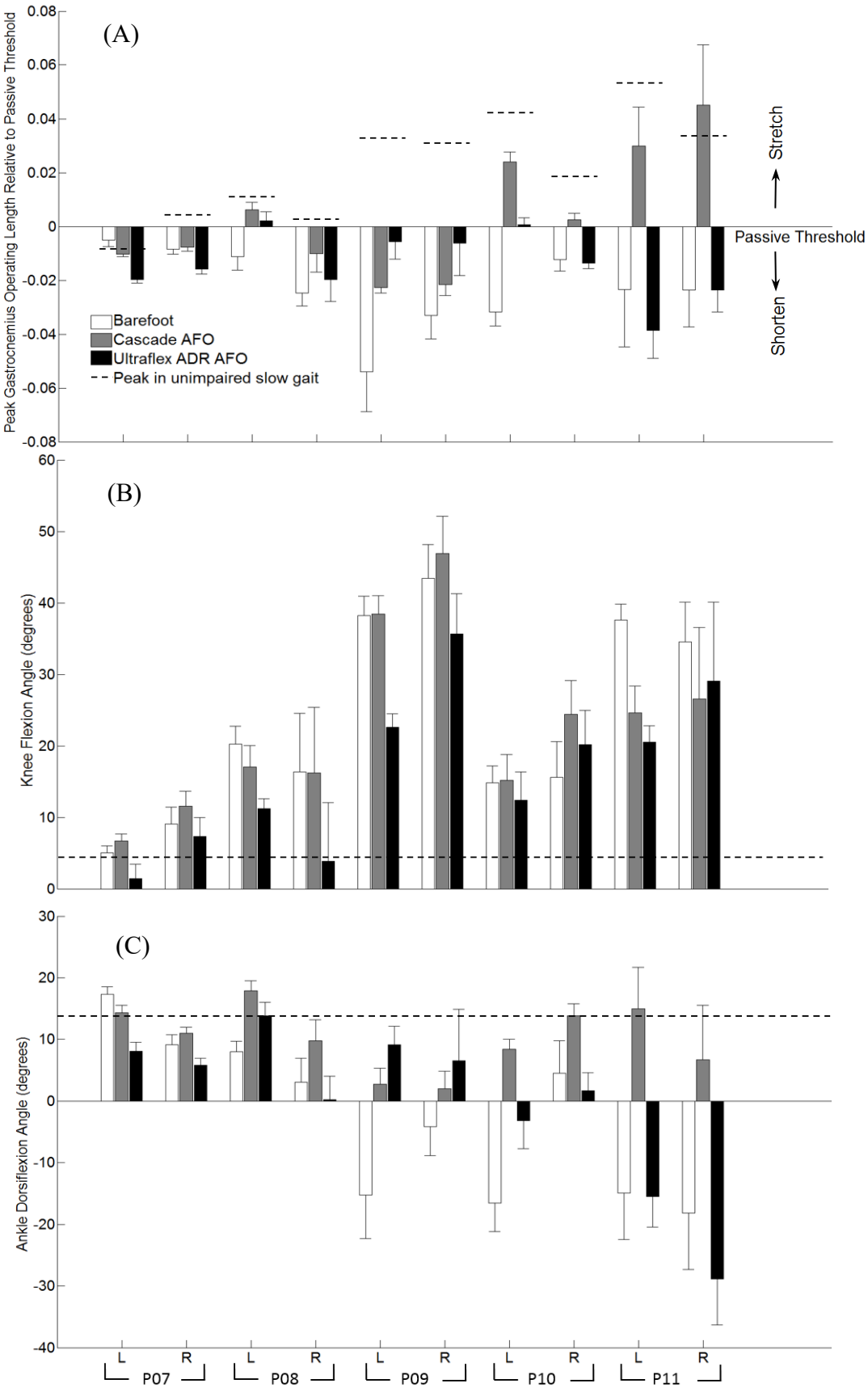
(A)
Peak Gastrocnemius Operating Length Relative to Passive Threshold
0.08
0.06
0.04
0.02
0
-0.02
-0.04
-0.06
-0.08
Stretch
Passive Threshold
Shorten
Barefoot
Cascade AFO
Ultraflex ADR AFO
Peak in unimpaired slow gait
(B)
Knee Flexion Angle (degrees)
60
50
40
30
20
10
0
(C)
Ankle Dorsiflexion Angle (degrees)
30
20
10
0
-10
-20
-30
-40
L
R
P07
P08
P09
P10
P11

Figure 11. GMFCS Level III Results: (A) Average normalized peak medial gastrocnemius operating length during gait compared to each individual's passive threshold from physical exam and sagittal plane kinematics at the knee (B) and ankle (C) at peak gastrocnemius operating length for all limbs that wore AFOs. Comparisons are shown during walking barefoot (white bars), with DAFOs (gray bars) and with ADR AFOs (black bars). Error bars describe one standard deviation across multiple gait cycles for each gait condition. Positive values of gastrocnemius length suggest stretching relative to the passive threshold and positive values of knee and ankle angles indicate flexion and dorsiflexion, respectively. Dashed lines depict the (A) peak operating length, (B) minimum knee flexion, and (C) maximum dorsiflexion during unimpaired gait at slow speeds.

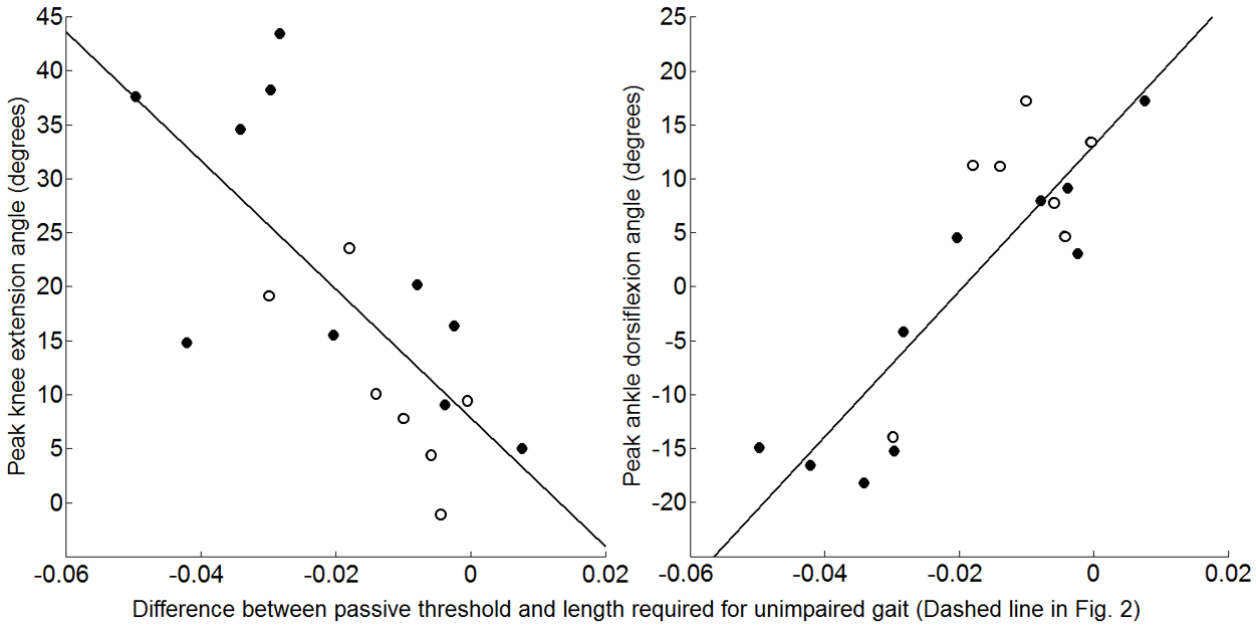

Figure 12. Correlation of (left) peak knee extension angle during barefoot walking and (right) peak ankle dorsiflexion angle during gait with the difference in normalized gastrocnemius operating length and passive threshold required for unimpaired gait.
White and black circles depict GMFCS Level I and GMFCS Level III participants, respectively.

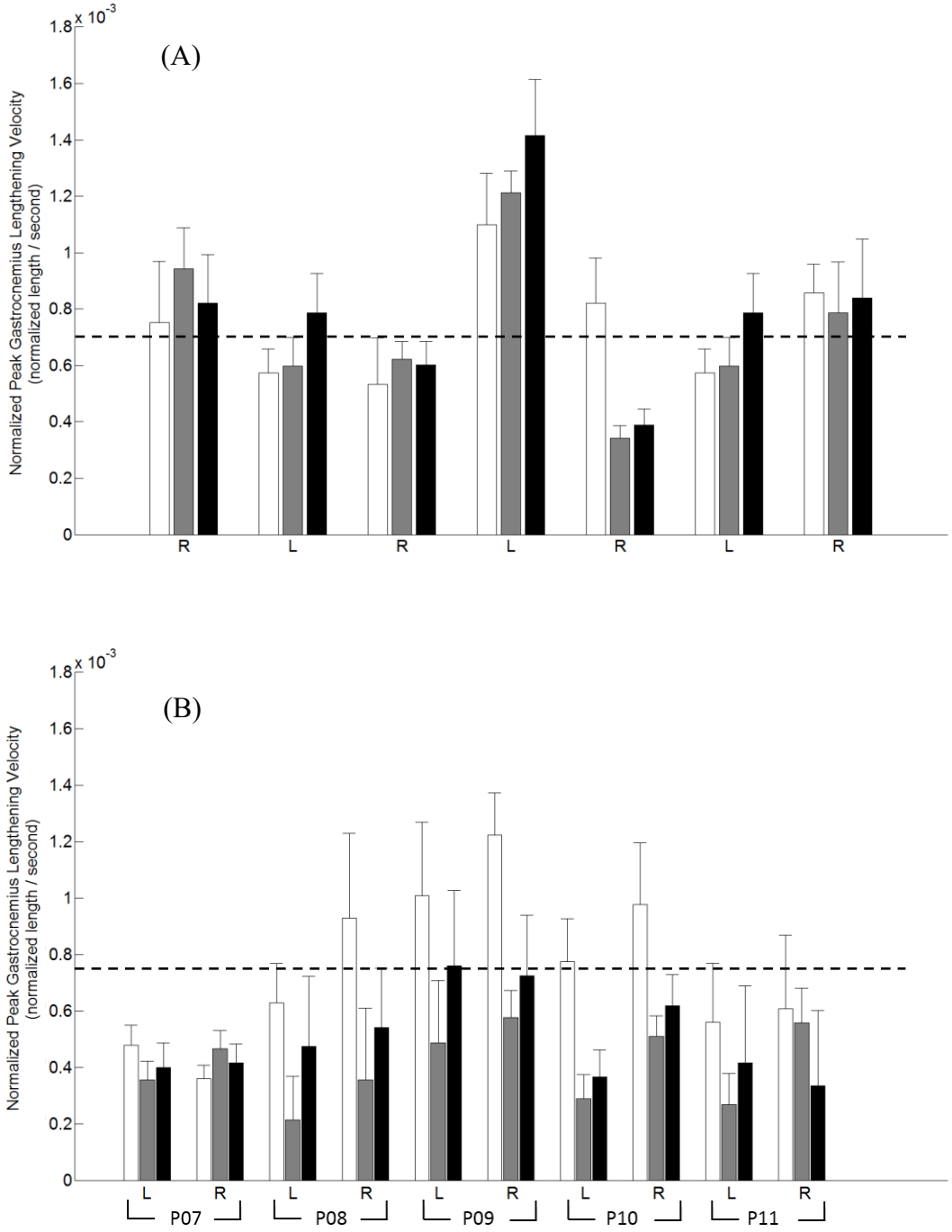

Figure 13. Average normalized peak medial gastrocnemius lengthening velocity during gait for the (A) GMFCS Level I and (B) GMFCS Level III participants. Comparisons are shown during walking barefoot (white bars), with DAFOs (gray bars) and with ADR AFOs (black bars). Error bars describe one standard deviation across multiple gait cycles for each gait condition. Dashed lines depict the peak medial gastrocnemius lengthening velocity during unimpaired gait at (A) slow speeds and (B) very slow speeds

2.4 Discussion

In this study, we used musculoskeletal modeling to evaluate the influence of different types of AFOs on MG operating length, lengthening velocity, and gait kinematics for individuals with CP. Our results demonstrate that current AFO prescriptions can stretch the MG during gait for some individuals with CP. However, changes in MG operating length and velocity were variable between participants and types of AFOs. The heterogeneity among participants in this study reflect the clinical reality faced by practitioners prescribing AFOs. These results illustrate the variability in response to different types of AFOs, emphasizing the need to understand the underlying mechanisms by which muscle function changes with AFOs. Stretching of the MG was driven by increases in knee extension and ankle dorsiflexion in terminal stance. However, in some participants, although the MG was stretched during gait with the AFOs, the participants had excessive knee hyperextension. The AFOs used in this study were prescribed according to current clinical recommendations, but these results highlight the interplay of potential competing priorities in orthotic prescription. While an orthosis may stretch the MG during gait, this stretching may be due to undesirable changes in kinematics. Balancing improvements in kinematics, metabolic costs, and other therapeutic goals is a continuing challenge.

There was a difference in the response between GMFCS Level I and III participants to the different AFOs. While GMFCS Level I participants had similar changes in MG operating length and gait kinematics with the DAFOs and ADR AFOs, the GMFCS Level III participants often exhibited different responses to the two types of AFOs. The DAFOs provided more rigid resistive support than the ADR AFOs, which may contribute to the greater change in ankle dorsiflexion with the DAFOs for the GMFCS Level III participants. ADR AFOs allow orthotists to tune the stiffness of the AFO; however, a quantitative measure of the stiffness set for each participant was

not available. The reported peak plantarflexion and dorsiflexion torques of ADR AFOs (40.7 and 27.1 Nm, respectively) may not be sufficient for some GMFCS Level III participants. Further, GMFCS Level III individuals generally have less strength [134] and these individuals may put more of their body-weight on external walking aids; impacting changes in kinematics and MG operating length with AFOs [135].

Evaluating the rate of change in musculotendon length (*i.e.,* velocity) can also be useful for evaluating points in the gait cycle where spasticity or other velocity-dependent effects may influence muscle function and motion. Among the GMFCS Level III participants, the peak MG lengthening velocity was less than that used during unimpaired gait for the majority of the participants. Both the ADR AFOs and DAFOs tended to further decrease MG lengthening velocity for this group, which could reduce the impact of spasticity during gait. Reducing MG lengthening velocity by constraining the ankle joint could improve knee joint kinematics by preventing excessive muscle activity [137]. However, if a participant has hamstring spasticity, a knee extension angular velocity could also trigger inappropriate muscle activity and limit improvements in knee kinematics during gait. Future studies that use quantitative assessments of spasticity [138] and monitor spastic thresholds could assist in understanding the role of spasticity on musculotendon dynamics with and without AFOs.

The variety of AFOs and pathological gait patterns in this study allowed us to evaluate how current AFO prescriptions may influence stretching or shortening of the MG during daily life. This variety introduced limitations, but also reflects the heterogeneity among individuals with CP and the diversity of AFO options currently available. We were unable to precisely quantify the stiffness of each AFO, which could provide valuable insight into the differences in response between individuals [71,139]. Musculoskeletal modeling lets us evaluate the overall operating length of a

muscle during movement; however, this reflects changes in length of both the muscle and tendon. An advantage of these methods is that they can be obtained from standard clinical gait analysis methods. To investigate if AFOs can stretch muscle fascicles, leading to long-term improvements in function, future studies should incorporate techniques such as ultrasound to evaluate relative stretching of muscle and tendon.

The musculoskeletal model used in this study was a generic model based on the anatomy of unimpaired adults. This models assumes no bone deformities such as femoral anteversion or tibial torsion, which are common in children with CP and may influence the results of modeling studies [140,141]. Among these bone deformities, tibial torsion could have an impact on gastrocnemius operating length. However, Hicks et al. [141] in 2007 demonstrated that tibial torsion deformity did not significantly affect gastrocnemius moment arms, which would suggest minimal effects of tibial torsion on the gastrocnemius musculotendon operating length estimated in this study. However, magnetic resonance imaging-based methods to create patient-specific musculoskeletal models for children with CP may enhance future research, although they are time and resource intensive [142,143]. In this study we were limited in our ability to statistically compare changes in MG operating length with kinematics due to the heterogeneity of participants' AFO prescriptions. However, this heterogeneity demonstrates the 'real-life' clinical situation and highlights the challenge for clinicians and orthotists to make patient-specific treatment decisions.

Muscles respond to the demands experienced in daily life, and this study represents a first investigation into whether AFOs may be able to help address short and stiff muscles among individuals with CP. Children with CP take fewer steps per day compared to typically-developing peers; however, even GMFCS Level III children with CP take over one thousand steps per day

[72]. If AFOs can help stretch short or stiff muscles, this may provide another tool for improving long-term function.

We found that the MG was stretched when walking with AFOs for some individuals. Whether this stretching is beneficial and could assist in rehabilitation during daily life will require further investigation. Further, potentially stretching tight muscles with AFOs would need to be balanced with other purposes of orthoses such as reducing energy costs, improving gait kinematics, and preventing bone deformities. Since muscle impairments contribute to pathologic gait in CP and are a common target of more invasive treatments, we should consider changes in muscle operating length and long-term adaptations in future orthotic design and prescription.

AIM 3: FABRICATION OF CUSTOMIZED 3D PRINTED VARIABLE STIFFNESS ANKLE FOOT ORTHOSES TO EVALUATE MUSCLE FUNCTION

3.1 Abstract

Ankle foot orthoses (AFOs) are an assistive device commonly prescribed for individuals with cerebral palsy and stroke to improve pathologic gait. AFOs impact gait kinematics and muscle function. Adjusting AFO stiffness has been suggested to improve gait kinematics and reduce energy costs. However, traditional AFO fabrication methods can be time and resource intensive to create a custom fit for each individual and make post-fabrication iterations challenging. This study introduce fabricating adjustable stiffness AFOs with 3D printing technology. The 3D printed adjustable stiffness AFO can adjust stiffness from 0 to 4 Nm / ˚ using different elastic polymer bands which covers free hinge to rigid standard care of AFO. 3D printing AFOs provides a platform to quickly fabricate and test adjustable stiffness AFOs. These AFOs can also accommodate additional sensors, such as ultrasound and electromyography (EMG), in experiment protocols. These techniques provide a platform for facilitating evaluation of muscle function and gait kinematics with respect to changes in resistance, as well as suggesting alternative AFO fabrication methods.

3.2 Background

Ankle foot orthoses (AFOs) are assistive devices commonly used to improve gait kinematics for individuals with cerebral palsy (CP) and stroke. AFOs influence gait kinematics and muscle function [88]. Moreover, adjusting AFO stiffness in the sagittal plane leads not only to improved kinematics but can also reduce energy costs during ambulation [71]. Traditional methods for fabricating AFOs are comprised of six steps. First, the orthotist determines the orientation and

configuration of the participants' leg into anatomic position, then marks protruded bony landmarks for determining trim lines and incorporating hinges. Second, cast tape is wrapped around the participant's leg and cut off when the cast tape is solidified. The cast is put back together to create a negative mold. Next, the cast material is filled with plaster to create a positive mold. Additional plaster material is added on the protruded bony land marks in order to make room for paddings and hinges. A heated thermoplastic is wrapped and vacuum formed around the cast model. Finally, a custom fit for each individual is achieved by trimming excess material.

These processes allow for flexibility and diversity in the design and prescription of AFOs, but can also be laborious and makes creating highly repeatable AFOs or iterating upon AFO designs challenging. Recent advances in 3D printing and scanning have been suggested as an additional toolset that may facilitate AFO fabrication [144-148]. Prior research has demonstrated that posterior leaf spring AFOs and other solid AFOs can be fabricated with additive manufacturing techniques and enable control of AFO stiffness [149]. These designs allow for the stiffness to be controlled based upon the shape and material properties of the solid AFO, but still make it challenging to determine the optimal stiffness for a given individual. The aim of this research was to use 3D-printing and scanning to create custom-fit AFOs whose stiffness could be quickly adjusted between walking trials. By harnessing interchangeable elastic polymer bands, the effect of AFO stiffness on muscle function during gait can be evaluated *in vivo* with ultrasound imaging and electromyography (EMG).

3.3 Methods

A combination of 3D scanning, 3D printing, and traditional AFO hardware was used to create a variable stiffness AFO. During the first visit, the participant's limb was scanned (Sense, 3DSystems). To create an articulated AFO, a commercially-available Camber Axis joint was integrated with the AFO design and the position of the Camber Axis joint was determined from the center of lateral and medial malleoli. The Camber Axis joint was attached to the participant's ankle and the foot and shank geometry were scanned while sagittal, frontal, and transverse planes were maintained in anatomical position (Fig. 14A). The acquired scanned data was post-processed using MeshMixer (MeshMixer, Autodesk, San Rafael, CA) software to trim unwanted areas of the mesh and assign a 3mm thickness, similar to current articulated AFOs. Two hooks, designed with Solid Works, were positioned posteriorly on the mesh for the shank and foot segments along the Achilles tendon to attach the elastic polymer bands (Fig. 14 B and 14 C). Designed AFOs were printed with a fused deposition modeling 3D printer (Replicator, Makerbot, Brooklyn, NY) with polylactic acid (PLA) filament. The print settings were as follows: 100% infill, 0.2mm layer height, 2 shells (Fig. 14 D). To adjust the stiffness for a wide range of values with a single elastic polymer band, the bands can be placed within a 2cm range to vary the moment arm. Using small clips, it is possible for the user to define the moment arm by adjusting the elastic band placement (Fig. 15)

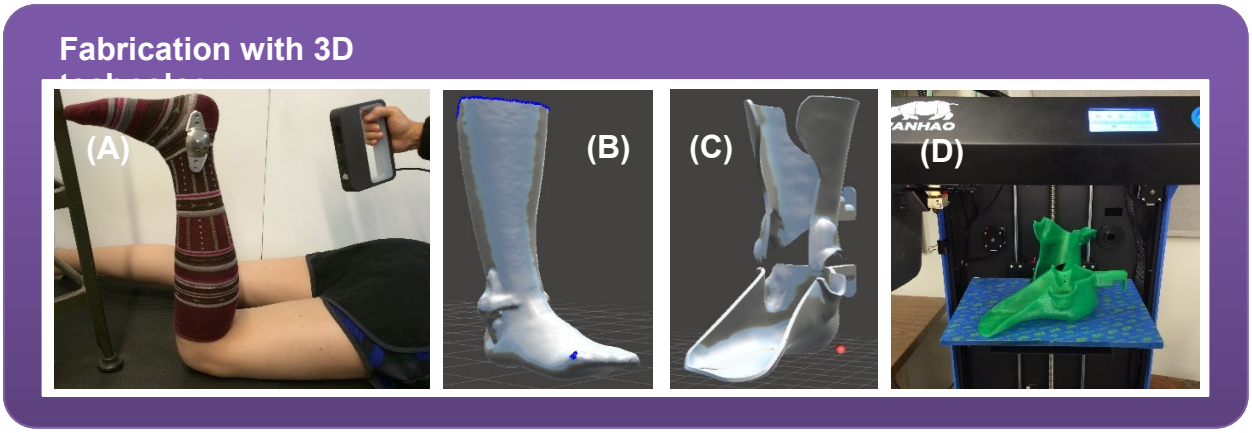

Figure 13 3D technology fabrication process of an ankle foot orthosis.

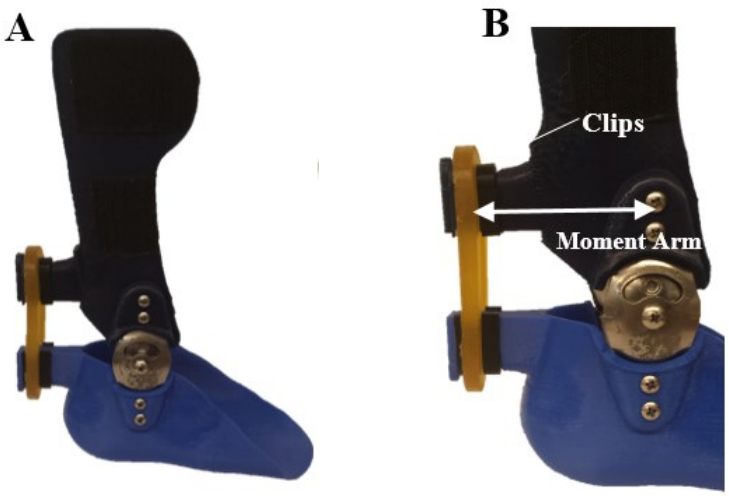

Figure 14 3D printed AFO
(A) 3D-printed AFO. (B) Momet arm of ealstic polymer bands and clips.

Molds were fabricated with 3D printing to create silicon negative mold to fabricate the elastic polymer bands. The elastic polymer bands were fabricated with polyurethane (PMC 780 Wet, Smooth-On) from the silicon negative mold (Fig. 16). Using a universal materials testing machine, tensile force of the polymer bands was measured to calculate AFO stiffness. The ankle

moment produced by the AFO (M) was calculated by multiplying the orthogonal distance from the Camber joint rotation axis to the elastic polymer band (MA), by the tensile force of the elastic polymer band (F) (Fig.15).

The resistive ankle moments during gait were quantified using OpenSim, an open-source musculoskeletal simulation software. Motion analysis data can be used to create a scaled musculoskeletal model of a participant's lower-extremities. Inverse kinematics and inverse dynamics are used to calculate joint angles and moments, respectively. From this information, we then calculate the resistive ankle moments of each elastic polymer band by multiplying ankle angle by the stiffness of each elastic polymer band.

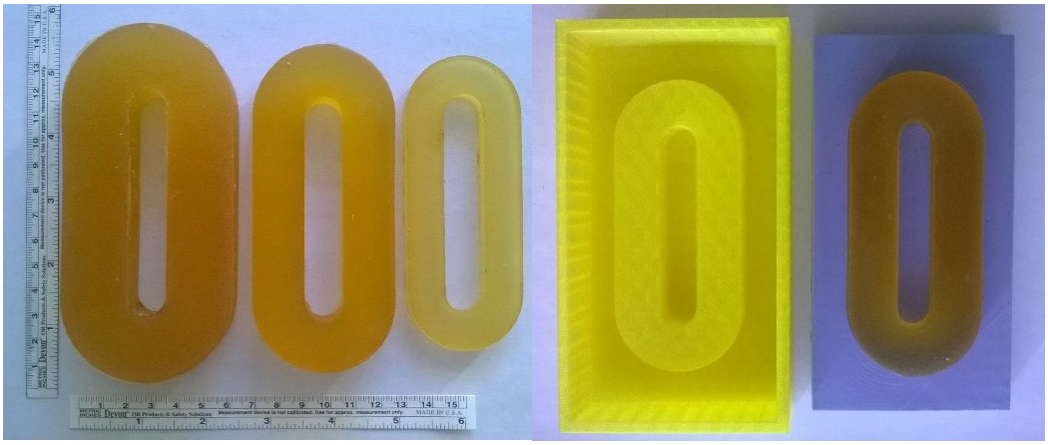

Figure 15 Different stiffness of elasatic polymer bands and its molds.

3.4 Results

The stiffness of the 3D printed AFO could be adjusted with different polymer bands. Existing rigid AFO stiffness is determined by medial and lateral trimlines around the malleoli. AFO stiffness is usually classified into compliant, moderate, and rigid [35]. Current designs of our polymer bands had a AFO stiffness range of 0 to 4.14 Nm / ˚, similar to the moderate stiffness range of current

AFOs (Fig. 17). We also accommodated a wide range of stiffness by using a wide attachment location and clips that allowed us to adjust the moment arm. On average, adjusting the moment arm to either side of the central position changed AFO stiffness by ±16% with a range in the central position of 0.23 Nm / ˚ to 3.95 Nm / ˚. By altering the moment arm length, this range was increased to 0.19 Nm / ˚ to 4.14 Nm / ˚ (Fig. 17 A). The range of stiffness values tested contributed up to 78% of the ankle moment (Fig. 17 B).

The 3D printed variable stiffness AFO can also be turned into a rigid AFO by inserting a metal key in the Camber Axis joint. Interchangeable polymer bands with variable quantifiable stiffness levels allow the stiffness of the AFO to be precisely manipulated and quantified to fit the user's needs. To evaluate the impact of AFO stiffness on muscle function during gait an ultrasound (Logicscan 128, Telemed) and EMG (BioPotential, Microsoft Research) can be used to record the muscle tendon junction and activation of the medial gastrocnemius (Fig. 18).

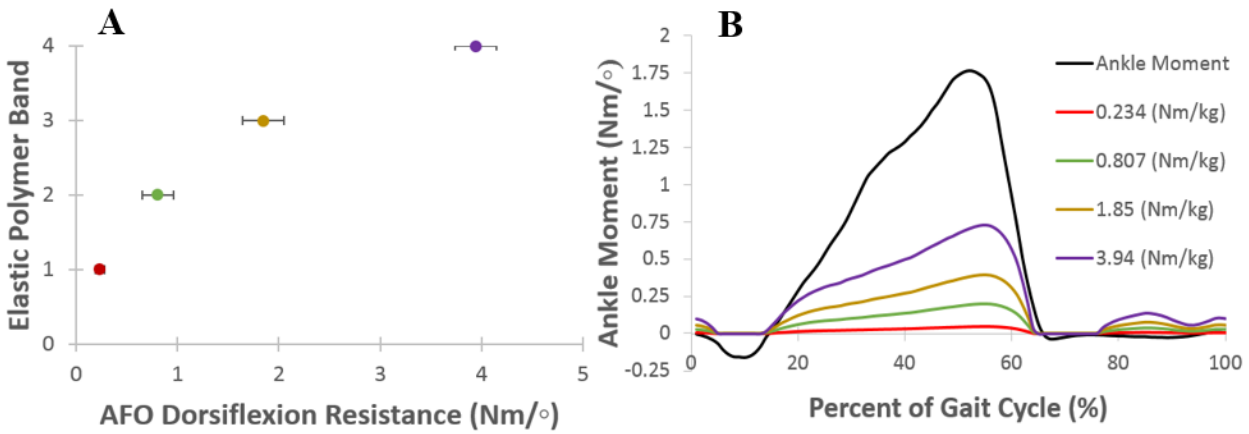

Figure 16 Stiffness of elastic polymer band and AFO moment. (A) AFO dorfiflexdion stiffness ranges for each elastic polymer band. (B) Ankle moment and AFO ankle dorsiflexion resistnace with each elastic polymer band during gait.

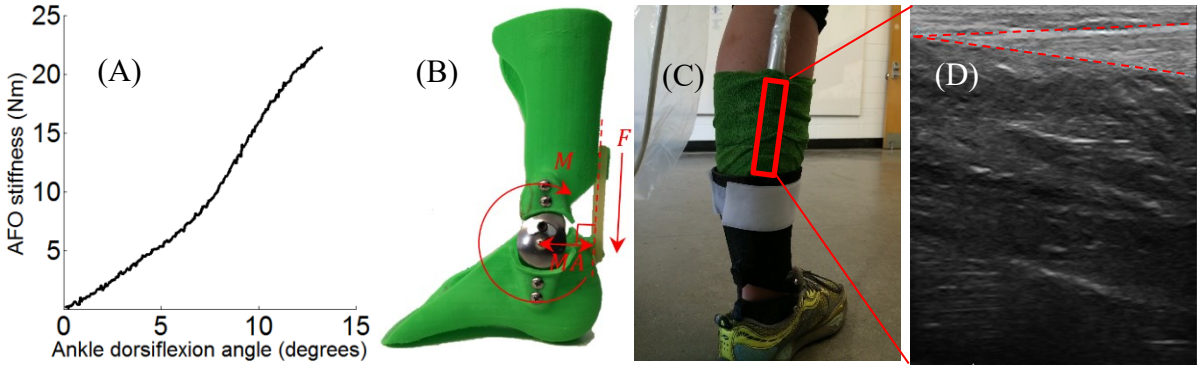

Figure 17 Sample utilization of 3D printed variable stiffness AFO.
(A) Sample AFO moment versus ankle angle for one polymer band. (B) 3D printed variable stiffness AFO with elastic polymer band. (C) Example of measuring medial gastrocnemius with ultrasound (red ractangle) in AFO condition. (D) Muscle tendon junction of medial gastrocnemius. Red dotted line depicts the boarder of medial gastrocnemius.

3.5 Discussion

3D-printed variable stiffness AFOs allow a pre-quantified stiffness value to be quickly adjusted by applying different polymer bands between walking trials. These techniques provide a foundation for not only expanding AFO fabrication techniques, but also facilitating evaluation of how pathologic muscle function and gait kinematics change with different AFO properties.

For this initial study, fabricating elastic polymer bands with specific stiffness values was performed by trial and error. However, finite element models could be used to predict elastic polymer band of AFO dimensions for a specified stiffness, reducing effort and time. This 3D printed AFO was not evaluated with rigorous fatigue testing for use in daily life. Evaluating fatigue testing and “real-world” testing such as exposure to sudden temperature changes would help determin the optimal material and fabrication settings for 3D printed AFOs. For example, PLA is affordable and is widely used for 3D printing products and it is rigid compared to the other plastic material. PLA also has less deformities from sudden temperature changes; however, it is vulnerable to brittle when the external force applied above the threshold. On the other hand, using acrylonitrile butadiene styrene (ABS) is more compliant compared to the PLA, but the level of

deformity is greater than PLA under a same amount of temperature changes [150]. 3D printing condition such as infill pattern and layer orientation also plays a significant role in determining AFO strength [151]. Therefore, determining the proper material and setting conditions will be critical for future fabrication of AFOs with 3D printing technologies.

AIM4: ACHILLES TENDON LENGTH DURING GAIT WITH DIFFERENT STIFFNESS ANKLE FOOT ORTHOSES

4.1 Abstract

Ankle foot orthoses (AFOs) are designed to improve gait for individuals with neuromuscular conditions and have also recently been used to reduce energy costs of walking for unimpaired individuals. AFOs influence joint motion and metabolic cost, but how they impact muscle function remains unclear. This study investigated the impact of different stiffness ankle foot orthoses (AFOs) on medial gastrocnemius muscle (MG) and Achilles tendon (AT) function during two different walking speeds. We performed gait analyses on eight unimpaired individuals. Each individual walked at slow and very slow speeds with a 3D printed AFO with no resistance (free hinge condition), and four levels of ankle dorsiflexion stiffness: 0.25 Nm / ˚, 1 Nm / ˚, 2 Nm / ˚, and 3.7 Nm / ˚. Motion capture, ultrasound and musculoskeletal modeling were used to quantify MG and AT length, and velocity with each AFO condition. Increasing AFO stiffness is related to increased peak AFO dorsiflexion moment, MG length, and AT length, as well as decreased peak ankle dorsiflexion angle and MG activation. Peak MG activity, length and velocity significantly decreased with slower walking speed; however, there was significant variability between participants in changes in MG activation level and length with varying speed. The influence of AFOs on MG and AT length indicate that AFO stiffness may be used to tune or optimize musculotendon function during gait, which can provide guidance for AFO design for rehabilitation, performance, or other goals.

4.2 Introduction

Ankle foot orthoses (AFOs) are assistive devices, which can be used to improve walking function [117]. Most AFOs are passive, exerting a torque about the ankle joint based upon the stiffness of the AFO's structure. In unimpaired individuals, passive AFOs have been shown to reduce metabolic costs of walking by up to 7% [152]. However, this reduction in metabolic cost is less than that predicted by various models and researchers have hypothesized this difference is due to complex musculotendon dynamics during gait [152,153]. Since the amount of force a muscle can produce is highly dependent on its length and velocity [154,155], if an AFO changes a muscle's length in unanticipated ways it may have counter-intuitive impacts on muscle force and metabolic costs. However, the impact of AFOs on the relative lengthening and shortening of key muscles, such as the gastrocnemius, have not been experimentally tested. Understanding musculotendon function during gait with AFOs has the potential to help optimize future designs and prescriptions.

The ankle plantarflexors play a critical role in supporting and propelling the body during gait [156,77] and are one of the muscle groups most impacted by wearing an AFO. The gastrocnemius is a bi-articular muscle, directly affecting both ankle and knee kinematics, making it a challenging muscle to understand functionally during gait. The gastrocnemius generates large forces during activities of daily living and harnesses a high efficiency system to manage these forces. The gastrocnemius muscle inserts into the Achilles tendon (AT), which is the thickest and strongest tendon in the human body [157], capable of handling large loads during dynamics tasks [158]. The AT is comprised of parallel arrays of collagen fibers [137], comparable with a mechanical spring [4]. The Achilles tendon stores mechanical energy during early- to mid-stance and releases energy during terminal stance [159,160], reducing gastrocnemius velocity and

allowing the gastrocnemius muscle to operate nearly isometrically during normal gait [155,161]. This reduction in muscle velocity helps increase walking efficiency [162]. However, AFOs can decrease ankle plantarflexor activity during gait, which may alter the efficiency of the gastrocnemius and AT during gait [77,117,155]. Using a mathematical model, one prior study suggested this decreased activity may reduce muscle fascicle shortening velocity, compromising muscle force production and metabolic costs during gait [153].

Quantifying muscle and tendon lengths and velocities during dynamic tasks like walking is challenging. The overall musculotendon unit (MTU) lengths and velocities can be estimated with musculoskeletal modeling using information about an individuals' joint kinematics, musculoskeletal geometry, and musculotendon moment arms [74]. Prior studies have evaluated the impact of various types of AFOs on MTU lengths and velocities in individuals with neurologic injuries, demonstrating AFOs can impact MTU stretching and shortening during gait, depending on AFO stiffness and other properties [88,125,166]. However, these methods are limited to estimating changes in overall MTU lengths, and do not differentiate between the relative muscle and tendon lengths.

Ultrasound is the most common method used to experimentally measure the relative length of the gastrocnemius muscle and AT during dynamic tasks. Prior studies have used ultrasound to quantify AT length by measuring the distance between the gastrocnemius musculotendinous junction (MTJ) and the insertion of the tendon at the calcaneus [163,167]. These studies have suggested that the gastrocnemius operates near isometrically during the stance phase of gait; however, changes in gastrocnemius function with AFOs or other assistive devices have not been investigated.

In this study we integrated ultrasound and musculoskeletal modeling to evaluate changes in AT and gastrocnemius length during gait with AFOs. Based upon prior research, we hypothesized that (1) as AFO stiffness increases, gastrocnemius muscle activity decreases leading to greater stretching of the gastrocnemius and a decrease in peak AT length during gait, and (2) as walking speed decreases, the gastrocnemius lengthens at a slower rate during stance, decreasing the sensitivity of musculotendon dynamics to different AFO conditions. By examining the impact of both AFO stiffness and walking speed on AT and gastrocnemius function, these results may inform future design and prescription of AFOs for both unimpaired individuals and individual with neurologic injuries.

4.2 Methods

Participant

We recruited 9 unimpaired individuals with no history of lower-extremity orthopedic surgery (5 males and 4 females) to participate in this study. One subject (male) was excluded due to excessive out-toeing during gait, resulting in a total of 8 participants whose data were analyzed for this study (mean ± standard deviation, height: 170.0 ± 7.9 cm, weight: 66.5 ± 8.5 kg, and age 25.3 ± 4.5 years). Institutional Review Board approval was obtained for this study and participants consented prior to testing.

AFO Fabrication

A combination of 3D scanning, 3D printing, and traditional AFO hardware was used to create an AFO whose stiffness could be easily changed during the experiment (Fig. 19). At the first visit, the participants' dominant foot and shank were scanned (HandySCAN 300, Creaform) while

their leg was maintained in anatomical position. To create an articulated AFO, a commercially-available metal hinge joint (Camber Axis Technic, Becker) was scanned and integrated with the AFO design. The acquired scanned data was post-processed using mesh design software (MeshMixer, Autodesk) to align the hinge joint to the medial malleolus [168] to minimize error between the AFO and participant's rotational ankle axes. Similar to current AFO fabrication methods, the hinge joint for the lateral malleolus was positioned parallel to the medial hinge joint. The foot of the AFO covered from calcaneus to metatarsal providing free motion of the phalangeal joint.

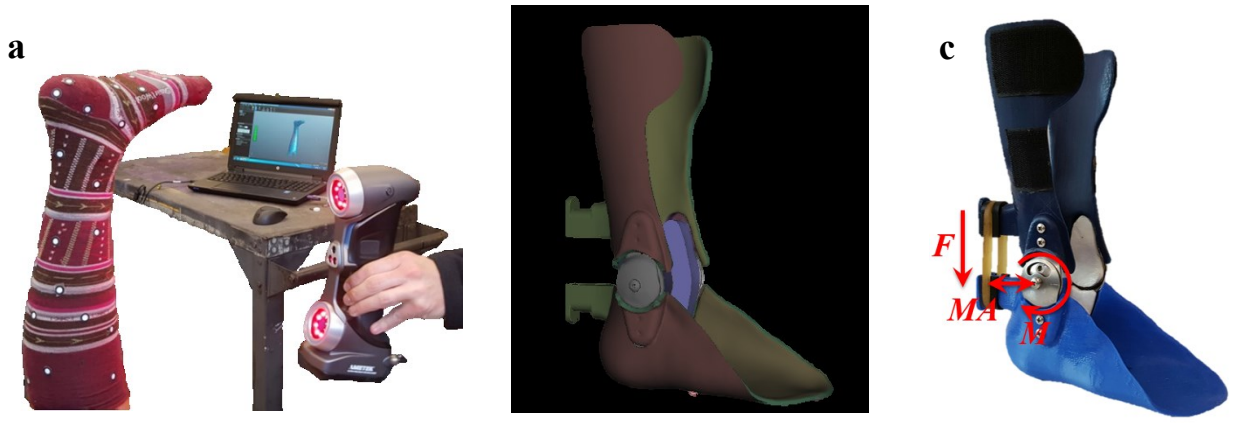

Figure 18 Variable stiffness 3D printed AFO fabrication process.
(a) Scanning a participant's foot and shank with a 3D scanner. Socks with patterns and markers help to improve the accuracy of the scan. The scans were used to customize the (b) AFO model with computer aided design software. The (c) variable stiffness AFO was printed with PLA and a polymer band was used to adjust stiffness between conditions. The stretch of the polymer band measured with markers determined the force (F), which multiplied by the moment arm (MA) was used to calculate the AFO moment (M) resisting ankle dorsiflexion.

Gait Analysis

Each participant walked on the treadmill with the five AFO conditions: free hinge mode (no resistance), and an AFO stiffness of 0.25 Nm / ˚, 1 Nm / ˚, 2 Nm / ˚, or 3.7 Nm / ˚ resisting ankle dorsiflexion. AFOs were worn on each participant's dominant leg. Since a previous study

demonstrated MTU length and joint kinematics vary with walking speed, each participant walked on the treadmill at two non-dimensional walking speeds of unimpaired individuals. The non-dimensional walking speed was defined as $\bar{v}^* = v/\sqrt{gravity \times leg\ length}$, and used to set very slow ($\bar{v}^* = 0.19$) and slow ($\bar{v}^* = 0.29$) speeds on the treadmill [113]. These speeds were selected to match the common speeds of individuals with neurologic disorders and provide sufficient capture frames from the ultrasound during each gait cycle. The order of each stiffness condition and non-dimensional walking speed was randomized for each participant. Participants were acclimatized to each walking speed and AFO condition for a minimum of 2 minutes, after which a recording of at least 25 gait cycles was collected for each condition.

For gait analysis, an eight-camera infrared motion capture system (Vicon, Motion Systems Ltd.,) was used to acquire three dimensional marker data at 100 Hz based on a modified Helen-Hays marker set with 23 markers [110]. Since ankle kinematics and AT length can be sensitive to the location of the foot markers, extra measurements were taken to evaluate the location of each marker with respect to the shoe and bony landmarks. An event switch (MA-153. Motion Lab Systems) placed beneath the calcaneus was also used to evaluate potential motion between the shoe and AFO during gait. All subjects wore the same shoe (UM311F102, Sintetico) which has a compliant sole (see Appendix A).

To evaluate the impact of AFO stiffness on AT length, an ultrasound (Logicscan 128, Telemed) recording at 61.4 Hz with a linear transducer (LV7.5/60/128Z-2, 59mm, Telemed) was attached to the shank and used to track the location of the medial gastrocnemius MTJ. An L-shaped ultrasound holder was fabricated with the 3D printer and used to provide a stable mount for the transducer and consistent marker locations. Three reflective markers were attached to the ultrasound holder to provide a coordinated system for tracking the position of the transducer

relative to the global coordinate system of the lab space. The location of the markers relative to the origin and axis of the ultrasound images was established by aligning the x' axis to the proximal side of ultrasound image and the y' axis to the lateral side of ultrasound image (Fig. 20).

Gastrocnemius activity was measured using a surface electromyography (EMG) measurement system (Trigno^{TM} Wireless EMG, Delsys). EMG data was recorded at 1111 Hz, with hardware signal processing including a band-pass filter (20-460 Hz). Using custom Matlab software, the EMG signal was rectified and low-pass filtered (6 Hz, 4th order Butterworth) to create a linear envelope for analysis. Muscle activity was normalized to the averaged maximum value across all trials walking with the hinged AFO condition. In this study, participant 2's EMG data was excluded due to poor signal quality.

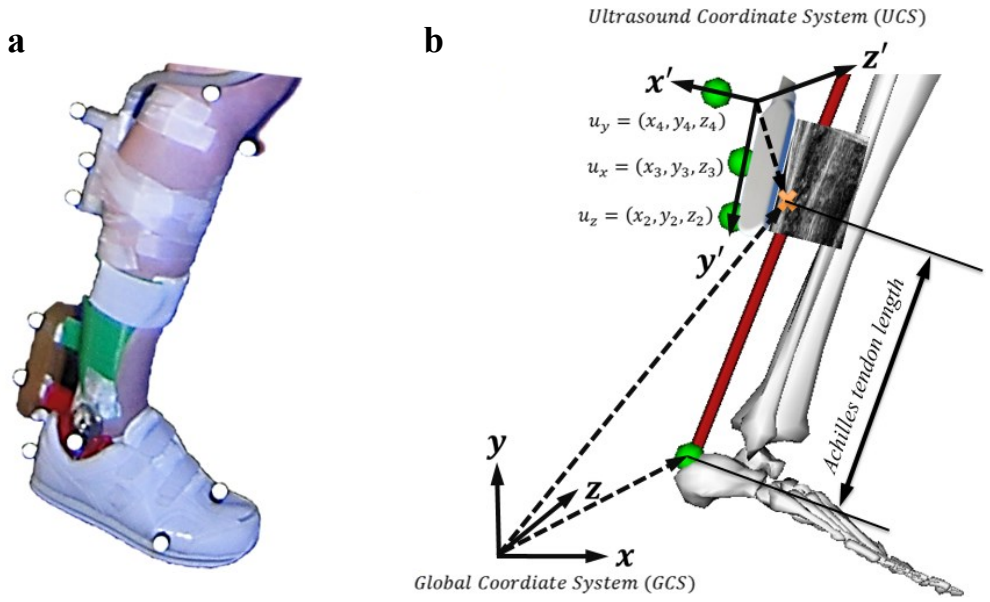

Figure 19 Quantification of Achilles tendon length.
(a) AFO, ultrasound, and position of experimental markers. (b) Scaled musculoskeletal model and schematic of coordinate systems for ultrasound to define AT length.

Musculoskeletal Modeling

OpenSim, an open-source musculoskeletal modeling and simulation software platform [111], was utilized to calculate gait kinematics, AT length, and medial gastrocnemius length. We used a generic musculoskeletal model with 37 degrees of freedom and 92 muscle actuators [169] which was scaled to each participant based on anatomical landmarks. The degrees of freedom in the model included a ball-and-socket joint at each shoulder, a hinge joint at each elbow, a combination saddle joint and condyloid joint at each wrist, three translations and three rotations of the pelvis, a ball-and-socket joint between the pelvis and the torso located at the third lumbar vertebrae, a ball-and-socket joint at each hip, a combination joint of translations and rotations at each knee, and a revolute joint at each ankle. We created an ultrasound object in OpenSim which allowed for 6 degrees of freedom (3 translations and 3 rotations) with respect to the tibia segment of the musculoskeletal model. For each trial, the distance between experimental reflective marker trajectories from gait analysis and virtual maker on OpenSim generic model was minimized to calculate joint angles and position of the ultrasound transducer using inverse kinematics. The medial gastrocnemius MTU length was calculated from the path between origin and insertion of the muscle during the gait cycle. The metatarsophalangeal movement was locked because foot markers were attached to the rear and mid foot.

Ultrasound images during each trial were acquired as movie data with a size of 823 by 512 pixels. Similar to prior studies, these images were used to manually track the MTJ position using ImageJ (NIH, Maryland), an open-source image processing software [170]. The horizontal pixel size of ultrasound image was correlated with the ultrasound linear sensor array to convert from the number of pixels to physical distances. The MTJ trajectories were manually identified at the point where the deep MG aponeuroses and external AT intersect on the ultrasound images

[171]. The two-dimensional pixel position representing the MTJ position was transformed into the ultrasound transducer coordinate system in OpenSim to visualize the position of the MTJ relative to the tibia during gait.

The insertion of the medial gastrocnemius MTU from OpenSim and MTJ trajectories from ultrasound were transformed into OpenSim's global coordinates to calculate changes in AT length during gait (Fig. 20). The medial gastrocnemius muscle length was calculated by subtracting the AT length from medial gastrocnemius MTU length at every time point. To compare between participants, changes in MTU, medial gastrocnemius muscle, and AT lengths were normalized to the length of the medial gastrocnemius MTJ length when the musculotendon model was positioned in anatomic position, full knee extension and neutral ankle angle, similar to previous studies [88,125,166]. Medial gastrocnemius muscle velocity was calculated by numerically differentiating the normalized muscle length with respect to time.

Data Analysis

We used R (R Core Team, 2012) and lme4 [172] to perform a linear mixed effect analysis to evaluate how different AFO stiffness and walking speed impact ankle angle, AT length, MTU length, medial gastrocnemius muscle length, and medial gastrocnemius eccentric velocity during stance. AFO stiffness and walking speed was entered into the model as fixed effects with random effects for the intercepts of each participant. Visual inspection of residual plots did not reveal any obvious deviations from homoscedasticity or normality. P-values were obtained by likelihood ratio tests of the full model with the effect in question against the model without the effect in question between participants and walking speeds. Significance was defined as $\alpha < 0.05$.

4.3 Results

AFO stiffness impacted joint kinematics and musculotendon lengths while walking on a treadmill. Figure 21 illustrates the impacts of AFO stiffness for a representative participant walking at a slow speed. As AFO stiffness increased, this participant exhibited increased hip extension in terminal stance, a slight increase in knee extension in stance, and decreased ankle dorsiflexion in terminal stance. These changes in knee and ankle kinematics contributed to a 3.3, 11.6, 20.3, and 31.4 Nm increase in the AFO moment with AFO stiffness conditions of 0.25, 1, 2, and 3.7 Nm/˚ compared to the hinged AFO condition. For this participant, while peak MG MTU length was similar across AFO stiffness conditions, peak AT length decreased and peak MG muscle length increased in terminal stance with increasing AFO stiffness. Changes in AT length contributed to the majority of the change in MTU length (57-58%) during stance across AFO conditions. With the hinged AFO, the MG length remained relatively consistent during mid-stance, but eccentric stretching of the MG in mid-stance increased with AFO stiffness.

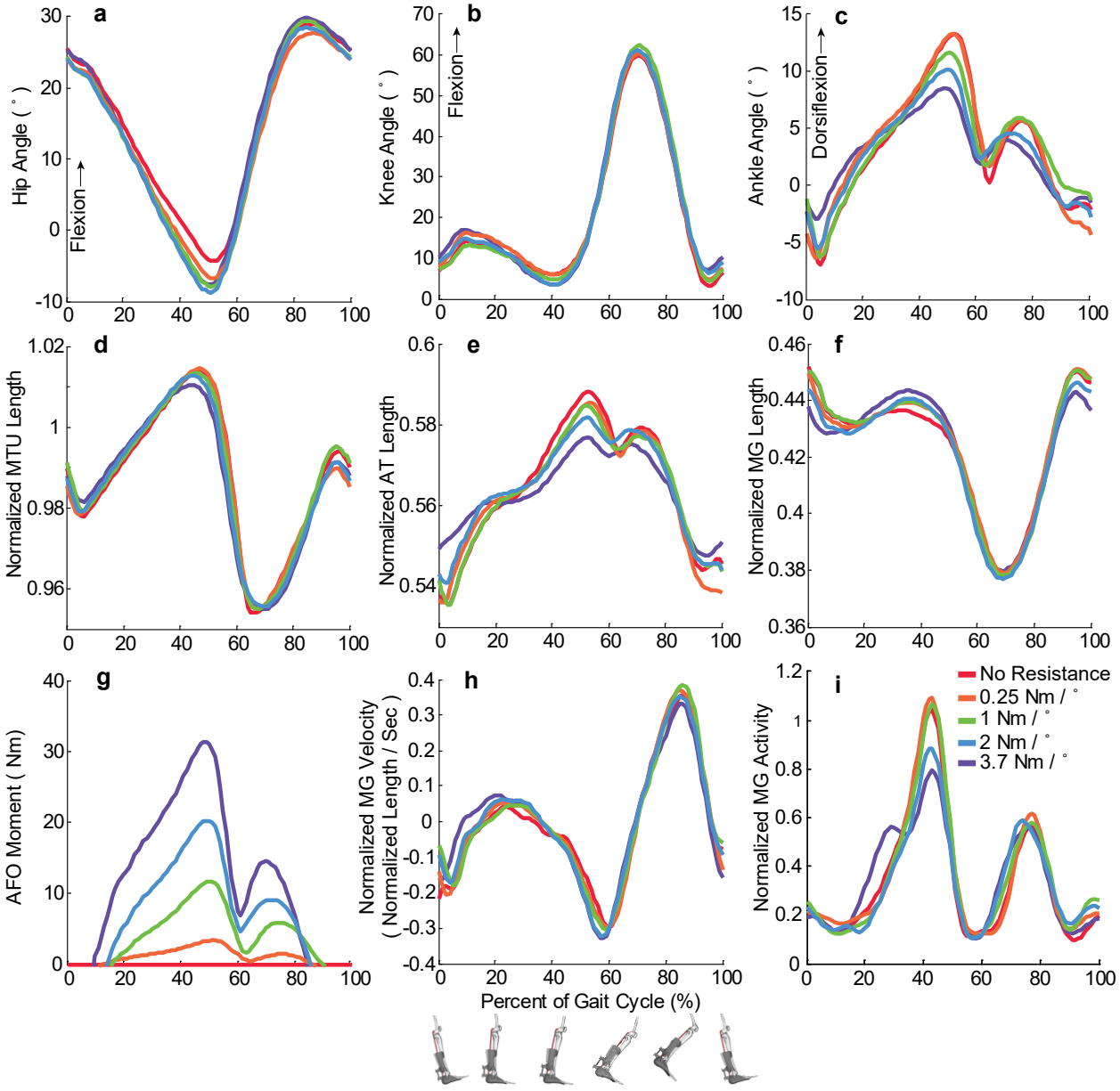

Figure 20 The average joint kinematics and muscle functions.

Average joint kinematics at the (a) hip, (b) knee, and (c) ankle for Participant 4 walking at a slow speed. There were minimal changes in (d) MTU length with AFO stiffness, while (e) peak AT length decreased and (f) peak MG length in terminal stance increased as (g) peak AFO moment increased. This participant showed minimal changes in (h) MG velocity, while (i) MG activity from EMG decreased. AT and MG lengths were normalized to the length of the MTU when musculoskeletal model was positioned in anatomic position.

Across participants, as AFO stiffness increased resistance to plantarflexion, peak knee extension angle ($p < 0.0001$) and peak ankle dorsiflexion angle ($p < 0.0001$) during single-limb stance significantly decreased, resulting in greater AFO moments with increasing stiffness ($p < 0.0001$) for both the slow and very slow walking speeds (Fig. 22). Peak gastrocnemius MTU length ($p < 0.0001$) and peak AT length ($p < 0.0001$) also significantly decreased during single-limb stance as AFO stiffness increased (Fig. 23a, d), although the effect size was small. On average, there was a 0.41 % change in MTU length and 2.89 % change in AT length between the hinge and 3.7 Nm / ˚ conditions during single-limb stance at slow walking speed and 0.81 % and 2.14 % change in MTU and AT lengths at the very slow walking speed. On the other hand, peak AT length at heel contact significantly increased as AFO stiffness increased ($p = 0.0002$) and walking speed decreased ($p < 0.0001$) (Fig. 23b). Peak AT length during terminal stance was greater than the length at heel contact (Fig. 23a, b).

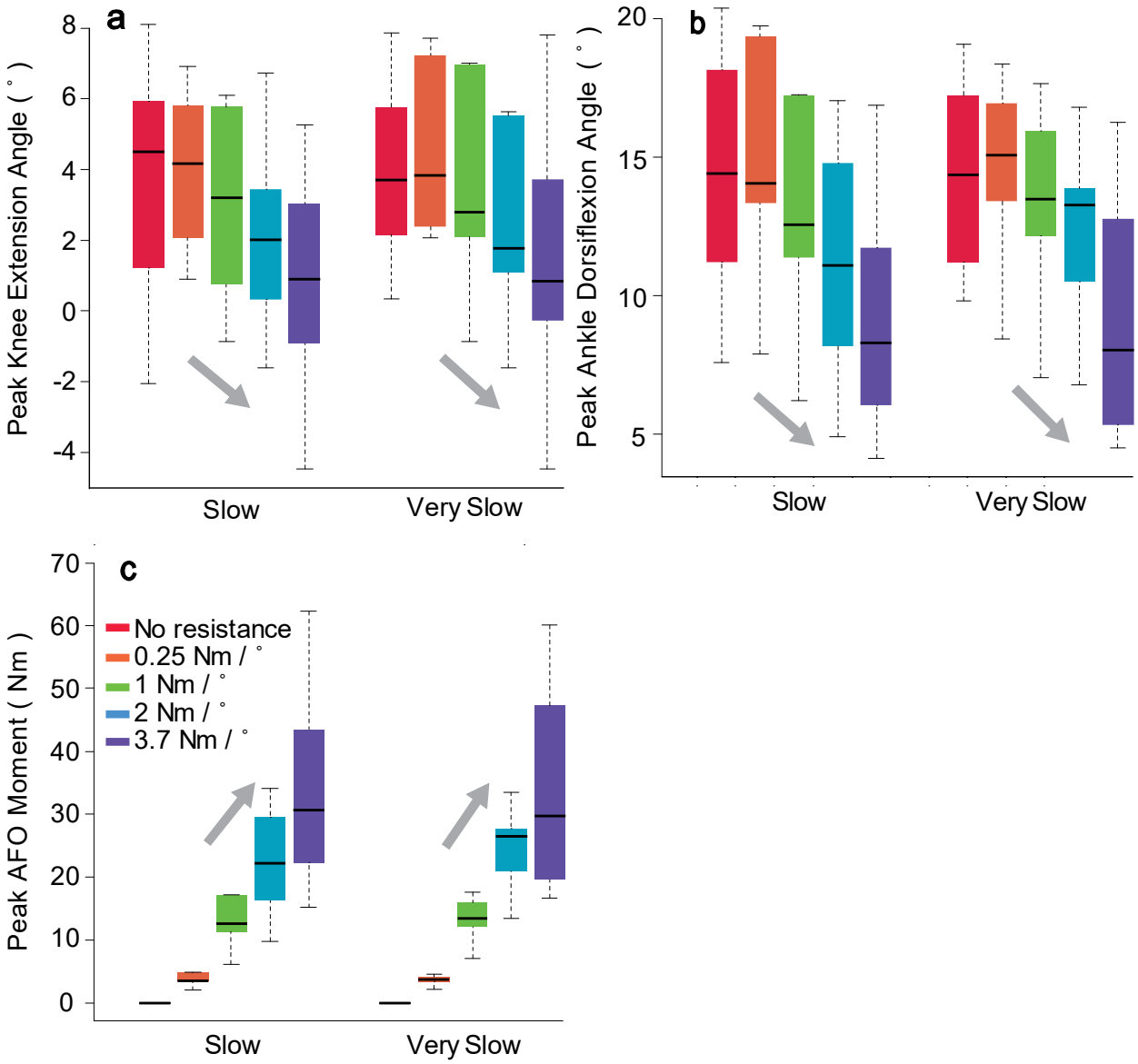

Figure 21 Effects of AFO stiffness and walking speeds on joint kinematics and AFO moment. Effects of AFO stiffness and walking speed on (a) peak knee extension angle, (b) peak ankle dorsiflexion angle, and (c) peak AFO moment during single limb support. Black horizontal line in each box depicts median value, upper and lower boundary of each box represents upper and lower quartile respectively. Upper and lower error bars represent maximum and minimum values respectively. Arrows represent a significant change ($p < 0.001$) with increasing AFO stiffness from the linear mixed-effects regression models.

Peak MG length ($p = 0.0016$) and activity ($p = 0.0025$) were significantly impacted by AFO stiffness in both walking speeds (Fig. 23 e, f), although there was more variability in responses across participants as compared to MTU and AT lengths. Figure 24 illustrates peak MG lengths, activities, and its correlation relative to no resistive AFO condition during mid to terminal stance for each participant. For example, during slow walking, three participants had decreased peak MG lengths as AFO stiffness increases beyond 2 Nm / ˚ while the other participants' peak MG length continued to increase. During very slow walking, two participants had a shortened peak MG length with an AFO stiffness of 3.7 Nm / ˚ compared to 2 Nm / ˚, but the other participants had consistent increases in peak MG length with increasing AFO stiffness. Increased peak MG length were associated with decreased MG activity except for two participants, suggesting as AFO stiffness increased, peak MG length increased due to less eccentric action of the MG. This suggests individuals adopt different adaptation to the AFO stiffness when greater than 2 Nm / ˚. Increasing AFO stiffness did not impact peak MG activity ($p = 0.5967$) and peak MG eccentric velocity ($p = 0.5967$) for both walking speeds (Fig. 23e, f).

Walking speed significantly reduced peak MG length ($p = 0.0009$), peak MG activity ($p = 0.0025$), and peak MG eccentric velocity ($p < 0.0001$) (Fig. 23c, e, f). However, peak knee extension angle ($p = 0.4381$), peak ankle dorsiflexion angle ($p = 0.4264$), peak AFO moment ($p = 0.7464$), peak MTU length ($p = 0.3510$), and peak AT length ($p = 0.1100$) were not significantly affected by walking speed. This suggests that walking speed significantly impacted the force generating capacity of the MG, with minimal changes in overall kinematics and MTU length.

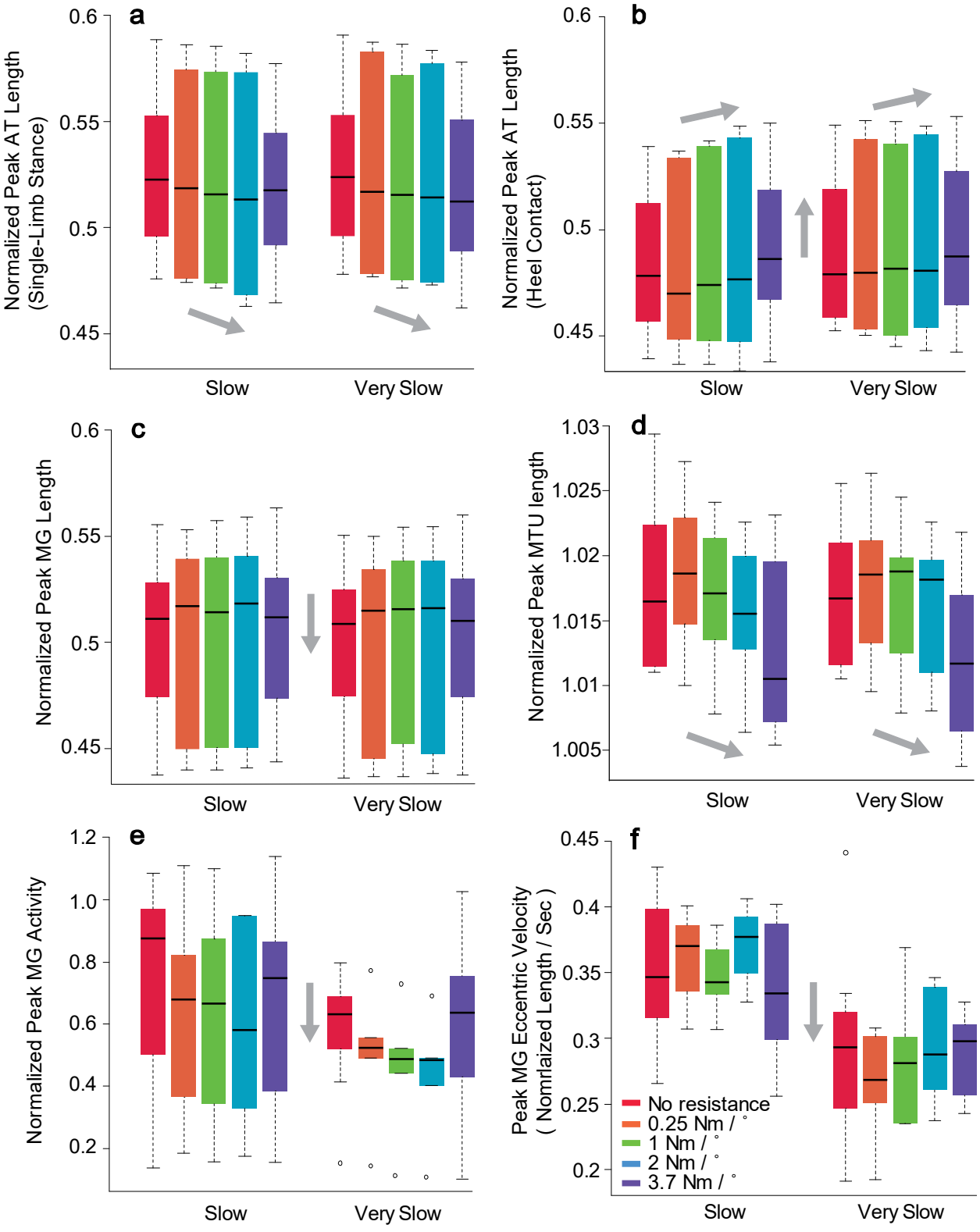
a
Normalized Peak AT Length (Single-Limb Stance)
0.6
0.55
0.5
0.45
Slow
Very Slow
b
Normalized Peak AT Length (Heel Contact)
0.6
0.55
0.5
0.45
Slow
Very Slow
c
Normalized Peak MG Length
0.6
0.55
0.5
0.45
Slow
Very Slow
d
Normalized Peak MTU length
1.03
1.025
1.02
1.015
1.01
1.005
Slow
Very Slow
e
Normalized Peak MG Activity
1.2
1.0
0.8
0.6
0.4
0.2
Slow
Very Slow
f
Peak MG Eccentric Velocity (Nomralized Length / Sec)
0.45
0.4
0.35
0.3
0.25
0.2
No resistance
0.25 Nm / °
1 Nm / °
2 Nm / °
3.7 Nm / °
Slow
Very Slow

Figure 22 Effects of AFO stiffness and walkig speeds on musculotendon length and velocity. Effects of AFO stiffness and walking speed on (a) normalized peak AT length during single-limb stance, (b) normalized peak AT length at heel contact, (c) normalized peak MG length during single-limb stance, (d) normalized peak MTU length during single-limb stance, (e) normalized peak MG eccentric velocity during single-limb stance, and (f) MG activation from EMG during single-limb stance. AT and MG lengths were normalized to the length of the MTU when musculoskeletal model was positioned in anatomic position. Black horizontal lines in each box depict median value, upper and lower boundary of each box represents upper and lower quartile, respectively. Upper and lower error bars represent maximum and minimum values, respectively. Circles in figure d depicts outliers (> 2 SD from mean). Inclined arrows and vertical arrows represent a significant change ($p < 0.001$) with increasing AFO stiffness and walking speed respectively from the linear mixed-effects regression models.

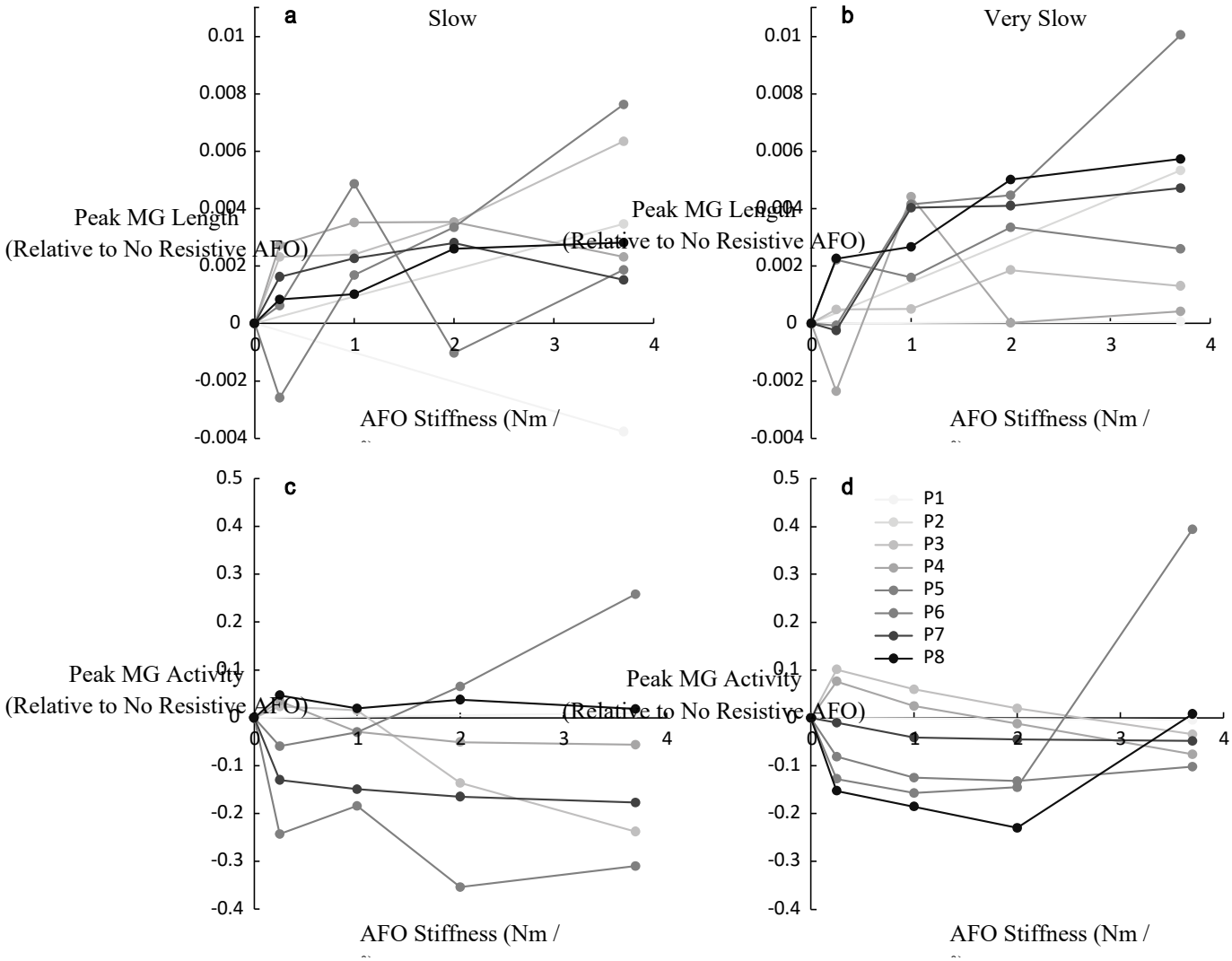

Figure 23 Changes in peak MG length during single-limb support relative to a hinged AFO. Change in peak MG length and activity during mid to terminal stance relative to a hinged (no resistive) AFO during (a / c) slow and (b / d) very slow speeds for each participant.

4.4 Discussion

In this study, we used 3D motion capture, ultrasound, and musculoskeletal modeling to evaluate the influence of AFO stiffness and walking speed on joint kinematics, induced AFO moment, and MG function. Our results demonstrated that AFO stiffness and walking speed significantly impact joint kinematics and musculotendon function during gait, with trends of increasing changes in MG and AT lengths with increasing AFO stiffness.

This study represents a first experimental investigation into how AFO stiffness and walking speed impact musculotendon function. Quantifying MG and AT lengths can provide insight into how the human neuromuscular system adapts and responds to assistance, such as from passive AFOs. The MG plays an important role supporting and propelling the body during gait [77]. Prior research suggests that the AT uses a catapult-like action [167] to improve walking efficiency. The amount of energy stored by the AT during is proportional to changes in AT length [154]. The MG uses the AT's passive elastic properties to operate near constant length during gait [167]. Prior studies with ultrasound [163-165] have confirmed the isometric operating length of the MG during unassisted walking, and we found similar results with our no resistance (hinged) condition. However, mathematical models have suggested that AFOs may increase lengthening velocity of the MG during gait, compromising force-generating capacity and AT energy storage [153].

This research demonstrated that AT and MG length were significantly impacted by AFO stiffness. Both AT length and MG activity deceased as AFO stiffness increased, suggesting the AT stores less energy and the MG's force-generating capacity can be compromised while walking with an AFO. A prior study found the peak net ankle moment, the sum of biological ankle moment and AFO moment, was conserved across different AFO stiffness conditions, suggesting the neuromuscular system adapts to use a consistent net ankle moment regardless of AFO assistance [152]. While kinetics were not available for this experiment, the changes in MG activity and length support these results. As MG activity decreased, the force in the series elastic AT also decreased, contributing to greater changes in MG length during gait.

Evaluating rate of change in peak MG length can also be useful to provide insights into mechanisms underlying the interplay between walking speed and AFO stiffness. During

unassisted walking, MG function is influenced by walking speed, with decreasing contributions to support and propulsion at slower walking speeds [113,156]. Our results demonstrated that slower walking speeds decreased MG's eccentric velocity [153]. Peak MG length and activity decreased during the very slow walking speed. These results suggest that when an individual with an AFO decreases their walking speed, decreasing the demand on the MG, they may not receive the level of energy savings expected due to changes in MG operating length and velocity.

This study also demonstrates the variability in responses to AFOs, even among unimpaired individuals. As AFO stiffness increased, some participants' gastrocnemius engaged more muscle force while others continued to decrease MG activity with increased AFO stiffness. Since no training or coaching was given to the participants in this study, the differences reflect variable responses to the potential assistance provided by a passive AFO. Prior studies of unimpaired individuals walking with active and passive AFOs have also reported variable changes in energy costs [152], which may be related to different strategies used to engage with or use the devices. Providing proper guidance which can maximally utilize the functionality of assistive devices may help to optimally reduce metabolic costs.

The methods described in this manuscript can also be used to evaluate musculotendon function and inform the prescription of AFOs for individuals with neurologic impairments, such as those with stroke and cerebral palsy. Individuals with cerebral palsy are commonly prescribed AFOs. Short and tight muscles are common for these individuals, which can contribute to pathologic gait, including excessive plantarflexion and/or knee flexion during walking. Since AFOs are worn all day, understanding whether they stretch or shorten the MG could have important implications for rehabilitation [38,73,180]. A prior study demonstrated that currently prescribed AFOs [166] and providing treadmill training with an incline can stretch the

gastrocnemius MTU during gait [181]. However, the relative stretching of the MG and AT with AFOs and other interventions remain unclear and represents an important area for future study.

While ultrasound provides insight into AT and MG muscle belly length, there are further musculotendon properties that may influence function with AFOs that cannot be quantified with ultrasound alone. In this study, we oriented the ultrasound probe so that the MTJ was positioned in the middle of the screen, so that MG belly length could be measured. We did not measure fascicle length or pennation angle, which would require a more proximal placement of the ultrasound transducer. Examining MG fiber length and pennation angle could provide insight on how AFO stiffness changes muscle force generating capacity relative to fascicle length [170]. Further, muscle force is dictated by sarcomere length, which cannot be estimated from ultrasound. While it often assumed that muscles adapts to operate near optimal sarcomere length, this assumption has not been experimentally tested in humans and may also not hold true for individuals with neuromuscular disorders.

This study evaluated how AFO stiffness impacts gait kinematics, MG, and AT function during walking with slow and very slow walking speeds. We found that, as AFO stiffness increased, peak AFO dorsiflexion moment, MG length, and AT length were increased, while peak ankle dorsiflexion angle and MG activation decreased. With slower walking speed, peak MG activity, length, and velocity also significantly decreased; however, there was significant variability between participants in changes in MG activation level and length with varying speed. Future studies are required to evaluate how AFO stiffness impacts musculotendon and walking function for individuals with neurologic injuries, such as cerebral palsy or stroke who are commonly prescribed AFOs. We believe these finding can help design optimal AFOs to improve both impaired and unimpaired gait during daily life.

CONCLUSION

Summary

This dissertation provides important evidence for how the human musculoskeletal system interplays with various AFO properties and advances AFO fabrication methods using 3D technologies. Specifically, this work suggests that:

- Adjusting heel wedge angles of AFOs can limit or alter short and tight muscle operating length. These changes can improve gait kinematics and speed for stroke survivors with stiff knee gait.
- Prescribing specific types of AFOs can be stretch short and tight muscles during gait, potentially assisting with rehabilitation goals.
- Fabricating AFOs with 3D printing and scanning technology can provide a research platform that reduces time and labor and allows for integration of novel sensors as compared to standard fabrication processes. This 3D printed AFO also allows for easy adjustment of stiffness by interchanging various elastic polymer bands.
- Quantifying AT length is possible using a novel method combining 3D motion capture, ultrasound, and musculoskeletal modeling to evaluate the impacts of different stiffness AFOs and walking speeds on joint kinematics and musculotendon function.

The evidence found in this dissertation may guide future development of an optimal AFO which may augment mobility and minimizes metabolic cost for both unimpaired and individuals with neurologic injuries, as well as maximizing rehabilitation goals in daily life.

Future Work

The work presented in this dissertation has created a foundation of knowledge about how AFOs impact musculotendinous function and joint kinematics. The results of these studies suggest many exciting avenues for future work, using both musculoskeletal modeling and experimental techniques. The following sections outline important areas of future work that can further expand our understanding of the impacts of AFOs to the human musculoskeletal system and lead to innovations in developing AFOs which minimize energy consumption and maximize human passive elastic elements:

- **How can we customize AFO to each individual?**

  Each individual has different musculotendon properties. Estimating AT stiffness could help determine how much energy we can utilize during dynamic tasks and guide AFO design. Evaluating AT length, as suggested in Aim 4, and ankle moment, which can be calculated from inverse dynamics, in two different stiffness levels of an AFO could quantify AT stiffness during dynamic tasks. For example, net ankle moment (biological ankle moment and AFO moment) in the hinged AFO condition ($M_{Net,H}$) and alpha stiffness AFO condition ($M_{Net,\alpha}$) can be calculated. From a previous study [152], humans uses almost the same amount of ankle moment during walking with different AFO stiffness conditions. However, there might be differences due to the changes in muscle contributions or energy dissipation between the human body and AFOs. This value can be used to compensate the difference between $M_{Net,H}$ and $M_{Net,\alpha}$.

$$M_{Net,H} = M_{Net,\alpha} + M_{\beta}$$

We can expand the moment into levels of stiffness ($K_{AT,H},\ K_{AT,\alpha},\ K_{AFO,H}$), moment arm length ($MA_{AT,H},\ MA_{AT,\alpha},\ MA_{AFO,H}$) and amount of elongation of AT and elastic polymer bands ($\Delta X_{AT,H},\ \Delta X_{AT,\alpha},\ \Delta X_{AFO,H}$).

$$K_{AT,H} \cdot \Delta X_{AT,H} \cdot MA_{AT,H} = K_{AT,\alpha} \cdot \Delta X_{AT,\alpha} \cdot MA_{AT,\alpha} + K_{AFO,H} \cdot \Delta X_{AFO,H} \cdot MA_{AFO,H} + M_{\beta}$$

Since AT stiffness within a participant is a near-constant material property, the moment arm can be calculated by differentiating the changes in muscle or elastic polymer band length by changes in ankle joint or AFO angle.

$$where,\ K_{AT,H} = K_{AT,\alpha} = K_{AT},\ MA = \frac{dl}{d\theta}$$

Finally, we can summarize the equation in terms of AT stiffness, which give us the level of AT stiffness.

$$K_{AT} = \frac{K_{AT,\alpha} \cdot \Delta X_{AT,\alpha} \cdot MA_{AT,\alpha} + K_{AFO,\alpha} \cdot \Delta X_{AFO,\alpha} \cdot MA_{AFO,\alpha} + M_{\beta}}{\Delta X_{AT,\alpha} \cdot MA_{AT,\alpha} + \Delta X_{AT,H} \cdot MA_{AT,H}}$$

Correlating each individual's AT stiffness and AT length in a specific AFO condition

may provide further evidence to identify the optimal stiffness which can minimize muscle effort by maximizing the utility of the AT during gait. This method can also be used to evaluate how AT properties are altered in individuals with neurologic injuries compared to unimpaired individuals.

- **How does changing AFO stiffness correlate to stretching short and tight muscles for individuals with neurologic injuries?**

  In Aim 2, we found specific AFO stiffness can stretch short and tight musculotendon length for children with CP. However, a question arose about which element, the muscle or the tendon, is stretched. The method in Aim 4 could be utilized to quantify how pathologic muscle can be stretched with different AFO properties during gait to determine whether it is feasible to stretch muscles during daily life.

- **Could dynamic stretching short and tight muscles with AFOs during walking be more effective compared to passive stretching exercise?**

  Unlike stretching exercises in the clinic where muscle is stretched without muscle activation, dynamic stretching with an AFO during walking provides some level of muscle activation. The method in Aim 4 could be utilized to evaluate how much muscle can be stretched with AFOs during walking and compared to passive stretching exercises.

- **Can a model predict adaptations to different stiffness AFOs?**

  The experimental results in Aim 4 used only two minutes of acclimatization time with changes in AFO properties, which may not allow sufficient adaptation to an AFO, but can

be used to generate an initial estimate of adaptations to different AFO properties. However, our body might have different strategies to adapt to the AFO with long period of time. Individuals with neurologic impairments may also have different strategies to adapt to the AFO with short and long periods of time. However, these experiments with different AFO properties can be very time consuming with many different conditions. Developing a model with experimental evidence that can predict locomotor and musculotendon adaptation to AFOs would enhance design and prescription.

The human musculoskeletal system is incredibly complex. In order to conclude precise interpretation of how our musculotendinous system interplays with AFOs or alternative types of assistive devices, various experimental data such as muscle force, muscle fascicle function, and other passive elements should be examined and considered for analysis. This dissertation provided several pieces of the complex puzzle to help investigate an entire phenomenon. This evidence provides more information to develop optimal AFO designs which can be fabricated in a more efficient way and help to maximize function for unimpaired individuals and individuals with neurologically impairments.

REFERENCES

1. Arneson, C.L., et al., *Prevalence of Cerebral Palsy: Autism and Developmental Disabilities Monitoring Network, Three Sites, United States, 2004*. Disabil Health J, 2009. **2**(1): p. 45–8.
2. Christensen, D., et al., *Prevalence of cerebral palsy, co-occurring autism spectrum disorders, and motor functioning - autism and developmental disabilities monitoring network, USA, 2008*. Dev Med Child Neurol, 2014. **56**(1): p. 59–65.
3. Kancherla, V., et al., *Medical expenditures attributable to cerebral palsy and intellectual disability among Medicaid-enrolled children*. Res Dev Disabil, 2012. **33**(3): p. 832–40.
4. Shefelbine, S.J., et al., *Mechanobiological predictions of femoral anteversion in cerebral palsy.* Ann Biomed Eng, 2004. **32**(2): p. 297–305.
5. Bagg, M.R., et al., *Long-term follow-up of hip sublucation in cerebral palsy patients*. J Pediatr Orthop, 1993. **13**(1): p. 32–6.
6. Murphy, D.J., et al., *Case-control study of antenatal and intrapartum risk factors for cerebral palsy in very preterm singleton babies*. Lancet, 1995. **346**(8988): p. 1449–54.
7. Carson, S.C., et al., *Value of sonography in the diagnosis of intracranial hemorrhage and periventricular leukomalacia: a postmortem study of 35 cases*. AJNR Am J Neuroradiol, 1990. **11**(4): p. 677–83.
8. Matsuda, Y., et al., *Comparison of neonatal outcome including cerebral palsy between abruptio placentae and placenta previa.* Eur J Obstet Gynecol Reprod Biol, 2003. **106**(2): p. 125–9.
9. Anat, E.G., *Axo-somatic and axo-dendritic synapses of the cerebral cortex*. J Anat, 1959. **93**(Pt 4): p. 420–33.
10. Miller, A.K., et al., *Variation with age in the volumes of grey and white matter in the cerebral hemispheres of man: measurements with an image analyser*. Neuropathol Appl Neurobiol, 1980. **6**(2): p. 119–32.
11. Marner, L., et al., *Marked loss of myelinated nerve fibers in the human brain with age*. J Comp Neurol, 2003. **462**(2): 144–52.
12. Dammann, O., et al., *Infection remote from the brain, neonatal white matter damage, and cerebral palsy in the preterm infant*. Semin Pediatr Neurol, 1998. **5**(3): p. 190–201.
13. Gonçalves, L.F., et al., *Intrauterine infection and prematurity*. Ment Retard Dev Disabil Res Rev, 2002. **8**(1): 3–13.
14. Verma, U., et al., *Obstetric antecedents of intraventricular hemorrhage and periventricular leukomalacia in the low-birth-weight neonate*. Am J Obstet Gynecol, 1997. **176**(2): 275–81.
15. Wren, T.A.L., et al., *Prevalence of specific gait abnormalities in children with cerebral palsy: influence of cerebral palsy subtype, age, and previous surgery*. J Pediatr Orthop, 2005. **25**(1): 79–83.
16. Rose, J., et al., *Neuromuscular activation and motor-unit firing characteristics in cerebral palsy*. Dev Med Child Neurol, 2005. **47**(5): p. 329–36.
17. Rodda, J.M., et al., *Sagittal gait patterns in spastic diplegia*. J Bone Surg Br, **86**(2): p. 251–8.
18. Rose, S.A., et al., *Kinematic and kinetic evaluation of the ankle after lengthening of the gastrocnemius fascia in children with cerebral palsy*. K Pediatr Orthop, **13**(6): p. 727–32.

19. Gage, J.R., The indentification and treatment of gait problems in cerebral palsy. In: Õunpuu, S., et al., *Classification of cerebral palsy and patterns of gait pathology*. 2nd ed. London: Mac Keith Press, p. 162–3.
20. Stackhouse, S.K., et al., *Voluntary muscle activation, contractile properties, and fatigability in children with and without cerebral palsy*. Muscle Nerve, 2005. **31**(5): p. 594–601.
21. Lance, J.W., *Symposium synopsis*. In: Feldman RG, Young RR, Koella WP, editors. *Spasticity: Disordered Motor Control*. Chicago: YearBook Medical, 1980. p. 185–203.
22. Tardieu, C., et al., *Muscle hypoextensibility in children with cerebral palsy: I. clinical and experimental observations*. Arch Phys Med Rehabil, 1982. **63**(3): p. 97–102.
23. Brown, P., *Pathophysiology of spasticity*. J Neurol Neurosurg Psychiatry, 1994. **57**(7): p. 773–7.
24. Barrett, R.S., et al., *Gross muscle morphology and structure in spastic cerebral palsy: a systematic review*. Dev Med Child Neurol, 2010. **52**(9): p. 794–808.
25. Mathewson, M.A., et al., *Stiff muscle fiber in calf muscles of patients with cerebral palsy lead to high passive muscle stiffness*. J Orthop res, 2014. **32**(12): p. 1667–74.
26. Zwaan, E., et al., *Synergy of EMG patterns in gait as an objective measure of muscle selectivityin children with spastic cerebral palsy*. Gait Posture, 2012. **35**(1): p. 111–5.
27. Wiley, M.E., et al., *Lower-extermity strength profiles in spastic cerebral palsy*. Dev Med Child Neurol, 1998. **40**(2): p. 100–7.
28. Rosa, M.C., et al., *Methodologies to assess muscle co-contraction during gait in people with neurological impairment – a systematic literature review*. J Electromyogr Kinesiol, 2014. **24**(2): p. 179–92.
29. Kaida, R., et al., *Effects of diazepam on evoked electrospinogram and evoked electromyogram in man*. Anesth Analg, 1981. **60**(4): p. 197–200.
30. Milla, P.J., et al., *A controlled trial of baclofen in children with cerebral palsy*. J Int Med Res, 1977. **5**(6): p. 398–404.
31. Koman, L.A., et al., *Management of cerebral palsy with botulinum-A toxin: preliminary investigation*. J Pediatr Orthop, 1993. **13**(4): p. 489–95.
32. Jahn, J., et al., *Calf muscle-tendon lengths before and after Tendon-Achilles lengthenings and gastrocnemius lengthenings for equinus in cerebral palsy and idiopathic toe walking*. Gait Posture, 2009. **29**(4), p. 612–7.
33. Baddar, A., et al., *Ankle and knee coupling in patients with spastic diplegia: effects of gastrocnemius-soleus lengthening*. J Bone Joint Surg Am, 2002. **84-A**(5): p. 736–44.
34. Rutz, E., et al., *Tibialis anterior tendon shortening in combination with Achilles tendon lengthening in spastic equinus in cerebral palsy*. Gait Posture, 2011. **33**(2): p. 152–7.
35. Gage, J.R., *The identification and treatment of gait problems in cerebral palsy.* In Ward, M., Pharmacologic treatment with oral medication. 2nd ed. Mac Keith Press; 2009, p. 352.
36. Eames, N.W., et al., *The effect of botullinum toxin A on gastrocnemius length: magnitude and duration of response*. Dev Med Child Neurol, 1999. **41**(4): p. 226–32.
37. Saw, A., et al., *Rectus femoris transfer for children with cerebral palsy: Long-term outcome*. J Pediatr Orthop, 2003. **23**(5): p. 672–8.
38. Pin, T., et al., *The effectiveness of passive stretching in children with cerebral palsy*. Dev Med Child Neurol, 2006. **48**(10): p. 855–62.
39. Dodd, K.J., et al., *A systematic review of the effectiveness of strength-training programs for people with cerebral palsy*. Arch Phys Med Rehabil, 2002. **83**(3): p. 1157–64.

40. Dodd, K.J., et al., *Partial body-weight-supported treadmill training can improve walking in children with cerebral palsy: a clinical controlled trial*. Dev Med Child Neurol, 2007. **49**(2): p. 101–5.
41. Ketelaar, M., et al., *Effects of a functional therapy program on motor abilities of children with cerebral palsy*. Phys Ther, 2001. **81**(9): p. 1534–45.
42. Franki, I., et al., *The evidence-base for basic physical therapy techniques targeting lower limb function in children with cerebral palsy: a systematic review using the International Classification of Functioning, DIsability and Health as a conceptual framework*. J Rehabil Med, 2012. **44**(5): p. 385–95.
43. Andersson, C., et al., *Adults with cerebral palsy: a survey describing problems, needs, and resources, with special emphasis on locomotion*. Dev Med Child Neurol, 2001. **43**(2): p. 76–82.44. Gage, J.R., The indentification and treatment of gait problems in cerebral palsy. In: Novacheck, T.F., et al., *Orthoses*. 2nd ed. London: Mac Keith Press, p. 332–3.
45. Cusick, B.D., *Splints and casts. Managing foot deformity in children with neuromotor disorders*. Phys Ther, 1988. **68**(12): p. 1903–12.
46. Hesse, S., et al., *Non-velocity-related effects of a rigid double-stopped ankle-foot orthosis on gait and lower limb muscle activity of hemiparetic subjects with an equinovarus deformity*. Stroke, 1998. **30**(9): p. 1855–61.
47. Convery, P., et al., *A three centre study of the variability of ankle foot orthoses due to fabrication and grad of polypropylene.* Prosthet Orthot Int, 2004. **28**(2): p. 175–82.
48. Bielby, S.A., et al., *Trimline severity significantly affects rotational stiffness of ankle foot orthosis*. AAOP, 2010. **22**(4): p. 204–10.
49. Schrank, E.S., et al., *Assessment of a virtual functional prototyping process for the rapid manufacture of passive-dynamic ankle-foot orthoses*. J Biomech Eng, 2013. **135**(10): p. 101011–7.
50. Wolf, S.I., et al., *Dynamic assist by carbon fiber spring AFOs for patients with myelomeningocele*. Gait Posture, 2008. **28**(1): p. 175–7.
51. Novacheck, T.F., et al., *Quantifying the spring-like properties of ankle-foot orthoses (AFOs)*. J Prosthet Orthot, 2007. **19**(4): p. 98–103.
52. Arch, E.S., et al., *Passive-dynamic ankle foot orthoses substitute for ankle strength while causing adaptive gait strategies: a feasibility study*. Ann Biomed Eng, 2015. **43**(2): p. 442–50.
53. Buckon, C.E., et al., *Comparison of three ankle-foot orthosis configurations for children with spastic hemiplegia*. Dev Med Child Neurol, 2001. **43**(6): p. 371–8.
54. Radtka, S.A., et al., *A comparison of gait with solid and hinged ankle-foot orthoses in children with spastic diplegic cerebral palsy. Gait Posture*, 2005. **21**(3): p. 303–10.
55. Lam, W.K., et al., *Biomechanical and electromyographic evaluation of ankle foot orthosis and dynamic ankle foot orthosis in spastic cerebral palsy*. Gait Posture, 2005. **22**(3): p. 189–97.
56. Buckon, C.E., et al., *Comparison of three ankle-foot orthosis configurations for children with spastic diplegia.* Dev Med Child Neurol, 2004. **46**(9): p. 590–8.
57. Brunner, R., et al., *Comparison of a stiff and a spring-type ankle-foot orthosis to improve gait in spastic hemiplegic children*. J Pediatr Orthop, 1998. **18**(6): p. 719–26.
58. Smiley, S.J., et al., *A comparison of the effects of solid, articulated, and posterior leaf-spring ankle-foot orthoses and shoes alone on gait and energy expenditure in children with spastic diplegic cerebral palsy.* Orthopedics, 2002. **25**(4): p. 411–5.

59. Bregman, D.J., et al., *Polypropylene ankle foot orthoses to overcome drop-foot gait in central neurological patients: a mechanical and functional evaluation*. Prosthet Orthot Int, 2010. **34**(3): p. 293–304.
60. Arch, E.S., et al., *Passive-dynamic ankle-foot orthoses substitute for ankle strength while causing adaptive gait strategies: a feasibility study*. Ann Biomed Eng, 2015. **43**(2): p. 442–50.
61. Lam, W.J., et al., *Biomechanical and electromyographic evaluation of ankle foot orthosis and dynamic ankle foot orthosis in spastic cerebral palsy*. Gait Posture, 2005. **22**(3): p. 189–97.
62. Romkes, J., et al., *Changes in muscle activity in children with hemiplegic cerebral palsy while walking with and without ankle-foot orthoses*. Gait Posture, 2006. **24**(4): p. 467–74.
63. Lairamore, C., et al., *Comparison of tibialis anterior muscle electromyography, ankle angle, andvelocity when individuals post stroke walk with different orthoses*. Prosthet Orthot Int, 2011. **35**(4): p. 402–10.
64. Bregman, D.J., et al., *Spring-like Ankle Foot Orthoses reduce the energy cost of walking by taking over ankle work*. Gait Posture, 2012. **35**(1): p. 148–53.
65. Bennett, B.C., et al., *The effects of ankle foot orthoses on energy recovery and work during gait in children with cerebral palsy*. Clin Biomech, 2012. **27**(3): p. 287–91.
66. Eddison, N., et al., *The effect of tuning ankle foot orthoses-footwear combination on the gait parameters of children with cerebral palsy*. Proshtet Orthot Int, 2013. **37**(2): p. 95–107.
67. Owen, E., *The importance of being earnest about shank and thigh kinematics especially when using ankle-foot orthoses*. Prosthet Orthot Int, 2010 **34**(3): p. 254–69.
68. Jagadamma, K.C., et al., *Effects of tuning of ankle foot orthoses-footwear combination using wedges on stance phase knee hyperextension in children with cerebral palsy – Preliminary results*. Disabil Rehabil Assist Technol, 2009 **4**(6): p. 406–13.
69. Gök, H., et al., *Effects of ankle-foot orthoses on hemiparetic gait*. Clin Rehabil, 2003. **17**(2): p. 137–9.
70. Crabtree, C.A., et al., *Modeling neuromuscular effects of ankle foot orthoses (AFOs) in computer simulations of gait*. Gait Posture, 2009. **29**(1): p. 65–70.
71. Bregman, D.J., et al., *The effect of ankle foot orthosis stiffness on the energy cost of walking: a simulation study*. Clin Biomech, 2011. **26**(9): p. 955–61.
72. Bjornson, K.F., et al., *Ambulatory physical activity performance in youth with cerebral palsy and youth who are developing typically.* Phys Ther, 2007. **87**(3): p.248–57.
73. Zhao, H., et al., *Changes of calf muscle-tendon biomechanical properties induced by passive-stretching and active-movement training in children with cerebral palsy*. J Appl Physiol, 2011. **111**(2): p. 435–42.
74. Delp, S.L., et al., *An interactive graphics-based model of the lower extremity to study orthopaedic surgical procedures*. IEEE Trans Biomed Eng, 1990. **37**(8): p. 757–67.
75. Holzbaur, K.R., et al., *A model of the upper extremity for simulating musculoskeletal surgery and analyzing neuromuscular control*. Ann Biomed Eng, 2005. **33**(6): p. 829–40.
76. Correa, T.A., et al., *Accuracy of generic musculoskeletal models in predicting the functional roles of muscles in human gait*. J Biomech, 2011. **44**(11): p. 2096–105.
77. Steele, K.M., et al., *Muscle contributions to support and progression during single-limb stance in crouch gait*. J Biomech, 2010. **43**(11): p. 2099–105.

78. Steele, K.M., et al., *Muscle contributions to vertical and fore-aft accelerations are altered in subjects with crouch gait*. Gait Posture, 2013. **38**(1): p. 86–91.
79. Bar-On, L., et al., *The relation between spasticity and musle behavior during the swing phase of gait in children with cerebral palsy*. Res Dev Disabil, 2014. **35**(12): p. 3354–64.
80. Rha, D.W., et al., *Biomechanical and clinical correlates of swing-phase knee flexion in individuals with spastic cerebral palsy who walk with flexed-knee gait*. Arch Phys Med Rehabil, 2015. **96**(3): p. 511–7.61.
81. Hicks, J.L., et al., *Crouched postures reduce the capacity of muscles to extend the hip and knee during the single-limb stance phase of gait*. J Biomech, 2008. **41**(5): p. 960–7.
82. Arnold, A.S., et al., *Evaluation of a deformable musculoskeletal model for estimating muscle-tendon lengths during crouch gait*. Ann Biomed Eng, 2001. **29**(3): p. 263–74.
83. Arnold, A.S., et al., *Computer modeling of gait abnormalities in cerebral palsy: application to treatment planning*. Theor. Issues Ergonomics Sci, 2005. **6**(3-4): p. 305–12.
84. Hsu, L.C., et al., *Distal hamstring elongation in the management of spastic cerebral palsy*. J Pediatr Orthop, 1990. **10**(3): p. 378–81.
85. Dhawlikar, S.H., et al., *Distal lengthening of the hamstrings in patients who have cerebral palsy. Long-term retrospective analysis*. J Bone Joint Surg Am, 1992. **74**(9): p. 1385–91.
86. Damron, T.A., et al., *Diminished knee flexion after hamstring surgery in cerebral palsy patients: prevalence and severity*. J Pediatr Orthop, 1993. **13**(2): 188–91.
87. Delp, S.L., et al*., Hamstrings and psoas lengths during normal and crouch gait: implications for muscle-tendon surgery*. J Orthop Res, 1996. **14**(1): p. 144–51.
88. Arnold, A.S., et al., *The role of estimating muscle-tendon lengths and velocities of the hamstrings in the evaluation and treatment of crouch gait*. Gait Posture, 2006. **23**(3): p. 273–81.
89. Thompson, N.S., et al., *Effect of a rigid ankle-foot orthosis on hamstring length in children with hemiplegia*. Dev Med Child Neurol, 2002. **44**(1): p. 51–7.
90. Wells, P.N.T., *Ultrasound imaging*. Phys Med Biol, 2006. **51**(13): p. R83–98.
91. Schafer, M.E., et al., *The influence of front-end hardware on digital ultrasonic imaging. IEEE Trans Sonics Ultrason*, 1984. **31**(4): p. 295–306.
92. Narici, M.V., et al., *Effect of aging on human muscle architecture*. J Appl Physiol, 2003. **95**(6): p. 2229–34.
93. Ohata, K., et al., *Measurement of muscle thickness as quantitative muscle evaluation for adults with severe cerebral palsy*. Phys Ther, 2006. **86**(9): p. 1231–9.
94. Mohagheghi, A.A., et al., *Differences in gastrocnemius muscle architecture between the paretic and non-paretic legs in children with hemiplegic cerebral palsy*. Clin Biomech, 2007. **22**(6): p. 718–24.
95. Malaiya, R., et al., *The morphology of the medial gastrocnemius in typically developing children and children with spastic hemiplegic cerebral palsy*. J Electromyogr Kinesiol, 2007. **17**(6): p. 657–63.
96. Wade, D.T. et al., *Functional abilities after stroke: measurement, natural history and prognosis*. J Neurol Neurosur Ps, 1987. **50**(2): p. 177–82.
97. Butler, P.B., et al., *The effect of fixed ankle foot orthoses in children with cerebral palsy.* Disabil Rehabil Assist Technol, 2007 **2**(1): p. 51–8.
98. Carse, B., et al., *The immediate effects of fitting and tuning solid ankle-foot orthoses in early stroke rehabilitation*. Prosthet Orthot Int, 2014. **34**(3): p. 270–6.

99. Jagadamma. K.C., et al., *The effects of tuning an ankle-foot orthosis footwear combination on kinematics and kinetics of the knee joint of an adult with hemiplegia*. Prosthet Orthot Int, 2010. **34**(3): 270–6.
100. Owen, E., *Shank angle to floor measures of tuned 'ankle-foot orthosis footwear combinations' used with children with cerebral palsy, spina bifida and other conditions*. Gait Posture, 2002. **16**: p. S132–3.
101. Butler, P.B., et al., *The biomechanics of fixed ankle foot orthoses and their potential in the management of cerebral palsied children*. Physiotherapy, 1991. **77**(2): p. 81–8.
102. Owen, E., *Proposed clinical algorithm for deciding the sagittal angle of the ankle in an ankle-foot orthosis footwear combination*. Gait Posture, 2005. **22S**: p. 38-9.
103. Owen, E., *A clinical algorithm for the design and tuning of ankle-foot orthosis footwear combinations (AFOFCs) based on shank kinematics*. Gait Posture, 2005. **22S**: p. 36-8.
104. Owen, E., *The point of 'point-loading rockers' in ankle-foot orthosis footwear combinations used with children with cerebral palsy, spina bifida and other conditions*. Gait Posture, 2004. **20S**: p. S86.
105. Bowers, R., et al., *Development of a best practice statement on the use of ankle-foot orthoses following stroke in Scotland*. Prosthet Orthot Int, 2010. **34**(3): p. 245–53.
106. Olney, S.J., et al., *Hemiparetic gait following stroke. Part I: Characteristics*. Gait Posture, 1996. **4**(2): p. 136–48.
107. Stauffer, R.N., et al., *Biomechanical gait analysis of the diseased knee joint*. Clin Orthop Relat Res, 1977. **126**: p. 246–55.
108. Hicks. J.L., et al., *Can biomechanical variables predict improvement in crouch gait?* Gait Posture, 2011. **34**(2): p. 197–201.
109. Owen, E., *From stable standing to rock and roll walking (part1) the importance of alignment, proportion and profiles*. The Association of Paediatric Chartered Physiotherapists, 2014. **5**(1): p. 7–18.
110. Kadaba, M.P., et al., *Measurement of lower extremity kinematics during level walking.* J Orthop Res, 1990. **8**(3): p. 383–92.
111. Delp, S.L., et al., *OpenSim: open-source software to create and analyze dynamic simulations of movement*. IEEE Trans Biomed Eng, 2007. **54**(11): p. 1940–50.
112. Agarwal-Harding, K.J. et al., *Variation of hamstrings lengths and velocities with walking speed*. J Biomech, 2010. **43**(8): p. 1522–6.
113. Liu, M.Q., et al., *Muscle contributions to support and progression over a range of walking speeds*. J Biomech, 2008. **41**(15): p. 3243–52.
114. Zajac, F.E., et al., *Determining muscle's force and action in multi-articular movement*. Exerc Sport Sci Rev, 1989. **17**: p. 187–230.
115. Anderson, F.C., et al., *Human walking.* In Jessica, R., et al., editors. *Simulation of walking*. 3rd ed. Lippincott Williams and Wilkins, 2006. p. 195–210.
116. Thomas, M.C., *The effects of heel height and ankle-foot-orthosis configuration on weight line location: A demonstration of principles*. Orthotics Prosthet, 1976. **30**(4): 43–6.
117. Figueiredo, E.M., et al., *Efficacy of ankle-foot orthoses on gait of children with cerebral palsy: systematic review of literature*. Pediatr Phys Ther, 2008. **20**(3): p. 207–23.
118. Brehm, M.A., et al., *Effect of ankle foot orthoses on walking efficiency and gait in chilren with cerebral palsy*. J Rehabil Med, 2008. **40**(7): p. 529–34.
119. Abe, H., et al., *Improving gait stability in stroke hemiplegic patients with a plastic ankle-foot orthosis*. Tohoku J Exp Med, 2009. **218**(3): p. 193–99.

120. Rao, N., et al., *The effect of two different ankle-foot orthoses on gait of patients with acute hemiparetic cerebrovascular accident*. Rehabil Res Pract, 2014. **2014**:301469.
121. Bassan, H., et al., *Neurodevelopmental outcome in survivors of periventricular hemorrhagic infarction*. Pediatrics, 2007. **120**(4): p. 785–92.
122. Lieber, R.L., et al., *Structural and functional changes in spastic skeletal muscle*. Muscle Nerve, 2004. **29**(5): 615–27.
123. Abel, M.F., et al., *Gait assessment of fixed ankle-foot orthoses in children with spastic diplegia*. Arch Phys Med Rehabil, 1998. **79**(2): p. 126–33.
124. Wren, T.A.L., et al., *Gastrocnemius and soleus lengths in cerebral palsy equinus gait-differences between children with and without static contracture and effects of gastrocnemius recession*. J Biomech, 2004. **37**(9): p. 1321–7.
125. Choi, H., et al., *Using musculoskeletal modeling to evaluate the effect of ankle foot orthosis tuning on musculotendon dynamics: a case study*. Disabil Rehabil Assist Technol, 2015. **11**(7): p.613–8.
126. Hullin, M.G., et al., *Gait patterns in children with hemiplegic spastic cerebral palsy*. J Pediatr Orthop B, 1996. **5**(4): p. 247–251.
127. Baddar, A., et al., *Ankle and knee coupling in patients with spastic diplegia: effects of gastrocnemius-soleus lengthening*. J Bone Joint Surg Am, 2002. **84-A**(5): p. 736–44.
128. Lance, J.W., *The control of muscle tone, reflexes, and movement Robert Wartenbeg Lecture*. Nuerology, 1980. **30**(12): p. 1303–13.
130. Engsberg, J., et al., *Ankle spasticity and strength in children with spastic diplegic cerebral palsy*. Dev Med Child Neurol, 2000. **42**(1): p. 42–7.
131. van der Krogt, M.M., et al., *Walking speed modifies spasticity effects in gastrocnemius and soleus in cerebral palsy gait*. Clin Biomech, 2009. **24**(5): p. 422–28.
132. Wren, T.A.L., et al., *Comparison of 2 orthotic approaches in children with cerebral palsy*. J Pediatr Orthop, 2005. **25**(1): p. 79–83.
133. Agarwal-Harding, K.J., et al., *Variabtion of hamstrings lengths and velocities with walking speed*. J Biomech, 2010. **43**(8): p. 1522–26.
134. Thompson, N., et al., *Muscle strength and walking ability in diplegic cerebral palsy: Implications for assessment and management*. Gait Posture, 2011. **33**(3): p. 321–25.
135. Youdas, J.W., et al., *Partial weight-bearing gait using conventional assistive devices.* Arch Phys Med Rehabil, 2005. **86**(3): p. 394–8.
136. Hoang, H.X., et al., *Crouched posture maximizes ground reaction forces generated by muscles*. Gait Posture, 2012. **36**(3): p. 405–8.
137. Orendurff, M.X., et al., *Length and force of the gastrocnemius and soleus during gait following tendo Achilles lengthening in children with equinus*. Gait Posture, 2002. **15**(2): p. 130–35.
138. Bar-On, L., et al., *Is an instrumented spasticity assessment an improvement over clinical spasticity scales in assessing and predicting the response to integrated botulinum toxin type a treatment in children with cerebral palsy?* Arch Phys Med Rehabil, 2014. **95**(3): p. 515–23.
139. Bregman, D.J.J., et al., *A new method for evaluating ankle foot orthosis characteristics: BRUCE*. Gait Posture, 2009. **30**(2): p. 144–9.
140. Bosmans, L., et al., *Hip contact force in presence of aberrant bone geometry during normal and pathological gait*. J Orthop Res, 2014. **32**(11): p. 1406–15.

141. Hicks, J., et al., *The effect of excessive tibial torsion on the capacity of muscles to extend the hip and knee during single-limb stance*. Gait Posture, 2007. **26**(4): p. 546–52.
142. Scheys, L., et al., *Personalized MR-based musculoskeletal models compared to rescaled generic models in the presence of increased femoral anteversion: Effect on hip moment arm lengths*. Gait Posture, 2008. **28**(3): p. 358–65.
143. Valente, G., et al., *Are subject-specific musculoskeletal models robust to the uncertainties in parameter identification?* PloS One, 2014. **9**(11): e112625.
144. Faustini, M.C., et al., *Manufacture of Passive Dynamic ankle-foot orthoses using selective laser sintering*. IEEE Trans Biomed Eng, 2008. **55**(2 Pt 1): p. 784-90.
145. Pallari, J.H., et al., *Design and additive fabrication of foot and ankle-foot orthoses.* Proceedings of the 21st Annual International Solid Freeform Fabrication Symposium – An additive Manufacturing Conference, 2010. p. 834–45.
146. Mavroidis, C., et al., *Patient specific ankle-foot orthoses using rapid prototyping*, 2011. J Neuroeng Rehabil. **8**(1): p. 1–11.
147. Schrank, E.S., et al., *Dimensional accuracy of ankle-foot orthoses constructed by rapid customization and manufacturing framework*, 2011. J Rehabil Res Dev. **48**(1): p. 31–42.
148. Creylman, V., et al., *Gait assessment during the initial fitting of customized selective laser sintering ankle foot orthoses in subjects with drop foot*. Prosthet Orthot Int, 2013. **37**(2): p. 132–8.
149. Takahashi, K.Z., et al., *Estimates of stiffness for ankle-foot orthoses are sensitive to loading conditions*. AAOP, 2010. **22**(4): p. 211–19.
150. Tymrak, B.M., et al., *Mechanical properties of components fabricated with open-source 3-D printers under realistic environmental conditions*. Materials & Design, 2014. **58**: p. 242–46.
151. Belter J.T. and Dollar A.M., *Strengthening of 3D printed fused deposition manufactured parts using the fill compositing technique*. PLoS One, 2015. **10**(4): e0122915.
152. Collins, S.H., et al., *Reducing the energy cost of human walking using an unpowered exoskeleton*. Nature, 2015. **522**(7555): p. 212–5.
153. Sawicki, S.H. and Khan, N., *A simple model to estimate plantarflexor muscle-tendon mechanics and energetics during walking with elastic ankle exoskeletons*. IEEE Trans Biomed Eng, 2016. **63**(5): p. 914–23.
154. Hill, A.V., *The mechanics of active muscle*. Proc R Soc London B Biol Sci, 1953. **141**(902): p. 104–17.
155. Hill, A.V., *The heat of shortening and the dynamic constants of muscle*. Proc R Soc Lond B, 1938. **126**(843): p. 136–95.
156. Neptune, R.R., et al., *The effect of walking speed on muscle function and mechanical energetics*. Gait Posture, 2008. **28**(1): p. 135–43.
157. Muffulli, N., *Rupture of the Achilles tendon*. J Bone Joint Surg Am, 1999. **81**(7): p. 1019–36.
158. Giddings, V.L., *Calcaneal loading during walking and running*. Med Sci Sports Exerc, 2000. **32**(3): p. 627–34.
159. Cavagna, G.A., et al., *Mechanical work in terrestrial locomotion: two basic mechanisms for minimizing energy expenditure*. Am J Physiol, 1977. **233**(5): p. R243–61.
160. Farris, D.J and Sawicki, G.S., *The mechanics and energetics of human walking and running: a joint level perspective*. J R Soc Interface, 2012. **9**(66): p. 110–18.

161. Fukunaga, T., et al., *In vivo behavior of human muscle tendon during walking*. Proc Biol Sci, 2001. **268**(1464): p. 229–33.
162. Ryschon, T.W., et al., *Efficiency of human skeletal muscle in vivo: comparison of isometric, concentric, and eccentric muscle action*. J Appl Physiol, 1997. **83**(3): p. 867–74.
163. Lichtwark, G.A., et al., *Interactions between the human gastrocnemius muscle and the Achilles tendon during incline, level and decline locomotion*. J Exp Biol, 2006. **209**(Pt 21): p. 4379–88.
164. Cronin, N.J., et al., *Achilles tendon length changes during walking in long-term diabetes patients*. Clin Biomech, 2010. **25**(5): p. 476–82.
165. Kalsi, G., et al., *Gastrocnemius muscle-tendon interaction during walking in typically-developing adults and children, and in children with spastic cerebral palsy*. J Biomech, 2016. **49**(14): p. 3194–99.
166. Choi, H., et al., *Gastrocnemius operating length with ankle foot orthoses in cerebral palsy*. J Prosthet Orthot Int, 2016. In press.
167. Ishikawa, M., et al., *Muscle-tendon interaction and elastic energy usage in human walking*. J Appl Physiol, 2005. **99**(2): p. 603–8.
168. Lundberg, A., et al., *The axis of rotation of the ankle joint*. J Bone Joint Surg Br, 1989. **71**(1): p. 94–9.
169. Hamner, S.R., et al., *Muscle contributions to propulsion and support during running*. J Biomech, 2010. **43**(14): p. 2709–16.
170. Randhawa, A. and Wakeling, J.M., *Associations between muscle structure and contractile performance in seniors*. Clin Biomech, 2013. **28**(6): p. 705–11.
171. Rosso. C., e. al., *Physiological Achilles tendon length and its relation to tibia length*. Clin J Sport Med, 2012. **22**(6): p. 483–87.
172. Bates, D., et al., *Fitting linear mixed-effects models using lme4*. arXiv preprint arXiv:1406.5823 2014.
173. Ryschon, T.W., et al., *Efficiency of human skeletal muscle in vivo: comparison of isometric, concentric, and eccentric muscle action*. J Appl Physiol, 1985. **83**(3): p. 867–74.
174. Whittington, B., et al. *The contribution of passive-elastic mechanisms to lower extremity joint kinemtics during human walking*. Gait Posture, 2008. **27**(4): p. 628–34.
175. Ikai, M. and Fukunaga. T., *Calculation of muscle strength per unit cross-sectional area of human muscle by means of ultrasonic measurement*. Int Z Angew Physiol, 1968. **26**(1): p. 26–32.
176. Arya, S. and Kulig, K., *Tendinopathy alters mechanical and material properties of the Achilles tendon*. J Appl Physiol, 2010. **108**(3): p. 607–5.
177. Edama, M., et al., *The twisted structure of the human Achilles tendon*. J Med Sci Sports, 2015. **229**(3): p. 610–14.
178. Zelik, K.E. and Kuo, A.D., *Human walking isn't all hard work: evidence of soft tissue contributions to energy dissipation and return*. J Exp Biol, 2010. **213**(Pt 24): p. 4257–64.
179. Zelik, K.E., *Quantifying physical interface dynamics: human-prosthesis and human-exoskeleton power transmission*. American Society of Biomechanics 2016.
180. Theis, N., et al., *Does long-term passive stretching alter muscle-tendon unit mechanics in children with spastic cerebral palsy?* Clin Biomech, 2015, **30**(10): p. 1071–6.

181. Lorentzen, J., et al., *Treadmill training with an incline reduces ankle joint stiffness and improves active range of movement during gait in adults with cerebral palsy*. Disabil Rehabil, 2016. **30**: p. 1–7.

APPENDIX A

Experimental worksheets for identifying marker and bony landmark positions for Aim 4.

Reflective marker dimension

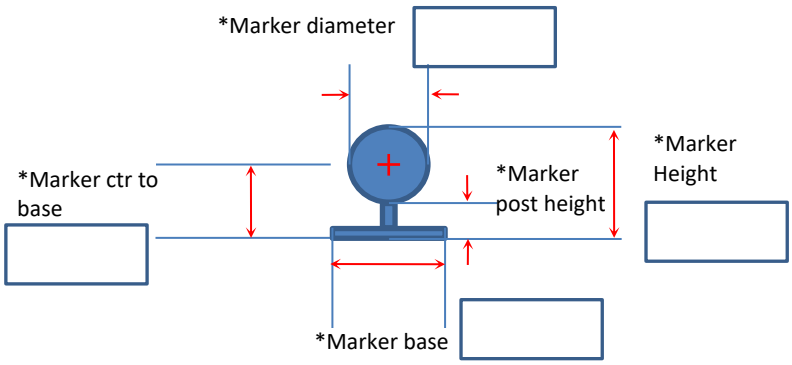

Foot marker position check sheet (Sagittal view)

UNIT: mm

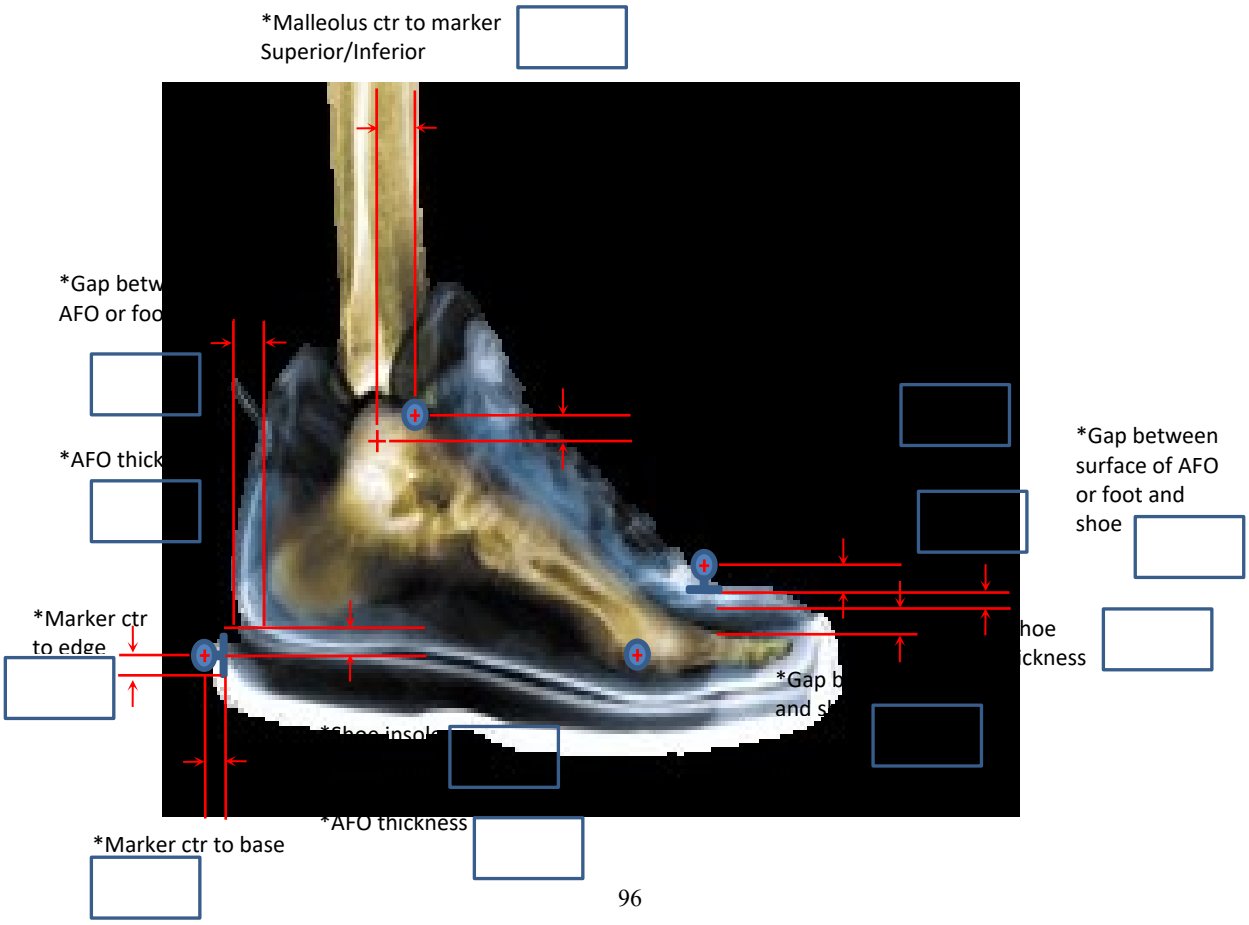

Foot marker position check sheet (Transverse view)

UNIT: mm

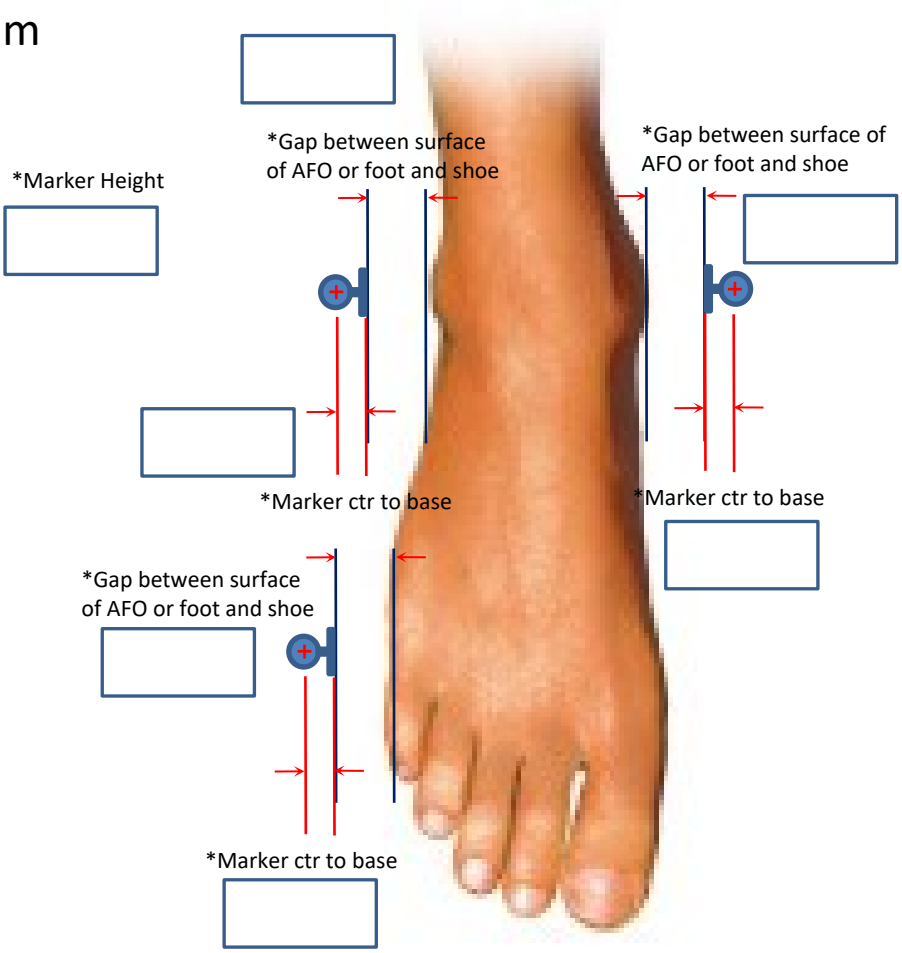

Test Protocol

Number: **Age:** **Height:**
Gender: **Weight:**

[I] 1st Visit

Date: / / **Testers:** _____

o Complete consent form and survey o Scanning the Leg

o Inform about TestDay 2:

o Short shorts, tight-fitting sleeveless shirt, no lotion on legs, shoe size,

[2] 2nd visit

Date: / / **Testers:** _____

To take from Ability lab:

o Goniometer, tapemeasure, aliper, yoga mat o Superglue for markers to AFO

o Attach velcro straps with glue

o 2 Laptops with power supply (Ultrasound, EMG)

o US box, probes, chargers, leads, triggers*2, gel, tissues, tape, coban, probe holders, o Charged battery, electrodes, double-sided tape, alcohol, razors

o Alcohol swabs, leads/headers, EMG boards

o socks, shoes, strap, foam, scissors, heat gun, dremel

o Gloves (heat and cloth), screwdrivers, extra screws, sticky notes, Volt meter o DSLR Camera, USB back-up * 2

o Biopotential fully charged and Lava.set file on SD card

o Printed out testing protocol and marker/picture documents * 3 o Delsys EMG Box

o Trigger System (Trigger junction box, Cables)

o Even Switches *5, Cables, + batteries

o AFO, Support Clips, Polymer bands (2394N/m, 7000N/m, 8247N/m, 19000N/m, 40600N/m)

VICON Lab:

Before participant arrives -

o Turn on Vicon desktop and camera (from the back of Vicon ethernet), laptops o Connect Vicon, US and EMG computers

o EMG sensors prepped tape, bilaterally, software ready o Reflective markers ready, double-sided tapes ready

o Camera calibration process

o Ensure the Vicon computer does not sleep

After participant arrives -

o Take Height, Weight, Age, Sex, and following measurements

Birth date		Height	cm
Gender		Weight	kg
A. Pelvis (LASIS-RASIS)	cm	A. Pelvis (LPSIS-RPSIS)	cm
R ASIS – R Med Knee	cm	L ASIS – L Med Knee	cm
A ASIS – R Lat Knee	cm	A ASIS – L Lat Knee	cm
RGT – R Knee	cm	LGT – L Knee	cm
R Lat Knee – R Lat Mal	cm	L Lat Knee – L Lat Mal	cm
R Heel – R 2nd Digit Prox. Phalanx (Wrap Lat under Mal)	cm	L Heel – L 2nd Digit Prox. Phalanx (Wrap Lat under Mal)	cm
R Knee (Med – Lat Con)	cm	L Knee (Med – Lat Con)	cm
R Ank (Med – Lat Mal)	cm	L Ank (Med – Lat Mal)	cm
R Acrom – L Acrom	cm		
R 5MT – R 2nd Digit Prox. Phalanx	cm	L 5MT – L 2nd Digit Prox. Phalanx	cm
R Heel – R 5 MT (Wrap Lat under Mal)	cm	L Heel – L 5 MT (Wrap Lat under Mal)	cm

R Ankle Passive Dorflexion w/Full Knee Extension		R Ankle Passive Dorsiflexion w/90˚ Knee Flexion	
R Knee Passive Extension (w/90˚ Hip Flexion)			
L Ankle Passive Dorflexion w/Full Knee Extension		L Ankle Passive Dorsiflexion w/90˚ Knee Flexion	
L Knee Passive Extension (w/90˚ Hip Flexion)			

o Fitting AFO (modify if necessary) -> Re-fit AFO, apply padding,
observe gait o Apply Motion capture marker set

o Apply Bilateral EMG Markers, pre-paired

o Apply US 1 with visual feedback (Check the interference without AFO and with AFO)

o Ask subject to stand on the treadmill

o Record Leg Length for Calculating Speed below

o Static calibration trial 1 (take photos with Hwan's reference sheet) -> remove
medial markers o MVC Trial

(**5 toes rasises**, standing with both feet shoulder width apart, raise up as high as they can on toes, and then slowly lower, **5 squats**, feet shoulder with apart, squat til knee at ~90˚, and **5 toe lifts on each side**, hold foot off the ground, lift up toes)

o Acclimatize the participant to the treadmill (2 min)

o Assist in increasing or decreasing speed of treadmill

o Calculating speed: ***normalized speed = Froude's number*SQRT(gravity*leg length)***

Rt. Leg length (RASIS to R LatMal) - ***Treadmill Speed***

Speed S (0.19) -	0.0000
Speed N (0.29) -	0.0000

*Record names here for each saved trial!

Trials	Vicon File Name	US File Name	EMG File Name	Stiffness	
Speed					
1	P11_Static_Shoe	P11_Static_Shoe	P11_Static_Shoe		
2	P11_MVC	P11_MVC	P11_MVC		
3	P11_Shoe_S	P11_Shoe_S	P11_Shoe_S		S
4	P11_Shoe_N	P11_Shoe_N	P11_Shoe_N		N
5	P11_Static_AFO	P11_Static_AFO	P11_Static_AFO		
6	P11_Hinge_N	P11_Hinge_N	P11_Hinge_N	**Hinge**	N
7	P11_10_N	P11_10_N	P11_10_N	**10**	N
8	P11_Rigid_S	P11_Rigid_S	P11_Rigid_S	**Rigid**	S
9	P11_314_N	P11_314_N	P11_314_N	**3.14**	N

10	P11_50_N	P11_50_N	P11_50_N	**50**	N
11	P11_Rigid_N	P11_Rigid_N	P11_Rigid_N	**Rigid**	N
12	P11_25_S	P11_25_S	P11_25_S	**25**	S
13	P11_314_S	P11_314_S	P11_314_S	**3.14**	S
14	P11_10_S	P11_10_S	P11_10_S	**10**	S
15	P11_50_S	P11_50_S	P11_50_S	**50**	S
16	P11_Hinge_S	P11_Hinge_S	P11_Hinge_S	**Hinge**	S
17	P11_25_N	P11_25_N	P11_25_N	**25**	N

Subject Notes:

Check List prior test

1. Treadmill speed setup □

2. All markers attachments Event switch wire connection AFO stiffness condition □

3. Vicon setup (file name, event switch setup) EMG trial setup/ Sensors Awake □

4. Ultrasound Setup □

Check List after each test

1. Is ultrasound image clear? □

2. Vicon data (Export trc file and check) □

3. Vicon event switch data (Export ASCII file and check) EMG data collected □

4. All markers attachment & visible □

5. Check AFO condition □

6. SAVE EMG/US/Vicon □

7. Export files □

VITA

Hwan Choi was born and raised in South Korea. He earned a Bachelor of Arts and Master of Arts in Control and Instrumentation Engineering at Korea University. In 2016, he earned a Doctor of Philosophy at the University of Washington in Mechanical Engineering.